

Alma Mater Studiorum-Università di Bologna

**Dottorato di ricerca in Scienze Farmacologiche, dello Sviluppo e del
Movimento Umano**

-XXVI ciclo-

Settore Concorsuale: 05/F1 Biologia

Settore Scientifico Disciplinare: BIO/13

Oxidative Stress and Friedreich's Ataxia

Presentata da: **Dott.ssa Alessandra Bolotta**

Coordinatore dottorato:

Prof. Giorgio Cantelli Forti

Relatore:

Prof. ssa Marina Marini

Co-Relatore:

Dott. ssa Provvidenza Maria Abruzzo

Esame Finale Anno 2014

Abstract

Friedreich's Ataxia (FRDA) is a neurodegenerative disorder caused by a deficiency of the protein frataxin and characterized by oxidative stress. The first aim of my research project was to analyze the effects of tocotrienol in FRDA patients. Patients received for 2 months a low dose of tocotrienol. A number of biochemical parameters related to oxidative stress were studied. We consistently showed that taking for 2 months a low dose of tocotrienol led to the decrease of oxidative stress indexes in FRDA patients. Also, this study provides a suitable model to investigate the efficacy of natural compounds to counteract the oxidative stress in FRDA.

Furthermore, we investigated whether the tocotrienol was able to modulate the expression of the frataxin isoforms (FXN-1, FXN-2, FXN-3) in FRDA patients. We demonstrated that tocotrienol leads to a specific and significant increase of *FXN-3* expression. As no structural and functional details were available for FXN-2 and FXN-3, 3D-models were built. FXN-1, the canonical isoform, was then docked on the human iron-sulphur complex and functional interactions were computed; when FXN-1 was replaced by FXN-2 or FXN-3, we found that the interactions were maintained, thus suggesting a possible biological role for both isoforms.

The second aim of my research project was to investigate the role of a single nucleotide polymorphism (SNP) in the protein Sirtuin 6 in FRDA patients. In fact, it was known that those who harbour a SNP (Asn46/Ser46) in the gene encoding Sirt6 show a better outcome than those individuals who are homozygous for the Asn 46 allele. We found that fibroblasts and iPSC-derived neurons from FRDA patients harboring the SNP (Asn46/Ser46) have a reduced amount of Sirt6 protein compared to cells from individuals who are homozygous for the prevalent Asn allele. Our studies provide new information on the role of Sirtuins in FRDA pathogenesis.

Index

Chapter I

1.1 Introduction to Friedreich's Ataxia (FRDA)	1
1.2 Clinical Features of Friedreich's Ataxia	3
1.3 Etiopathogenesis of Friedreich's Ataxia	7
1.4 Epigenetic Mechanisms in Friedreich's Ataxia	13
1.5 Structure and Function of the Frataxin Protein	15
1.6 Pharmacological Treatments and Therapeutic Strategies for Friedreich's Ataxia.....	20

Chapter II

Oxidative Stress

2.1 Radical Oxygen Species (ROS)	30
2.2 Physiological and Pathological Functions of ROS	32
2.3 Cellular Antioxidant Systems	37
2.4 Oxidative Stress and Biomarkers of Oxidative Stress	44
2.5 Role of Oxidative Stress in Friedreich's Ataxia	47

Chapter III

Research Project

Part I: Aims	50
Part II: Aims.....	51

Chapter IV: Role of Oxidative Stress in the Friedreich's Ataxia

Materials and Methods Part I.....	53
Supplementary materials Part I.....	61
Results Part I.....	64
Discussion and Conclusions Part I.....	77

Chapter V: Generation of human induced Pluripotent Stem Cells (hiPSCs) from Friedreich's Ataxia (FRDA) patients

Materials and Methods Part II.....	81
Supplementary materials Part II.....	86
Results Part II.....	88
Discussion and Conclusions Part II	105

References.....	107
-----------------	-----

Chapter I

1.1 Introduction to Friedreich's Ataxia (FRDA)

Friedreich's Ataxia (FRDA, OMIM #229300) is a progressive neurodegenerative disorder; it was described for the first time by the German physician Nikolaus Friedreich (1863). It is the most frequent inherited autosomal recessive ataxia with a prevalence of 1:50,000 in Caucasian populations, while it is rare in sub-Saharan African populations and is very rare in the Far East (Vankan. 2013). FRDA is characterized by a progressive degeneration of the central and peripheral nervous system and is also associated to cardiac hypertrophic myopathy and diabetes mellitus. The cardiomyopathy and the subsequent cardiac failure are the common cause of death in FRDA patients. The first symptoms that occur during the puberty include gait instability, dysarthria, areflexia, sensory loss and pyramidal signs (Santos et al., 2010). In the majority of cases, FRDA is caused by a (GAA)_n trinucleotide repeat expansion in the first intron of FXN gene (Fratxin encoding gene) located on chromosome 9q13, that encodes the protein Frataxin (Campuzano et al., 1996). A small percent of patients are heterozygous, with point mutations found on the other allele. The (GAA)_n repeats cause a epigenetic silencing of FXN gene and consequently a decreased of levels of FXN mRNA. In FRDA patients, the levels of FXN mRNA are around 4-25%, whereas in the asymptomatic carriers FXN mRNA levels are about 50% with respect to the normal subjects. It has been suggested that the mechanism responsible for the silencing of the FXN gene is due to the ability of the expanded triplets to adopt an alternative DNA structure GAA-TTC-GAA. This unusual conformation would be able to hamper the process of FXN mRNA transcription, with consequent reduction of the quantity of the transcript. Additionally, (GAA)_n repeats can induce the heterochromatinization of the FXN gene, which can contribute to gene silencing (Ohshima et al., 1998).

Frataxin is a mitochondrial protein involved in the regulation of mitochondrial iron homeostasis, in the biosynthesis and assembly of iron-sulfur (Fe-S) clusters and is involved in, nuclear damage and chromosomal instability (Karthikeyan et al.,2002). Deficiency of frataxin cause the imbalance of iron homeostasis, increased oxygen radical production and a major hypersensitivity to oxidative stress (Rustin et al.,2011).

There is no approved treatment for FRDA. Current drug screening studies are focused on ameliorating neuronal cardiac iron accumulation using iron chelators and enhancing respiratory

chain function using idebenone, a synthetic analog of coenzyme Q10 and/or reducing oxidative damage with antioxidant compounds. Alternative therapeutic approaches are based on molecules able to revert the silencing of FXN gene and restore the frataxin expression: To this purpose, chromatin-modifying molecules such as histone deacetylase inhibitors (HDACi) and compounds that increase the level of frataxin protein with neuroprotective and cardioprotective activities, such as the recombinant human erythropoietin (rHuEPO) are being currently tested. The effectiveness of these treatments in improving cardiac and neurological outcomes in Friedreich ataxia patients is under evaluation.

1.2 Clinical Features of Friedreich's Ataxia

The Quebec Collaborative Group in 1976 and Harding in 1981 have defined the essential clinical criteria for the diagnosis of FRDA (Fig.1.1). Additionally, with the application of molecular genetic methods, it has become possible to perform also the molecular diagnosis of atypical phenotypes FRDA. Currently, there are no valid outcome markers to monitor the progression of the disease. Therefore, the following clinical scales are applied to the assessment of disease severity and progression in FRDA: The International Cooperative Ataxia Rating Scale (ICARS), the Friedreich's Ataxia Rating Scale (FARS) and the Scale for the Assessment and Rating of Ataxia (SARA) (Bürk et al., 2013).

-The International Cooperative Ataxia Rating Scale (ICARS) has been validated for use in patients with focal cerebellar lesions and was tested for acceptability, reliability and validity in FRDA. The ICARS scale is scored out of 100 with 19 items and 4 subscales of postural and gait disturbances, limb ataxia, dysarthria, and oculomotor disorders.

-The Friedreich's Ataxia Rating Scale (FARS) has been validated specifically for neurological features of FRDA. It is based on a neurological examination of bulbar, upper limb, lower limb, peripheral nerve, and upright stability/gait functions. Further, functional staging and activities of daily living (ADL) assessment are incorporated. The scales are supplemented by quantitative performance measures including 8 m walk at maximum speed (8MW), the 9-hole peg test (9HPT), PATA rate (number of repetitions of the bisyllabic phrase 'PATA' within 10 s) and low-contrast letter acuity.

-The Scale for the Assessment and Rating of Ataxia (SARA) is a clinical scale restricted to cerebellar clinical symptoms and does not take into account any extracerebellar features. The eight measuring items are related to gait, stance, sitting, speech, finger-chase test, nose-finger test, fast alternating movements and heel-shin test. A maximum score of 40 reflects most severe ataxia.

All scales measure motor aspects of cerebellar dysfunction including ataxia of stance, gait and limbs. SARA being the shortest scale, FARS and ICARS also covering further aspects of the neurological examination (e.i. dysarthria or oculomotor symptoms). Only FARS considers features not directly related to the physical examination, such as activities of daily living (Bürk et al; 2013).

Based on the clinical features, FRDA is classified into two phenotypes, classical and atypical. In the classical phenotype of FRDA, at the onset around puberty neurological and non neurological features arise. The neurological features are gait and limb ataxia, areflexia and dysarthria. The ataxia is of mixed origin and is caused by cerebellar degeneration, peripheral sensory neuropathy, cerebellar and vestibular pathology (Delatycki and Corben 2012). The first pathological changes occur in the dorsal root ganglia (DRGs) with thinning of dorsal roots (DR), loss of large sensory neurons associated with neurodegeneration in Clark's and posterior columns, pyramidal signs and spinocerebellar tracts of spinal cord (Puccio et al., 2000). Neuropathological examinations have confirmed overall reduction in the size of DRG, atrophy or active destruction of nerve cells, "residual nodules" (also known as nodules of Nageotte) and gray discoloration of the thinned DR (Koeppen et al., 2009). Gait and limb ataxia causes increasing difficulties in daily activity, walking, washing and dressing. Pyramidal weakness and areflexia are prominent in the lower limbs (LLs) compared to the upper limbs (ULs) in the early stage associated with a reduction of muscle tone, cramps and spasms (Delatycki et al; 2012). Moreover, dysarthria characterized by consonant imprecision, decreased pitch variation and reduced phrase length is frequent as early sign in more than 90% of patients. In the early stage of disease the ophthalmic system with fixation instability, square wave jerks and nystagamus is also involved. Hearing difficulties caused by auditory neuropathy are a common and understated problem, which can be socially very disabling even in the early stages of disease. Almost, all patients show disordered neural conduction in the central auditory pathways which functionally results in impaired speech understanding in conditions of background noise typical of everyday listening conditions, which can lead patients to be able to access only 50% of information available, compared to unaffected individuals (Rance et al. 2010). Non neurological manifestations such as cardiomyopathy, diabetes and skeletal abnormalities are common in FRDA classical phenotypes. The hypertrophic and progressive cardiomyopathy is a common cause of death in FRDA patients. The cardiac symptoms occur early during the first or second decade of life, but the clinical signs of cardiac involvement develop only later in the course of the disease and include palpitations and uncontrolled arrhythmias. The echocardiographic hallmark of Friedreich's cardiomyopathy is left ventricle (LV) hypertrophy to which it may be added that of the posterior wall and of septa. The histological changes in the LV mainly consist of cellular hypertrophy, diffuse fibrosis, and focal myocardial necrosis. In most FRDA patients, the QRS duration is normal. Electrocardiographic signs of LV cardiomyopathy which arise during the advanced stages are high S-wave in V1 and V2, and high R-wave in V5 and V6 and T-wave abnormalities (i.e., inversion or flattening) (Weidemann et al. 2012).

Approximately 10-20 % of FRDA patients develop diabetes mellitus and about 24%- 50% have intolerance to carbohydrates. The pathogenetic mechanism of diabetes is complex and includes both a dysfunction of pancreatic β islands and peripheral insulin resistance similar to that at the base of other mitochondrial disorders (Santos et al. 2010). Data derived from a study performed in FRDA patients, suggested that diabetes in FRDA is caused by loss of islet cells similar to common Type 1 diabetes, but without HLA-association and without serologic evidence for autoimmune destruction of the islet cells (Schonele et al., 1989). The diabetes onset is often acute and the FRDA patients require insulin administration. In a number of cases, the first presentation of diabetes was ketoacidosis, which may be fulminant. (Cnop et al; 2012). Other non-neurological complications arising in FRDA patients affect the skeletal system, particularly scoliosis and foot deformities with pes cavus and talipes equinovarus.

In addition to classic FRDA phenotypes, atypical variants have been described. They include the Acadian type, late-onset FRDA (LOFA), very late-onset FRDA (VLOFA) and FRDA with retained reflexes (FARR). In atypical variants of FRDA, neurological manifestations typical of the classical phenotype remain frequent, which gait and limb ataxia, dysarthria and pyramidal involvement. However, the non neurological clinical complications (cardiomyopathy, diabetes and skeletal deformities) are less frequent or absent. Finally, in literature few cases of early-onset FRDA, have been described; they display an atypical and more severe phenotype characterized by onset before age of 5, associated with faster progression of disability, frequent cardiomyopathy and skeletal complications.

<i>Clinical Features</i>	<i>Mean Frequency (%)</i>
<i>Ataxia</i>	98
<i>Areflexia</i>	92.1
<i>Dysarthria</i>	93.6
<i>Extensor plantar responses</i>	83.5
<i>Decreased position and vibratory sense</i>	92.7
<i>Foot Deformity</i>	76.8
<i>Scoliosis</i>	84.3
<i>Abnormalities on ECG</i>	80.3
<i>Abnormalities on cardiac ultrasound</i>	50
<i>Diabetes</i>	8
<i>Nystagmus</i>	32
<i>Hearing loss</i>	20

Fig. 1.1 Clinical Features of Friedreich's ataxia.

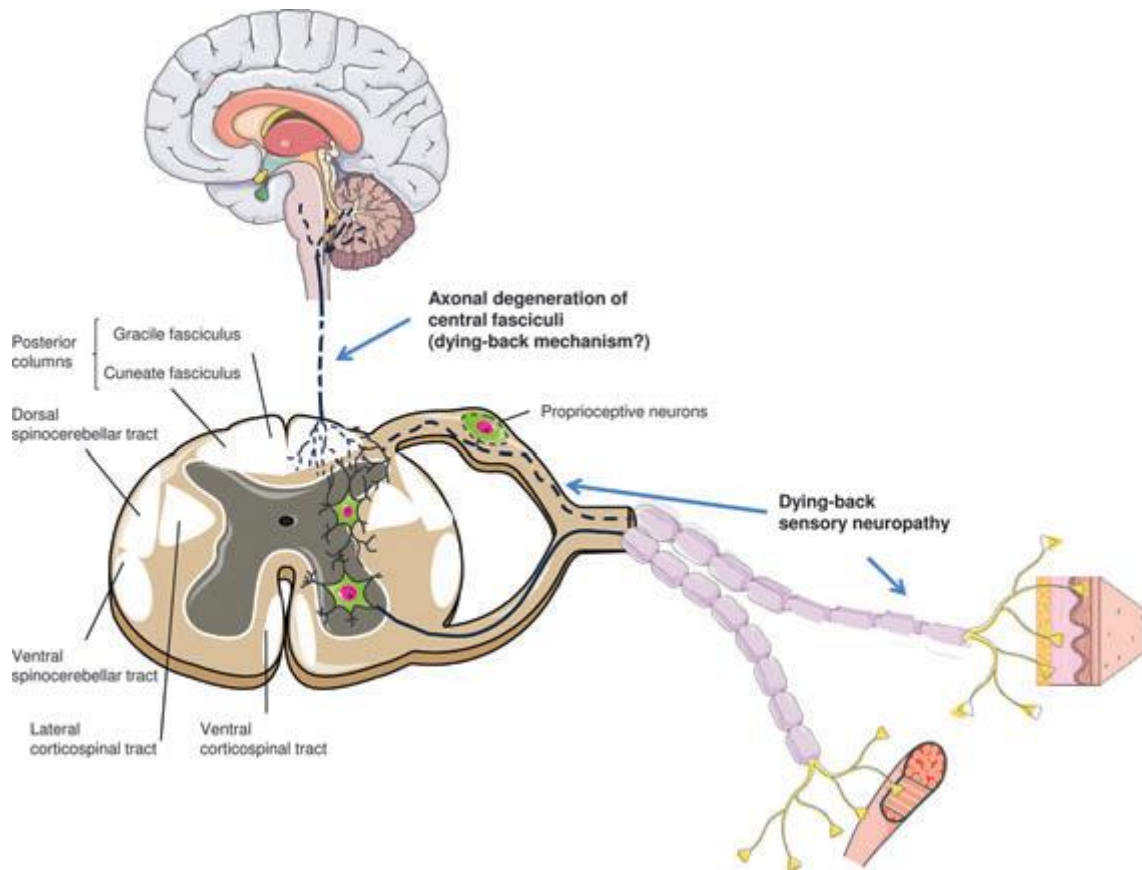


Fig.1.2 Schematic drawing of axonal pathology in peripheral and central nervous systems.

1.3 Etiopathogenesis of Friedreich's Ataxia

Genetic Mechanisms

As already mentioned in the introduction, the majority of FRDA cases are caused by a (GAA)_n trinucleotide repeat expansion in the first intron of FXN. The human FXN gene was identified in 1996 by Campuzano; it is localized on the chromosome 9q13. The genomic region containing the FRDA locus was analyzed using new polymorphic microsatellite markers. The only gene within the minimum candidate region was X25 (subsequently named *FRDA* and now *FXN*) and the FRDA locus was at last identified. Two studies showed evidence of genetic heterogeneity in FRDA. Occasional reports appearing in literature describe patients who present FRDA clinical symptoms, but in whom a mutation in the *FXN* gene cannot be detected. Thus, a second locus *FRDA2*, mapping to chromosome 9p23-p11, was proposed (Christodoulou et al., 2001), but no subsequent studies have confirmed these observations.

FXN gene is composed of seven exon (1-4, 5a, 5b and 6); exon 6 is not transcribed. The main messenger RNA is composed of five exons and encodes the protein frataxin (isoform FXN 1 of 7168bp). There are also two other transcripts with different lengths that are denominated isoform 2 (FXN2) and 3 (FXN 3), the formation of which is due to alternative splicing. Comparing the 1 and 2 isoform, it is possible to note that the variation of splicing is between exon 4 and 5a; this causes an increase of nucleotides at the end of the fourth exon in the second isoform FXN-2 (7176bp). In the third isoform, FXN-3 (980bp), mRNA alternative splicing produces a transcript identical to isoform 1 until the end of the fourth exon, then there is a skip in the transcript that causes the deletion of exon 5a but includes exon 5b (*Figure 1.3*). Isoform 3 is produced at lower levels than isoforms 1 and 2. No functional data about the protein isoforms have been reported. *FXN* gene expression and production of the protein frataxin are ubiquitous and have an essential role especially during the early stages of embryonic development. Studies of mouse *FXN* expression homologue during embryonic development by Northern blot analysis and RNA *in situ* hybridization confirmed that the *FXN* expression is not detectable at E8.5, is weak at E12.5, then increases until E16.5, when no further change is observed until the neonatal period. At E14.5, the expression is high in the ventricular zone of the brain, the anterior horns of the spinal cord, the large neuronal cells in the DRG and in the granular layer of the cerebellum (Jiralerspong et al., 1997). The levels of *FXN* mRNA and protein show tissue specificity that partially correlates with the main sites

affected by the disease. In humans, adults show the highest levels of expression in the heart and spinal cord, with intermediate levels observed in the cerebellum, liver, skeletal muscle, and pancreas and very low levels in the cerebral cortex. Furthermore, FXN mRNA is found in non-neural tissues as kidney and brown fat (Campuzano et al., 1996 and Pianese et al., 2002). Recently, Xia and co-workers (2012) have identified two novel isoforms of frataxin specifically expressed in affected cerebellum and heart. The transcripts were alternately spliced using exons 1a/1b and generated either an exon 1a-containing transcript encoding a 164 amino acid protein (isoform III), or an exon 1b-containing transcript encoding a protein of 135 amino acids (isoform II). b. Exons 2-5a are present in all three frataxin isoforms (Xia et al., 2012). Frataxin isoforms II and III were expressed as transcripts and proteins in the cerebellum and heart of individuals with FRDA, respectively. Importantly, both isoforms could facilitate iron-sulfur cluster assembly in vitro (Xia et al., 2012). Additional FXN transcripts have also been identified; however, their physiological relevance remains unclear (Pianese et al., 2004; Xia et al., 2012).

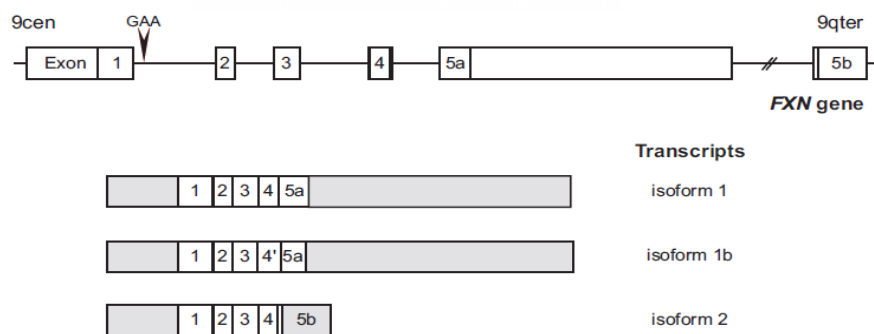


Fig.1.3 Structure of human FXN gene

The promoter region of the human FXN gene consists of 1,255 bp and bears different repetitive elements. They include L2 (LINE) and Alu (SINE) elements as well as Mammalian-wide Interspersed Repeats (MIRb) and mariner DNA transposons (Greene et al., 2007). In addition, in the first intron of the gene an E-box element that modulates the activity of the promoter is present, in fact, its deletion leads to a significant reduction in the detection of a reporter (Cossès et al., 2000). The regulation of human gene FXN is very little known, although it is known that the sequence E-box is able to bind transcription factors belonging to the family of proteins basic helix-loop-helix (bHLH). A protein that could bind to this sequence is the factor muscle-specific Mt, however its biological importance is not clear (Greene et al., 2007). Many reports have recently shown that the

expression of frataxin is regulated by iron. The addition of the iron chelator deferoxamine in the culture medium of fibroblasts and lymphoblasts of patients with FRDA leads to a reduction of the level of frataxin both as mRNA and protein amounts. Studies based on the use of promoter-luciferase constructs have shown that the iron acts as a transcriptional regulator, but the mechanism remains to be clarified (Li et al., 2008). Moreover, other authors have demonstrated that the murine gene FXN seems to be directly regulated by the transcription factor HIF-2 α (Hypoxia-Inducible Factor 2 α , encoded by the gene EPAS1). The levels of frataxin, both mRNA and protein, are reduced by 50% in the liver of Knock-out *Epas*^{-/-} mice compared to control. However, it is not known whether the human gene FXN is also regulated by HIF-2 α . (Oktay et al., 2007). Finally, two new regulatory factors influencing the frataxin expression, TFAP2 and SRF were identified. TFAP2 (activating enhancer binding protein AP2) is a developmentally-regulated, retinoic-acid inducible transcriptional activator, which directly binds to the promoter region of the FXN gene. Also, the expression of TFPAP2 is significantly down-regulated in HEK293 and SH-SY5Y cells in an iron-dependent manner, suggesting that iron may in turn alter the levels of FNX mRNA expression by FFAP2 regulation. SRF (c-fos serum response factor) is a ubiquitously expressed factor able to influence, in a cell-line specific way, the FXN mRNA levels (Li et al., 2010). Finally, low levels of FXN expression were also found in association with the depletion of PGC1a, the co-activator of peroxisome proliferator-activated receptor gamma 1-alpha (PPARGC1A) (Coppola et al. 2009; Marmolino et al. 2010).

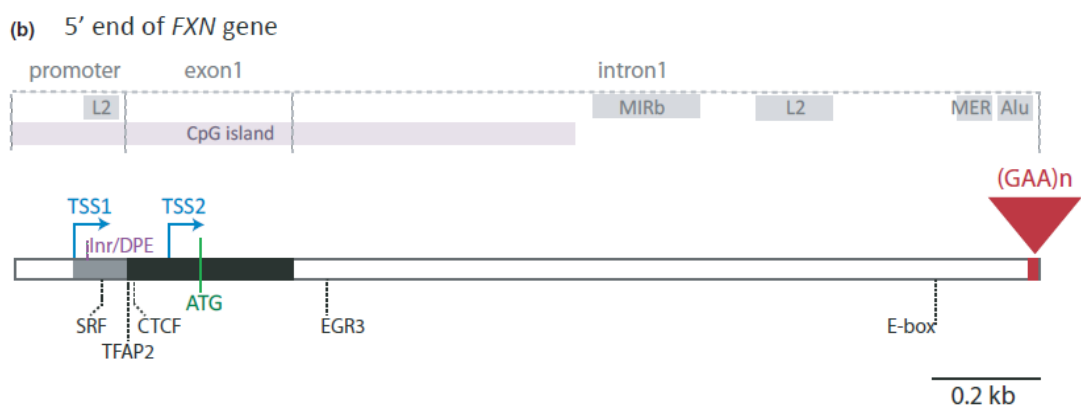


Fig.1.4. Regulatory component of human FXN gene.

Molecular Mechanisms

Most FRDA patients (about 96%) are homozygous for (GAA)_n trinucleotide repeat expansions and the remaining 4% of cases are compound heterozygous for a (GAA)_n expansion and point mutations in the coding region of the gene. The (GAA)_n repeats derive from an expansion of poly (A) sequence A5TACA6 placed in the center of the element AluSx, flanked by a repeat of 13 bp (AAAATGGATTTC) (Campuzano et al., 1996).

The expansion of (GAA)_n repeats arises from inter-generational instability in the germinal maternal line (oocyte) through expansion and/or contraction events, whereas the alleles transmitted by the father (sperm) undergo only contraction (Delatycky et al., 1998 and De Michele et al., 2000). Moreover, a trend of increase of (GAA)_n expansions has been demonstrated to occur via somatic mitosis. This instability is age-dependent, and is most common in certain individual cells, such as pseudo-unipolar neurons of the dorsal root ganglia (De Biase et al., 2007). It is suggested that errant DNA mismatch repair may be a common denominator amongst the array of alterations caused by DNA repeat expansion. Recently, it has been shown that MSH2, MSH3 and MSH6 enzymes of mismatch repair (MMR enzymes), are highly expressed in induced pluripotent stem cells (iPSCs) derived from FRDA patients cells compared with fibroblasts and neuronal stem cells (Ku et al., 2010 and Du et al., 2012). Moreover, in a cellular model of instability-related repeats, the knockdown of the mismatch repair proteins, MSH2 and MSH3 slows down the GAA•TTC expansion (Grabczyk et al., 2012). Expanded (GAA)_n repeats (67-1700 bp) were associated with decreased levels of FXN mRNA (4-29% of normal in FRDA, ~50% of normal in asymptomatic carriers). The length of (GAA)_n trinucleotide repeats correlates positively with the disease severity and correlates negatively with the age of onset. Several studies have described a relation between the size of the GAA repeat expansion and the presence and timing of several features of the disease. The GAA•TTC expansion in FXN does not alter the protein sequence. Although, the precise mechanism remains unclear, there is substantial evidence that the expanded (GAA)_n repeats do not affect the RNA splicing of the FXN gene but occur during the transcription process (Campuzano et al., 1996).

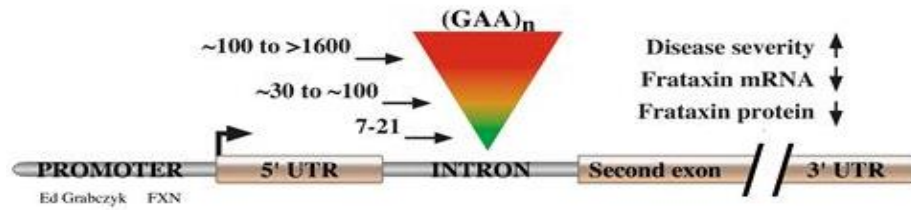


Fig.1.5. GAA repeat expansion in FXN gene (Graczyk)

Currently it has been proposed that the mechanism responsible for the silencing of the gene FXN can be attributed to two models; 1) formation of non-B-DNA structure and 2) formation of hybrid DNA-RNA non coding (Figure 1.6.) duplexes. In both cases, heterochromatin formation occurs (Figure 1.7).

These secondary structures include purine:purine:pyrimidine and pyrimidine:purine:pyrimidine triplexes, which may down regulate FXN expression through a physical blockage effect on transcription by making it more difficult for the transcription RNAPII complex to unwind the DNA template and move forward (Sakamoto et al., 2001). In addition, triplex structures known as “sticky DNA” are formed by unusual hydrogen bonds between G•G, G•A or A•A. (Kumari and Usdin 2012). Furthermore, triplex structures formed by (GAA)_n repeats allow the formation of stable RNA•DNA hybrids (R-loops) during the transcription (LeProust et al. 2000). Triplex structures inhabited by expanded (GAA)_n repeats were shown to be recognized by the DNA repair machinery in various models including hiPSCs derived from FRDA patients (Ku et al. 2010 and Du et al. 2012).

In addition to these alternative structures of DNA characteristic of the FXN gene, the repeated sequences of triplets can induce a packaging of the genomic regions involved in inaccessible heterochromatin, further contributing to FXN genic silencing.

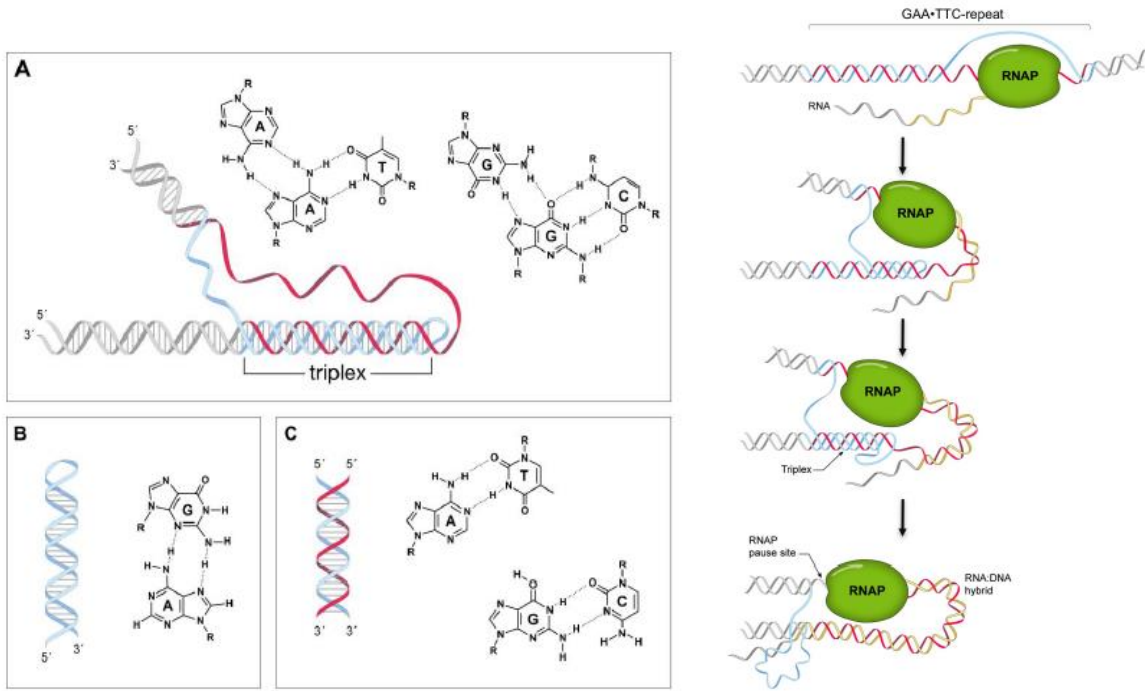


Fig. 1.6 Examples of different structures formed by GAA•TTC repeats

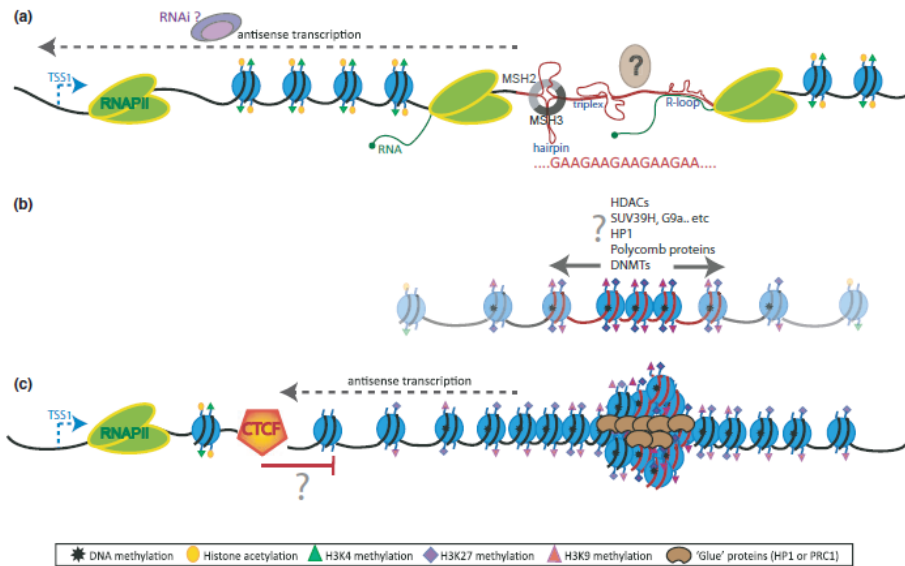


Fig.1.7 A hypothetical model for the heterochromatinization of FXN gene

1.4 Epigenetic Mechanisms in Friedreich's Ataxia

There are different neurological disorders caused by triplet expansions such as myotonic dystrophy, spinal muscular atrophy, and fragile X syndrome, in which epigenetic modifications play a pivotal role in the pathogenesis of these diseases. Numerous studies have confirmed that the silencing of FXN gene mediated by (GAA)_n repeats expansions is originated by epigenetic changes, as the direct methylation of DNA, histone modifications and alternative mechanism of transcription in antisense direction. FXN gene contains a CpG island covering the promotor, the first exon and the beginning of the first intron. Bisulfite mapping demonstrates that the regions adjacent to the repeats in intron 1 of FXN gene are methylated in both unaffected and affected individuals. However, an increase in the number of methylated residues has been reported in FRDA cells (Green et al., 2007). Also, autopsy of patients arise the elevated levels of CpG methylation upstream of (GAA)_n (Al-Mahdawi et al., 2008). Moreover, elevated levels of CpG methylation upstream of (GAA)_n have been observed in autoptic tissues from FRDA patients (Mahdaw et al., 2008). Finally, two large scale studies on peripheral blood mononuclear cells also confirmed that higher degree of DNA methylation was proportional to the length of (GAA)_n and positively correlated to FXN gene silencing and to disease severity (Castaldo et al., 2008). In addition, the acetylation status of histones and other proteins involved in transcription regulation is crucial for the regulation of gene expression. Heterochromatin is characterized by histone hypoacetylation, histone H3 lysine 9 and lysine 27 methylation, and the association of histone deacetylase enzymes, specific histone methyltransferases and heterochromatin proteins such as members of the Heterochromatin Protein (HP1 family) and Polycomb group proteins. The first report in support of an epigenetic silencing mechanism in FRDA came from Festenstein and colleagues (2006), who showed that a transgene containing GAA•TTC repeats was silenced in vivo, in a manner reminiscent of the position-effect variegated gene silencing. In this study, repeat-induced silencing was augmented by over-expression of the heterochromatin protein HP1, and the silenced transgene was packaged into condensed chromatin, as evidenced by resistance to nuclease digestion (Saveliev et al. 2003). In addition, it has been shown that the alleles of FRDA patients are enriched with a variety of histone modifications characteristic of silenced genes, including hypoacetylated H3 and H4 and dimethylation and trimethylation of histone H3 lysine 9 (H3K9). Herman and co-workers (2006) have shown for the first time that H3K9 methylation, which is typical of heterochromatin, is present at the *FXN* locus in primary lymphocytes and in lymphoblastoid cell lines from individuals with Friedreich's ataxia. Furthermore, they have shown that it is possible to reverse the aberrant

silencing of *FXN* using a new HDAC inhibitor. A similar pattern of epigenetic changes has also been found in the affected tissues (brain and heart) from mouse models of the disease and in Friedreich's ataxia autopsy-derived brain, cerebellum, and heart (Al-Mahdawi et al. 2008 and Rai et al. 2008). Results obtained from ChIP data reporting the histone modifications on the *FXN* locus have confirmed high levels of heterochromatin marks in the first intron of the *FXN* gene (Saveliev et al., 2003). Furthermore, ChIP DNA analysis using primers specific to the (GAA)_n has revealed that the classical heterochromatin marks histone H3 lysine 9 dimethylation (H3K9me₂), histone H3 lysine 9 tri-methylation (H3K9me₃) and histone H3 lysine 27 tri-methylation (H3K27me₃) are enriched particularly in the immediate flanking regions of expanded (GAA)_n repeats, whereas acetylation marks were reduced (Green et al., 2007, Al-Mahdawi et al., 2008, Castaldo et al., 2008 and Soragni et al., 2008). This suggests that heterochromatin is bidirectionally spreading from the expanded (GAA)_n tract within the *FXN* locus (Chan et al., 2013). Important is also the discovery by De Biase and co-workers of a CTCF binding site 154bp downstream of TSS1 within the 5'UTR of the *FXN* gene. CTCF (a zinc finger protein) is a chromatin insulator protein known to prevent the spreading of heterochromatin, that results to be depleted in FRDA patient fibroblasts; its depletion is associated with increased antisense transcription (De Biase et al. 2009). Finally, *FXN* silencing may be due to a mechanism of reverse transcription via the activity of the RNA-interference complex. An *FXN* antisense transcript called "FXN antisense transcript 1" (FAST1) has been identified, which seems to be produced at higher levels in the fibroblasts derived from FRDA patients.

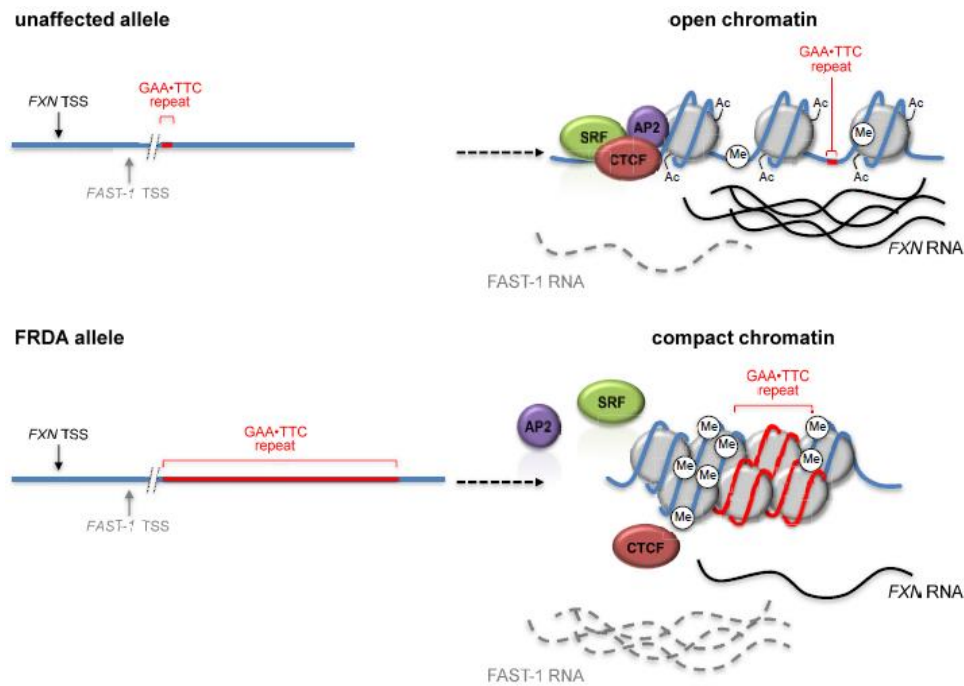


Fig.1.8. A epigenetic model for FRDA

1.5 Structure and Function of the Frataxin Protein

Structure of frataxin

Frataxin is a small acidic protein (with isoelectric point around pH 4.9). It is highly conserved in most organisms from bacteria to mammals (Gibson et al. 1996 and Adinolfi et al. 2002). A frataxin homolog was also identified in the human parasite *Trichomonas vaginalis* (Dolezal et al. 2007). Due to its small size, it was possible to solve the structure of frataxin by Nuclear Magnetic Resonance analysis (NMR). The structure of the human frataxin was determined both in solution and in crystalline form (Musco et al., 2000 and Dhe Paganon 2000) as well as that of its homologues CyaY in *E. coli* (Noir et al., 2004 and Cho 2000) and Yfh1 in the yeast *Saccharomyces cerevisiae* (He et al., 2004 and Kalberg et al., 2006). Frataxin is characterized by a flat β -sheet platform supported by two parallel α -helices at N and C terminus. Frataxin protein contains two structural elements that are conserved in all frataxin orthologs: (i) the presence of acidic residues in the first α -helix (α -1) and β -strand (β -1) which form a negatively charged surface; (ii) a neutral flat area on the β -sheet surface that probably allows the interaction of protein partners on frataxin (Sirano et al., 2000).

An N-terminal block of 81–92 residues, completely absent in prokaryotes and poorly conserved among eukaryotes, is unfolded and highly flexible (Huynen et al., 2001). The conserved C-terminal

domain fold in a mixed $\alpha\beta$ structure that consists of two helices packing against a contiguous anti-parallel beta-sheet assembled in the sequence alpha-(beta) 5-7-alpha of the protein and comprises a highly conserved block of ca. 100–120 amino-acids. Frataxin is a nuclearly encoded protein, expressed in the cytoplasm and imported in the mitochondrion through an import signal (mitochondrial targeting sequence; MTS) contained in the N-terminus. The MTS sequence is removed by proteolytic cleavage in two steps, to produce the mature protein (Branda et al., 1999 and Cavadini et al., 2000). The maturation of human frataxin, as well as that of yeast, depends on the MPPs (mitochondrial processing peptidases). Using an YTH (yeast two-hybrid) assay, it was shown that the N-terminus of murine frataxin interacts with the β subunit of the MPP (Koutnikova et al., 1998). These enzymes cut the first precursor of frataxin to produce an intermediate form, which will then be converted into the mature frataxin.

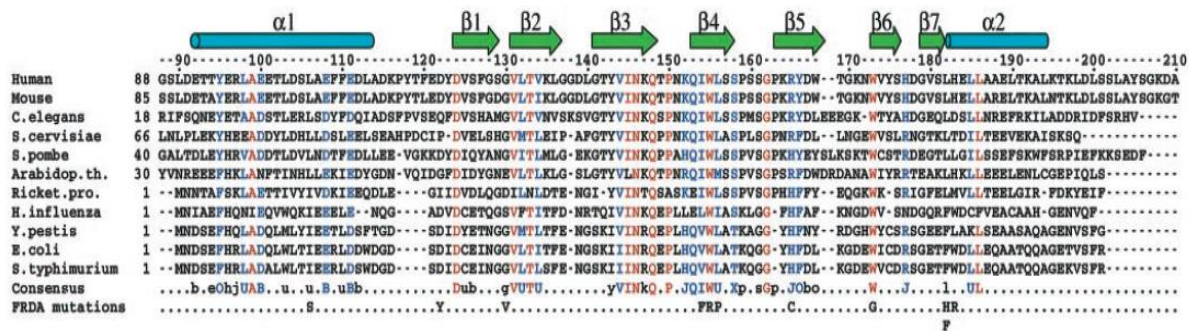


Fig1.9. Structure-based sequence alignment of human frataxin with homologues from prokaryotes and other eukaryotes

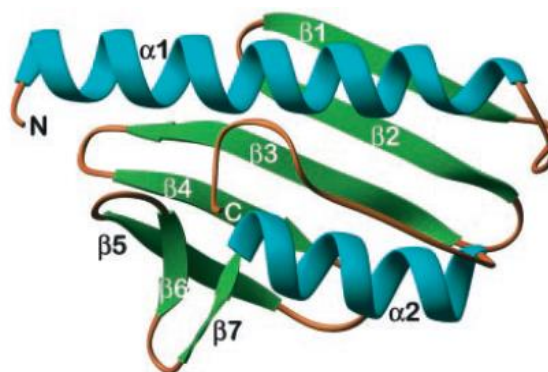


Fig.1.10 Structure of frataxin

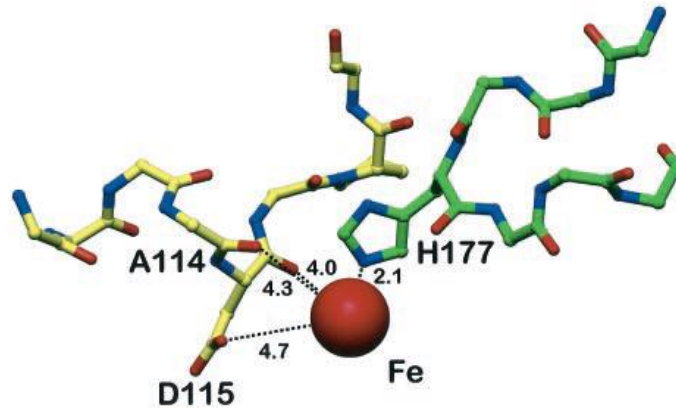


Fig.1.11. Iron binding of frataxin

In yeast frataxin ortholog Yfh1, the first mitochondrial processing peptidase (MPP) cleavage site lies between residues Y20 and M21 (RRY ↓ MIA), while the second cut is made between residues F51 and V52 (KRF ↓ ESR). Detailed analysis of the two sequences, residues 1-20 (domain I) and 21-51 (Domain II), have established that the domain I is the matrix- targeting signal (MTS). Furthermore, it was observed that in the absence of domain II, the MTS is unable to mediate transport of frataxin in mitochondria (Gordon et al., 2001). Maturation of pre-Yfh1 protein requires also the sequential action of Ssc1 and Ssq1, mitochondrial chaperones members of the Hsp70 family (Knight et al., 1998 and Voisine et al., 2000). Finally, Tim4 plays a pivotal role in importing into the mitochondrial inner membrane and is required for the binding of Ssc1 to Yfh1 (Geissler 2000).

Human frataxin is synthesized as a precursor of 210 amino acids imported to the mitochondrion, and undergoes maturation by the MMP through a two-step process that leads to the successive generation of an intermediate form of 19 kDa cleaved between G41 and L42 (residues 42-210) and a mature form of 14 kDa (residues 81-210) (Koutnikova et al. 1998; Condò et al. 2007 and Schmucker et al. 2008). Another form starting at S56 was also reported (Cavadini et al., 2000), but it is now widely accepted that the 81-210 form is the most abundant species, both in normal individuals and in FRDA patients (Condò et al. 2007; Schmucker et al. 2008; Gakh et al. 2010).

Function of Frataxin

Frataxins are essential proteins whose deficiency causes a range of metabolic disturbances such as oxidative stress, deficit of iron-sulphur clusters, and defects in heme synthesis, energy metabolism, stress responses, and mitochondrial dysfunction. Numerous studies, also confirmed the role of frataxin in physiological and pathological processes such as embryonic development, cellular differentiation, cancer and regulation of antioxidant defense (Santos et al., 2009). Although, the precise function of frataxin remains to this day unknown, it is clear that frataxin is involved in the cellular iron homeostasis. The first hypothesis about the role of frataxin derives from studies in yeast (*S cerevisiae*), in which it was observed that deletion of frataxin ortholog ($\Delta yfh1$) gene results in a reduced cellular respiration, high sensitivity to hydrogen peroxide and copper, low levels of cytosolic iron and a constitutive activation of the system of iron transport in the plasma membrane. Also, in the yeast $\Delta yfh1$ mutant, deletion of frataxin homolog 1 (YFH1) produces a 10-fold increase in mitochondrial iron and increased sensitivity to oxidants (Babcock et al., 1997 and Foury et al., 1997) These data suggested a role of frataxin in mitochondrial iron homeostasis, and a role of frataxin as a mitochondrial iron chaperon was proposed. Iron is a well-known catalyst of free radicals, and excess iron in mitochondria most probably explains the increased sensitivity to hydrogen peroxide and oxidative stress. Subsequent works with mice completely deficient in frataxin demonstrated cardiac degeneration and iron accumulation (Cosseè et al., 2000). Further, in human FRDA patients, excess iron is observed in hearts, liver, pancreas and neural tissue (Bradley et al., 2000 and Lamarche 1980). Indeed, it was suggest that the iron accumulated in mitochondria of FRDA patients causes their hypersensitivity to oxidative stress, as a consequence of Fenton Reaction (Fe^{2+} catalysed production of hydroxyl radicals). A second hypothesis for frataxin function is its role in the biogenesis of iron–sulfur clusters (ISCs) (Foury et al., 1999). It was shown that yeast carrying the YFH1 mutation was deficient in multiple ISC-dependent enzyme activities. ISCs are complexes of iron and sulphur atoms that serve as prosthetic groups for a series of enzymes with different functions, including energy metabolism (i.e. aconitase; complexes I, II, and III of the respiratory chain), iron metabolism (i.e. iron responsive protein I and ferrochelatase), purine synthesis, and DNA repair. ISC containing enzymes are localized in various cellular compartments, including mitochondria, cytosol, and nucleus. Rotig and co-workers (1997) found selective deficiencies of respiratory chain complexes I, II and III and a reduction of the cytosolic and mitochondrial aconitase activities in heart biopsies of FRDA patients. All the deficient enzymes and the complexes containing iron sulfur (Fe –S) clusters in their active sites are particularly

sensitive to free radicals. Deficiency restricted to Fe-S proteins has not been found in 60 biopsies of patients with cardiomyopathy, indicating that this inactivation is associated specifically with depletion of frataxin. Another hypothesis on the function of frataxin proposed by Isaya and collaborators (2004), is that frataxin could be a binding protein that stores iron in a bioavailable and non-toxic form for the synthesis of the clusters Fe -S and heme groups. Furthermore, studies performed in cultured cells from patients with FRDA have confirmed that frataxin deficiency causes anomalies in sulphur amino acids, energy metabolism and mitochondrial function (Tan et al., 2003). Also, the absence of frataxin in yeast also leads to DNA damage, as evidenced by increased nuclear and mitochondrial DNA damage, increased chromosomal instability including recombination and mutation, and greater sensitivity to DNA-damaging agents. Excess iron in the presence of oxygen also can generate superoxide and hydroxyl radicals, both of which are ROS. High ROS levels could cause damage to nuclear and mitochondrial DNA which are both radical-sensitive. (Karthikeyan et al., 2002). Frataxin was also reported to be necessary for the embryonic development and differentiation in different model organism. In the plant *Arabidopsis thaliana*, frataxin knock-out results in early embryonic lethality (Vazzola et al., 2007). Mutant *atfh-1* plants with less than 50% of normal frataxin levels show retarded growth, without any morphological abnormalities in roots, leaves and flowers, and impaired fructification. Total deletion of the frataxin gene in the mouse resulted in embryonic lethality (Cosseè et al., 2000). Several studies suggest that frataxin has the role as tumor suppressor by increasing cellular oxidative metabolism and apoptotic Bax-dependent and p53-independent pathway (Schulz et al., 2006).

Finally, it has been proposed that frataxin is involved in controlling oxidative stress by reducing the production of reactive oxygen species (ROS): Such a role could be linked easily with either the chaperone or the ferritin-like hypothesis, or with both. According to a ferritin-like model, the protein could first bind to Fe^{2+} , transform it into Fe^{3+} through ferroxidase chemistry, and retain the bound metal in a bioavailable form (Park et al., 2003). Frataxin deficient cells have increased intracellular ROS levels and decreased antioxidant defenses. The exact sequence of events that occur in FRDA cells has not been clarified yet. Paupe and colleagues (2009) have shown that the Nrf2-dependent Phase II antioxidant pathway is defective in frataxin-deficient fibroblasts. Under normal conditions, the activity of the transcription factor Nrf2 is regulated by the actin-associated Keap1 protein, which sequesters Nrf2 in the cytoplasm and promotes its degradation via ubiquitination. Under conditions of stress, this interaction is disrupted and Nrf2 is translocated into the nucleus, where it binds to DNA sequences of the *cis*-acting ARE (antioxidant responsive

element), activating the expression of Phase II antioxidant genes, including SODs, catalase, glutathione S-transferase and NADH quinone oxidoreductase.

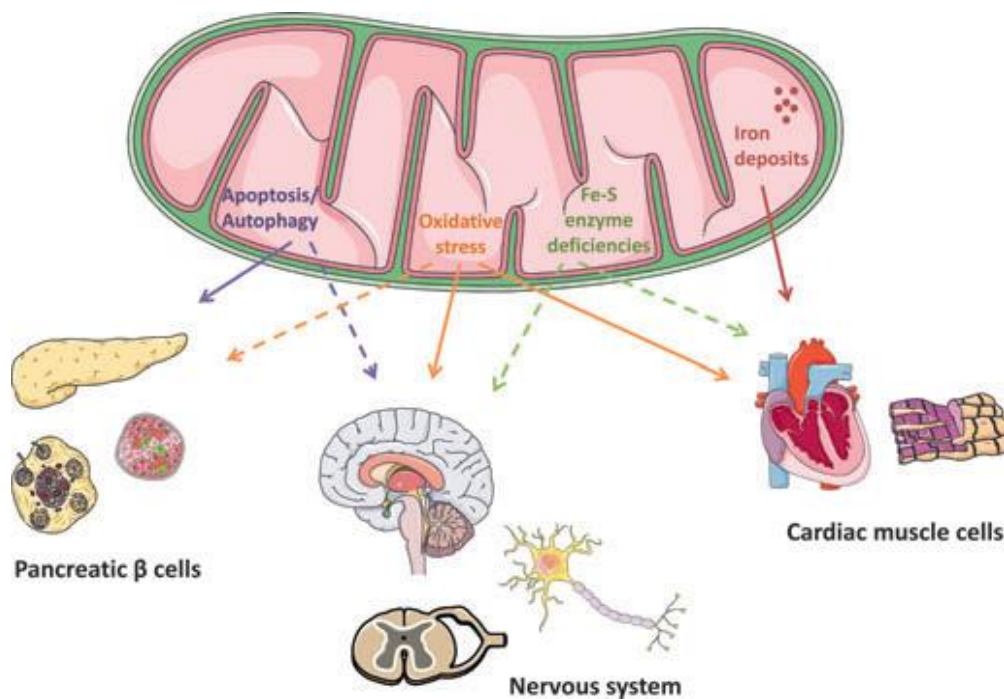


Fig.1.12 Schematic representation of the biological pathways altered in Friedreich's ataxia (FRDA) as consequences of frataxin deficiency in mitochondria.

1.6 Pharmacological Treatments and Therapeutic Strategies for Friedreich's Ataxia

No approved cure is currently available to FRDA patients. Therapeutic strategies are based on the use of anti-oxidants or iron chelators, with controversial results. Other strategies are in earlier clinical phases or pre-clinical stage. Ongoing clinical trials are illustrated (Figure 1.17).

Antioxidant molecules

Based on the studies that frataxin deficient cells are more sensitive to oxidative stress, different molecules with antioxidant activities were evaluated as potential therapeutic agents in FRDA.

Among these molecules, CoQ10 (coenzyme Q10), idebenone and mitochinone (MitoQ) (respectively, an analogue and a derivative of CoQ10) and vitamin E have been extensively tested in FRDA. Co-enzyme Q10 (2,3-dimethoxy-5-methyl-6-decaprenyl benzoquinone or ubiquinone) is a small lipophilic molecule present within the inner mitochondrial membrane in association with the electron transporter chain (ETC) complexes, which transfers electrons between complexes I and II, and from oxidation of fatty acids and branched chain amino acids to complex III resulting in the ultimate production of ATP. Structurally, it has a benzoquinone nucleus which is readily reduced to ubisemiquinone and ultimately to ubiquinol, as well as a 10-unit polyisoprenoid side chain conferring hydrophobicity (Orsucci et al. 2011; Hargreaves 2003; Lenaz et al. 2007). Because of its facility at undergoing redox reactions, coenzyme Q10 acts as a potent antioxidant preventing oxidation of proteins, lipids, lipoproteins and DNA, and maintaining other antioxidants such as ascorbic acid and vitamin E. It is the only endogenously synthesized lipid-soluble antioxidant. It also contributes to preventing the opening of the mitochondrial membrane transition pore which permits passage of enzymes and other molecules which can contribute to the depolarization of the mitochondrial membrane potential as the DNA fragmentation and apoptotic events. Co-enzyme Q10 may also have anti-inflammatory and anti-atherosclerotic properties (Bentinger et al. 2010). Clinical trials of co-enzyme Q10 were initiated treating 10 FRDA patients with 400 mg/day co-enzyme Q10 and 2100 IU/day vitamin E for 6 months (Lodi et al. 2001). However, in this study no significant change was found in ICARS and in the echocardiography parameters. Likewise to Co-enzyme Q10, the idebenone (2,3-dimethoxy-5-methyl-6-(10-hydroxydecyl)-1,4-benzoquinone) can act as an electron carrier within the electron transporter chain (ETC) (Suno and Nagaoka 1984). Results derived from a first preliminary study have demonstrated an improvement of cardiac function with variable neurological results secondary (Mariotti et al., 2002). Currently, FRDA patients regularly take idebenone, an analogue of coenzyme Q10, which exerts its beneficial effects by ameliorating cardiac and cerebellum function and modulating oxidative stress (Meier et al., 2009 and Santos et al., 2010). Nevertheless, a recent research has shown that in a 6-month randomized, double-blind, controlled study, idebenone did not improve cardiac or neurological function (Lynch et al., 2010 and Lagedrost et al., 2011). For this reason, researchers are focused on development a new molecules with higher antioxidant, neuroprotective, and cardioprotective proprieties

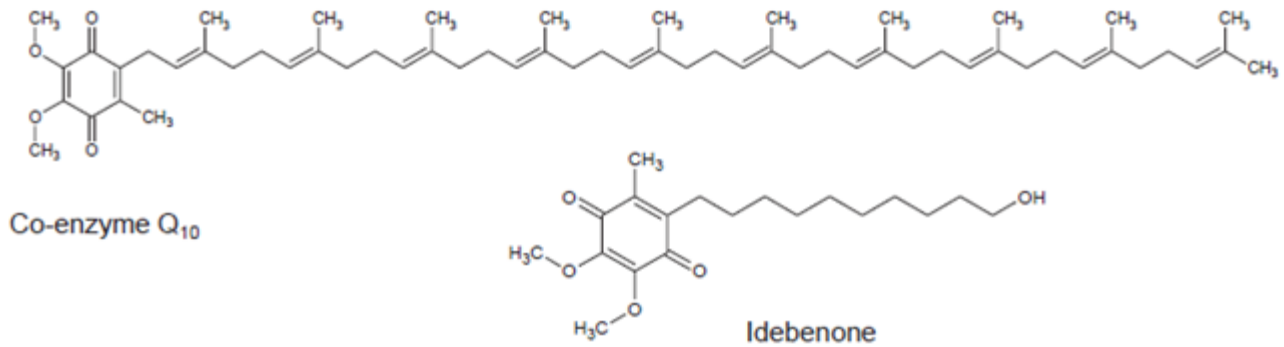


Fig.1.13 Chemical structure of Co-Enzyme Q10 and Idebenone

Further molecule which has antioxidant activity and can be considered as a possible therapeutic approach for the FRDA is Vitamin E. The term Vitamin E is the generic name used to denote a family of lipidic-soluble antioxidants, which includes two classes of compounds:

- tocopherols (α , β , γ and δ);
- tocotrienols (α , β , γ and δ).

Vitamin E is present to various extents in most edible oils, including those extracted from wheat germ oil, wheat, rice, bran, barley, oats, coconut and palm. (<http://www.tocotrienol.org>). (Aggarwal et al., 2010). Tocopherols consist of a chromanol ring and a 15-carbon tail. The presence of three trans double bonds in the tail distinguishes tocopherols from tocotrienols. The isomeric forms of tocotrienol are distinguished by the number and location of methyl groups on the chromanol rings: α -tocotrienol is 5, 7, 8-trimethyl; β -tocotrienol is 5,8-dimethyl; γ -tocotrienol is 7,8-dimethyl and δ -tocotrienol is 8-monomethyl. (Sen et al., 2007)

Vitamin E acts as an antioxidant "chain breaker" able to prevent the propagation of radical reactions. Various studies indicate that tocotrienols exhibit antioxidant, antiproliferative, antisurvival, proapoptotic, antiangiogenic, and anti-inflammatory activities. The antioxidant properties of tocotrienols are mediated through induction of antioxidant enzymes such as superoxide dismutase, NADPH, quinone oxidoreductase and glutathione peroxidase. (Lee et al., 2009). Tocotrienols also have cardioprotective effects due to their antioxidant mechanisms and their ability to suppress inflammation, inhibit HMG-CoA reductase, a rate-limiting enzyme in cholesterol biosynthesis (Pearce et al., 1992 and Parker et al., 1993), and reduce the expression of adhesion molecules and monocyte–endothelial cell adhesion (Therriault et al., 2001). Tocopherols

and tocotrienols are essential for neurological function. Deficiency of this vitamin is now known to cause severe degenerative diseases such as Ataxia, Duchenne muscular dystrophy-like muscle degeneration (Aggarwal et al., 2010). Recent results have documented the neuroprotective potential of tocotrienols. Also, Anderson and colleagues (2003) have shown that tocotrienol is able to regulate directly the expression of IKBKAP whose alteration is responsible for a neurodegenerative disease, familial dysautonomia

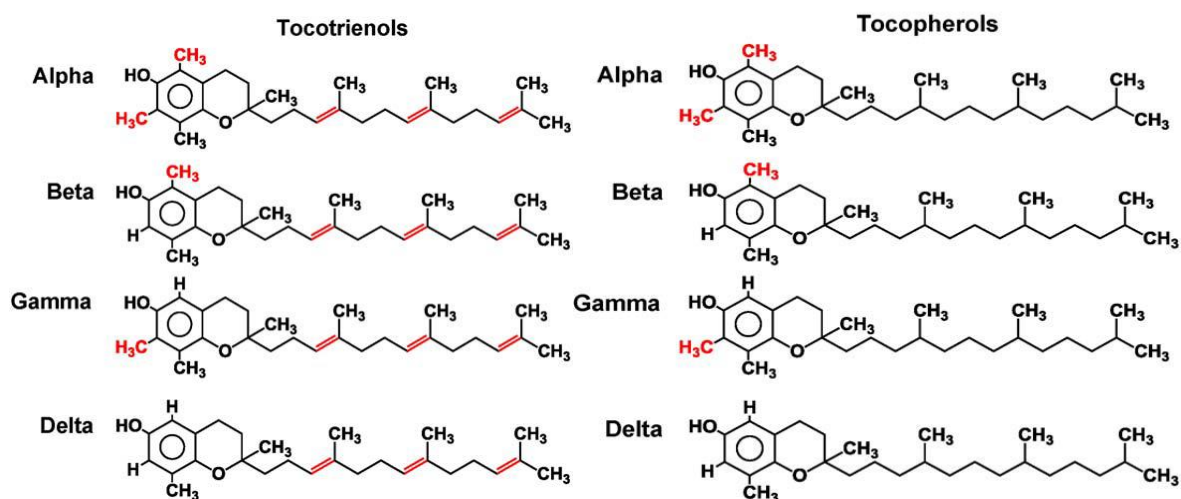


Fig.1.14 Chemical structure of tocotrienols and tocopherols.

Finally, analogues of CoQ10 have also been developed: one of these, called MitoQ, protects the fibroblasts of patients from oxidative stress with endogenous high efficiency (Jauslin et al., 2003) while the α -tocopherol-quinone EPI-A0001, seems lead an improvement in the neurological function assessed by FARS scale in the preclinical phase II studies.

Iron Chelators

The use of iron chelators in FRDA was first proposed as mean to eliminate the excess iron accumulating in mitochondria, thus decreasing free radical generation through the Fenton reaction.

The possible role of iron chelation in the treatment of FRDA and other neurological diseases is still largely debated in literature (Richardson et al., 2001 and Kalinowsky et al., 2005). MRI studies in FRDA have shown that iron accumulates typically in the heart, in the dentate nucleus of the cerebellum while the plasma levels of iron, ferritin, and heme are generally maintained to normal levels (Waldvogel et al., 1999). Currently, the research is aimed at designating a molecule orally active and permeable to membranes, able to chelate specific areas of the brain without reducing the bioavailability of iron essential to heme biosynthesis. Deferiprone, an orally administered, lipidsoluble iron chelator used in several countries as an alternative to desferoxamine to treat iron overload in polytransfused individuals with hemoglobinopathies, can easily cross the blood–brain barrier and cellular membrane. Results derived from studies in various cells type, have shown that the deferiprone is able to act as a siderophore and to chelate the labile iron that is present in both cytosolic and mitochondrial compartments and redistribute it between all cellular compartments. (Sohn et al., 2008). In a pilot, open label study, the administration of deferiprone (20-30 mg/kg/day for 6 months) in eight of the 13 young patients FRDA enrolled, was able to reduce the iron deposits at the level of the dentate nucleus, after only two months of treatment (Boddaert et al., 2007). However, the variegated appearance of adverse reactions observed in four patients, has imposed a careful and constant monitoring of hematological and biochemical parameters. In conclusion, the chelation of mitochondrial iron may be beneficial at an early stage of the disease, but more studies are necessary to monitor, in order to avoid undesirable effects. To overcome these serious side effects a valid alternative is the chelator Fe aroilidrazone (PCTH), resulting from another family of chemical molecules (compounds PCIH) which in vitro do not show the same systemic toxicity of deferiprone, while presenting the same ability to chelate the iron (Lim et al., 2008).

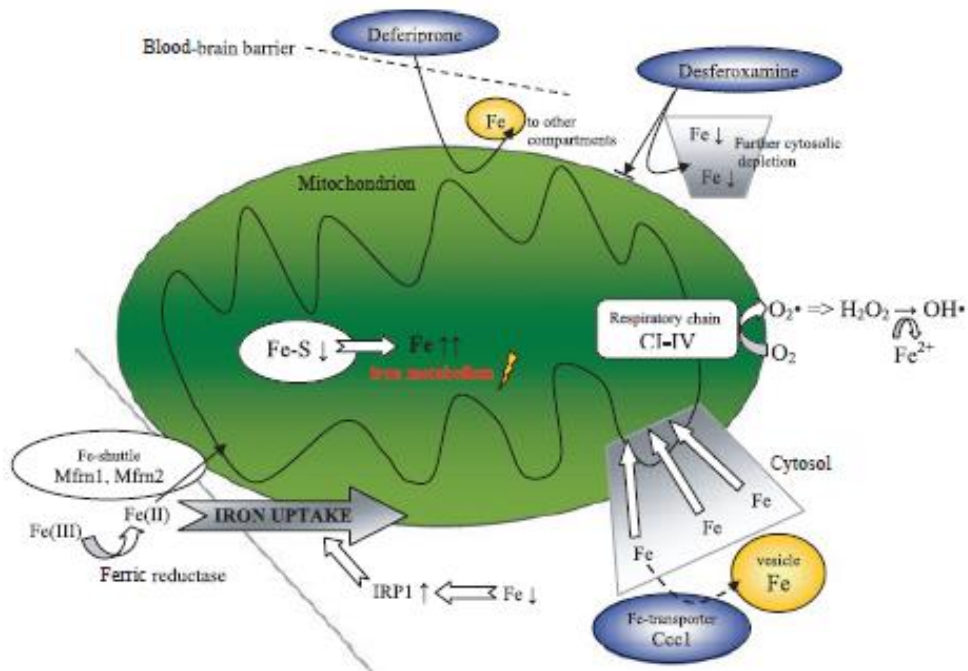


Fig.1.15 Mechanism of action Deferiprone

Histone inhibitors deacetylase (HDACi)

Histone deacetylase inhibitors (HDACi) are a new class of molecules which have been proposed for their ability to restore the frataxin expression and represent an innovative approach in the treatment of FRDA. Indeed, in FRDA the (GAA)_n repeats seem to predispose the FXN gene to a series of epigenetic modifications that cause its silencing which appear to be caused by epigenetic modifications. For this reason, it has been suggested that the use of HDACi may be able to correct the epigenetic changes. Eighteen histone deacetylase enzymes have been identified in the human genome, including the zinc-dependent (class I, class II, and class IV) and the NAD⁺-dependent enzymes (class III or Sirtuins) (Gottesfeld 2013). Numerous studies have shown that small molecule inhibitors of the histone deacetylase (HDAC) enzymes are able to revert silent heterochromatin to an active chromatin conformation, and restore the normal function of genes that are silenced in various human diseases, including neurodegenerative and neuromotor diseases (Di Prospero et al., and Fischbeck et al., 2005). The efficacy of 2-aminobenzamide HDAC inhibitors 106, has been tested in two mouse models for FRDA (Rai et al. 2008, 2010 and Sandi et al. 2011), in which it was proved able to correct the deficiency of frataxin both at transcriptional and post-transcriptional levels, by increasing histone H3 and H4 acetylation near the GAA•TTC repeat. This study also

showed that the elevation of frataxin mRNA and protein was sustained, persisting 48 h after drug exposure in the case of the protein. There was no effect in "wild type" animals, thus indicating that the effect of this compound is due to removal of inhibition due to the expansion GAA (Rai et al. 2010).

Recently a HDAC, 109/RG2833, has completed a Phase 1 clinical trial in FRDA patients. Results derived from this study have shown that the treatment was well tolerated and there was an increase in frataxin mRNA. These results are significant in that they provide proof of principle that an HDAC inhibitor delivered orally (in a pill) can increase frataxin gene expression measured in blood from subjects (Gottesfeld 2013). An alternative therapeutic approach provides the use of polyamides. Polyamides are polymers which contain repeating amide, -CO-NH- linkages, able to interact with the unusual non B-DNA structures such a "sticky" or double/triples helix structure of DNA derived from the repeated sequences (GAA)_n. It has been shown that Beta-alanine-linked pyrrole-imidazole polyamides bind GAA.TTC tracts with high affinity and disrupt the intramolecular DNA:DNA-associated region of the sticky-DNA conformation formed by long GAA.TTC repeats and restore the transcriptional repression of FXN gene (Burnett et al., 2006). Furthermore, Du and co-workers (2012) have demonstrated that the specific polyamide (FA1) is able to block the (GAA)_n expansion by displacing MSH2 from *FXN* intron 1 in FRDA human induced pluripotent stem cells (iPSCs) derived from FRDA patients.

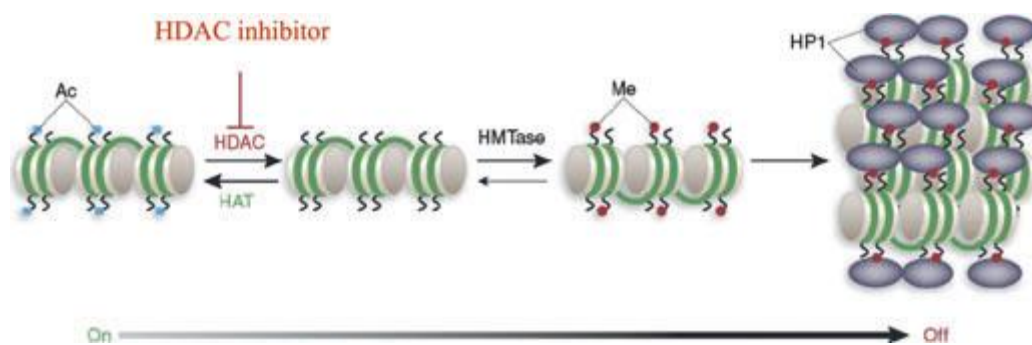


Fig.1.16 Putative silencing pathway in Friedreich's ataxia.

Recombinant human erythropoietin (rHuEPO) and Carbamylated erythropoietin (CEPO)

Among the various therapeutic perspectives that are being considered, there are substances that subvert gene silencing and restore the synthesis of frataxin. An interesting therapeutic candidate in the treatment of FRDA is the recombinant human erythropoietin (rHuEPO). Erythropoietin (EPO) is a 30 400-Dalton glycoprotein that was initially recognized as a regulator of red cell production. EPO acts as a protective multifunctional protective molecule and exercises neuroprotective and cardioprotective effects (Sakanaka et al., 1998). Furthermore, EPO may attenuate the production of radical oxygen species (ROS) or glutamate-stimulated excitotoxicity (Calapai et al. 2000 and Kawakami et al. 2001). rHuEPO is a 165 amino acid glycoprotein manufactured by recombinant DNA technology with the same biological activities as endogenous erythropoietin and able to cross the blood–brain barrier (Brines et al.,2000). It was discovered that the rHuEPO increases frataxin expression in lymphocytes derived from FRDA patients and in primary cultures of human cardiomyocytes obtained from donor hearts (Sturm et al., 2005). Furthermore, in a fibroblast cell line from FRDA patients, rHuEPO, increases the levels of frataxin protein in the absence of observed changes in the expression of mRNA frataxin (Acquaviva et al., 2008). These results suggest a post-transcriptional regulation of frataxin by rHuEPO. Moreover, encouraging results have been obtained from a pilot clinical trial in which a reduction in urinary markers of oxidative stress such as the 8-oxo-7-hydrodeoxyguanosine (8-oxodG) and peroxides in serum after administration of 5000 IU rHuEPO for eight weeks, three times a week was observed. The average increase in frataxin observed in this trial was 27%, with a high range of variability from 15% to 63%. Despite the commercial availability of rHuEPO as a drug with proven safety, these preliminary results should be interpreted with caution, as longer trials with a higher number of patients will be conducted where the presence of significant endpoints (Boesch et al., 2007) will be examined. Finally, a chemically modified EPO called Carbamylated erythropoietin (CEPO) was shown to stimulate the synthesis of frataxin in the lymphocytes from FRDA patients. However, a sponsored randomized controlled trial to evaluate secondary endpoints of the CEPO showed no positive results (Lundebeck.com).

Interferon gamma (IFN γ)

Recently, Tomassini and co-workers (2012) have demonstrated that interferon gamma (IFN γ) can up-regulate the frataxin expression in different cell types, including primary cells derived from FRDA patients. Furthermore, in vivo IFN γ treatment is able to prevent the degeneration of DGR neurons of FRDA mice. The beneficial effects of IFN γ could be attributed to its ability to regulate the iron distribution by directly modulating the important targets of iron homeostasis as ferritin, the transferrin receptor (Byrd et al., 1993), the iron exporter ferroportin, its peptide ligand hepcidin IRP1 and the iron symporter NRAMP1 (Feelders et al., 1998 and Kim et al., 2000).

Gene Therapy

Fusion proteins containing the transactivator of transcription TAT, a small peptide derived from the human immunodeficiency virus are able to effectively deliver proteins across cell membranes and intracellularly (Del Gaizo et al., 2003). Recently, Piyush and colleagues (2011) have shown that a TAT frataxin fusion protein is correctly processed in FRDA fibroblasts and is able to bind the iron in free cell systems and rescue the frataxin expression by the control of “iron-oxidative” stress. The same study has also demonstrated that the injection of TAT–FXN protein into mice with a conditional loss of FXN increased their lifespan and cardiac function. Finally, the gene therapy through the viral vector HSV1 is still at the stage of preclinical research but can represent a curative treatment of the FRDA as well as for all diseases in which the alteration is found at the level of a gene (Gomez-Sebastian et al., 2007).

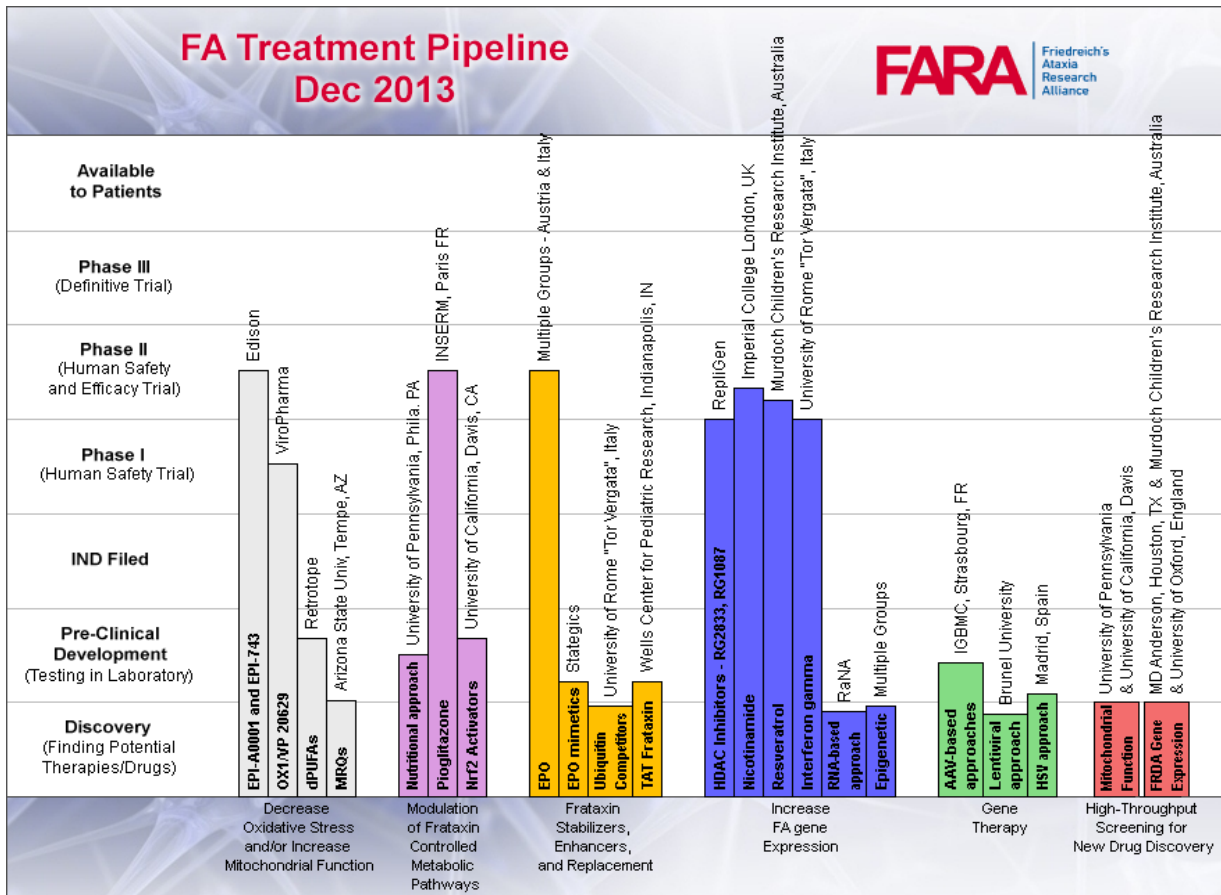


Fig.1.17 A schematic representation of the drugs research status in FRDA

Chapter II

Oxidative Stress

2.1 Radical Oxygen Species (ROS)

Oxygen is a molecule essential for the survival of aerobic organisms, however because of its atomic structure that does not allow him to accept electron pairs can generate highly unstable intermediates known as reactive oxygen species (ROS) (Figure 2.1) (Gutteridge et al., 2000). These species are the result of successive reductions until the complete reduction of oxygen to H₂O and can be divided into two categories; oxygen free radicals (i.e. superoxide anion (O₂⁻) and hydroxyl radical (OH[•]) containing an unpaired electron and the non- radical species (i.e. H₂O₂).

Superoxide anion

The superoxide anion is the first free radical that is formed as an intermediate during the biochemical reactions of oxygen reduction. It has a negative charge and unlike other free radicals, has a relatively long half-life and is able to attack a large number of substrates to complete its orbital. The superoxide anion can be formed through different reactions: by interaction of O₂ with electrons sometimes leak the respiratory chain when it runs at high speeds, especially in the transition between the redox coenzyme Q, and cytochromes, during metal-dependent oxidation of molecules such adrenaline, noradrenaline or even some thiol compounds, or during some specific enzymatic reactions such as those catalyzed by xanthine oxidase, tryptophan dioxygenase and indolamines dioxygenase. The inflammatory cells produce large amounts of superoxide anion as a defense mechanism against bacteria or potentially harmful organisms (Fuchs, 1992). Finally, the dismutation of superoxide anion, either spontaneously or catalyzed by superoxide dismutase (SOD), is the major source of hydrogen peroxide in the cell (1)



Hydrogen peroxide

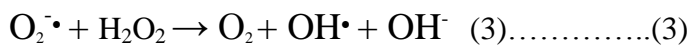
The hydrogen peroxide (H₂O₂) is a reactive molecule relatively stable, able to cross the membranes and with a rather long half-life. It is rather cytotoxic, but it is considered a weak oxidizing agent. The toxicity lies in the fact that it is able to give rise to hydroxyl radical via reactions catalyzed by metal ions (2).



Hydroxyl radical

In the Haber-Weiss process, a molecule of superoxide and a molecule of hydrogen peroxide are combined to produce one molecule of oxygen, one equivalent of hydroxyl radical and a hydroxyl anion.

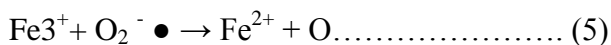
This process is catalyzed by the ions Fe²⁺ or Cu²⁺ (3)



In Fenton reactions, one molecule of hydrogen peroxide is converted into a hydroxyl radical and a hydroxyl anion with simultaneous oxidation of Fe²⁺ to Fe³⁺ (4)



The Fe³⁺ so produced can in turn react with a superoxide radical according to the following reaction, regenerating Fe²⁺ which can again react with H₂O₂ in the Fenton reaction (5) .



It should be specified that the iron content in the cells and in plasma is usually bound to transport, storage and functional proteins, and in this form is never responsive. The Fenton reaction can then occur only in the presence of free iron. Iron chelators can be released from the proteins subsequent to a decrease of pH by the accumulation of lactic acid as a result of ischemia, hemorrhage, trauma, and by interaction of with O²⁻ ferritin .The hydroxyl radical OH[•] is a highly reactive molecule with

strong oxidizing ability and is the agent that promotes the initial phase of peroxidative processes in human tissues. It is able to collide with, and damage, all cellular macromolecules; proteins, nucleic acids, glycosaminoglycans and especially polyunsaturated fatty acids of membrane phospholipids.

Singlet oxygen

Singlet oxygen (O_2^*) is a highly reactive form of molecular oxygen that can be harmful to living systems by oxidizing organic molecules. It is a derivative of the oxygen molecule in which all valence electrons have opposite spin. In vitro studies have showed that O_2^* oxidizes many organic molecules including membrane lipids, proteins, amino acids, nucleic acids, nucleotides, pyridine nucleotides, carbohydrates and thiols. O_2^* can be produced by exposure to ultraviolet light (320-380nm) or during the macrophages activation. The action of NADPH oxidase produces the superoxide radical anion, which spontaneously or enzymatically, dismutates to form hydrogen peroxide. Myeloperoxidase, or peroxidase of macrophages, then catalyze the reduction of hydrogen peroxide to hypochlorous acid. The hypochlorous acid and H_2O_2 react in turn to generated singlet oxygen (Powers SK et al., 2008).

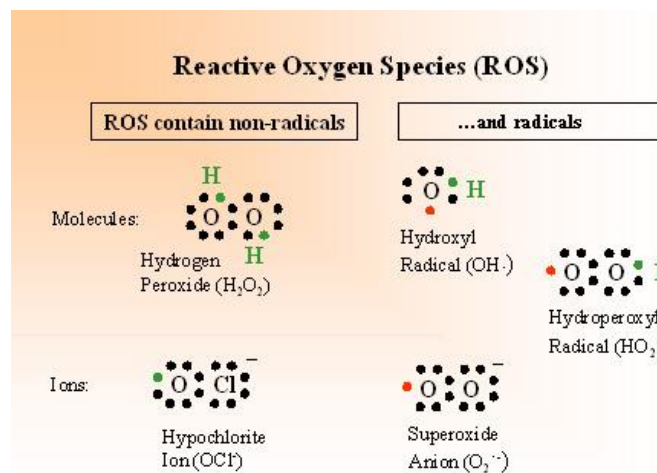


Fig.2.1 Reactive Oxygen Species (ROS)

2.2 Physiological and Pathological Functions of ROS

At high concentrations free radicals, radical-derived and non-radical reactive species damage all biological macromolecules but at moderate concentrations the ROS play a pivotal role as regulatory

mediators in signaling processes. In the many organisms, the ROS mediated responses provide to maintaining the redox homeostasis and to protect the cells against oxidative stress (Dröge 2001). The physiological redox signaling required the increase in ROS concentration or the decrease in antioxidant activities. Many organisms use the ROS-mediated signaling to regulate different physiological processes. For example, phagocytic cells generate singlet oxygen to enhance immunological responses. Similarly, the superoxide anion produced by phagocytes, performs an action of defense against bacterial infections, while the hydrogen peroxide as a product resulting from the dysfunction of the mitochondrial chain, can act as a key regulator in apoptotic mechanisms (Gogvadze et al., 2008). In the same fashion, various type of non- phagocytic cells (i.e. fibroblasts, endothelial cells, cardiac myocytes) produce superoxide and hydrogen peroxide via NADPH oxidase activity, to regulate intracellular signaling cascades. ROS produced by enzymes such as lipoxygenase (5-LOX) and cyclooxygenases (COX) are considered important mediators in inflammatory responses (Bonizzi et al., 200). Vascular tone, platelet adhesion and ventilation also are physiological process regulated by changes ROS production (Dröge 2001). Therefore, appears evident the dual role of ROS: on one hand these molecules are potentially harmful to the cell, on the other play a regulatory role in various processes. This dual function, probably due to differences in the production of ROS for both duration and quantity, and can be explained with the concept of “hormesis”, a concept that is used in toxicology to express the trend of the response of the biological systems in response to exposure to toxic agents. It is a dose-response curve with a bell-shaped trend. In the case of ROS, an increase in moderate amount and of short duration of these molecules may activate these molecular mechanisms that lead the cell to adapt and protect it against subsequent stress. However, high concentrations of ROS for long periods may activate other signaling pathways resulting in proteolysis and cell death (Ji et al., 2006). Small levels of ROS are deactivated by antioxidants. In contrast, the persistence of high levels of ROS damage cell components, which in turn, cause the pathological manifestations (*Fig.2.2*). Indeed, the excessive or sustained increase in ROS production has been implicated in the pathogenesis of cancer, diabetes mellitus, atherosclerosis, neurodegenerative diseases and other pathologic conditions.

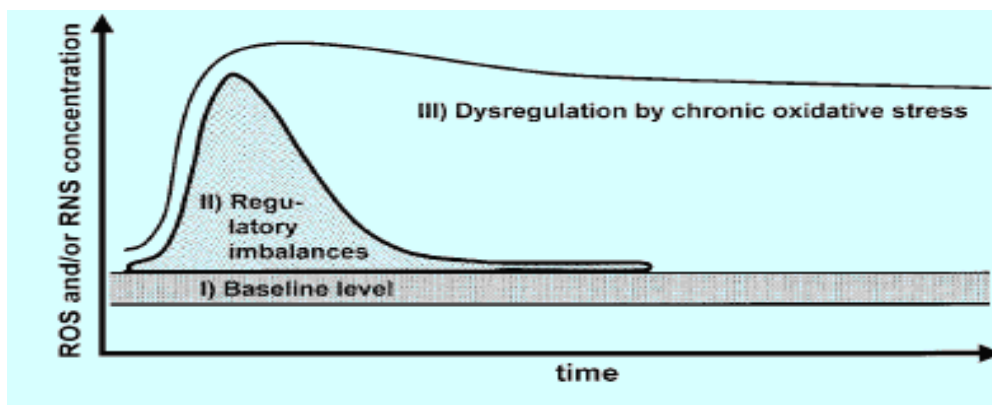


Fig. 2.2. Regulatory events and their dysregulation depend on the magnitude and duration of the change in ROS concentration.

The chemical modifications caused by ROS can affect all macromolecules that constitute the cell; lipids, proteins, carbohydrates and nitrogenous bases of nucleic acids.

Lipid peroxidation

ROS cause lipid peroxidation (LPO), which modifies the three-dimensional structure of the lipids that make up cell membranes, by changing their fluidity and permeability and compromising their function. The process consists of a series of chain reactions in which the unsaturated fatty acids of membrane phospholipids are progressively transformed into lipid radicals ($L\cdot$), peroxy radicals ($LOO\cdot$) and lipid peroxide ($LOOH$). Lipid peroxide can easily decompose into different lipid species such as alkoxides ($LO\cdot$), aldehydes (malondialdehyde, MDA), alkanes, lipid epoxides and alcohols. Similarly, the cholesterol can suffer modifications of the same type, giving rise to epoxides and alcohols. Following these degenerative processes, cell membranes become rigid losing the fluidity and function of selective permeability that distinguishes it (Spiteller, 2006).

Protein oxidation

The protein oxidation may determine a change in the three-dimensional structure of the molecule and also can change the catalytic site of an enzyme preventing the binding with the substrate. An example of protein oxidative modification is carbonylation, caused by oxidation of the R-groups of the amino acids (Davies 1987). This process is associated to the irreversible loss of function of the protein that is deleted in the proteasome, allowing cell survival (Dalle Donne et al., 2006).

Nucleic Acid Damage

The DNA damage consists of chemical modifications of nucleotides which often give rise to breakage of the nucleic acid strand or errors in the replication with the introduction of mutations. Oxidative alterations irreversibly inhibit the processes of transcription, translation and DNA replication, leading to premature senescence and cell death (Harman, 1981; Schraufstatter et al., 1988). Oxidative damage to DNA can result in breakage of the filaments (double and single), in the formation of DNA-DNA (or DNA-protein) cross-links, in sister chromatid exchange, and in modifications of the nucleotide bases. Given the close proximity to the site of ROS production, mitochondrial DNA is the primary target of the toxicity of ROS. In fact, an elevated occurrence of spontaneous mutations arise in mitochondrial DNA compared to nuclear DNA, given also the lower efficiency of DNA repair in this compartment (Kakkar et al., 2007). Mutations in mitochondrial DNA cause further superoxide production and activation of the mitochondrial apoptotic cascade (Ricci et al. 2008). Most likely DNA damage is mediated by the hydroxyl radical OH⁻. One of the most characteristic alterations is the addition of OH at C-8 position of an adenine or guanine. These modifications can be converted by oxidation into 8 - idrossiadenine or 8 - idrossiguanine, which can form formamidodiammino purines, able to induce the block of DNA replication (Halliwell 2002). The 7,8-Dihydro-8-oxodeoxyguanosine (8 OXO-dG) is one of the most frequent oxidative products of DNA and is often used to measure oxidative damage (Tarnig 2000). The 8-OXO-dG showed a documented mutagenic potential which is expressed in various ways, including errors or loss of specificity of coupling between the bases, such as GC → AT transversions and reading errors on adjacent bases (Cooke, 2000). Finally, this adduct is quantitatively the most present in biological extracellular matrices easily accessible, such as blood and urine, and in recent years several analytical methods have been developed that allow a sensitive and specific determination. Since the 8 - OXO -dG excreted in the urine is a product of oxidized DNA, it has been used as a potential biomarker in many environmental exposure studies (Pilger, 2006). Furthermore, it appears to be elevated in several neurodegenerative disorders such as Parkinson's disease, Amyotrophic Lateral Sclerosis (ALS), Alzheimer's disease and Autism.

Nitrogen radicals have the same mechanism of action as oxygen radicals. NO-and ONOO- directly interact with DNA causing deamination reactions and cross-linking, thus increasing the mutagenesis or determining the formation of sugar adducts that cause the breakage of the DNA strand (Davis, 2001). The structural changes that affect cellular macromolecules may influence the fate of the cell. In fact, limited cellular damages are usually repaired by enzyme complexes capable of restoring the natural molecular structures as the DNA repair enzymes. However, if the cell suffers more

consistent damage, the normal cellular architecture is lost and the cell either accumulates breaks and mutations or undergoes death by necrosis or apoptosis.

2.3 Cellular Antioxidant Systems

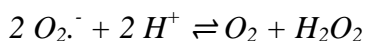
ROS are potentially harmful chemical species that can attack any molecule in our body, making several changes. For this reason, organisms have developed, in the course of evolution, a complex antioxidant defense system, consisting of a set of enzymes, vitamins and trace elements, which allow to neutralize ROS and to block their oxidizing activity. The antioxidants can be classified according to different criteria: on the basis of the origin, in endogenous and exogenous, on the basis of the chemical nature, in enzymatic and non-enzymatic, and finally, on the basis of the solubility, in fat-soluble and water-soluble.

Enzymatic or primary antioxidants

Primary antioxidants belong to the class of a wide range of enzymes able of detoxifying ROS in the cell through enzymatic reactions in which the reactive oxygen species lose their reactivity and are transformed into harmless substances for the cell.

Superoxide dismutase

The superoxide dismutase (SOD) is an enzyme belonging to the family of metalloproteins discovered in 1969 by McCord; the function is to convert the $O_2^{\cdot -}$ in O_2 and H_2O_2 (Rahaman, 2007) according to the following reaction of dismutation:



In this reaction, one molecule of $O_2^{\cdot -}$ oxidizes becoming oxygen and the other molecule is both reduced and protonated becoming H_2O_2 .

SOD is present in different isoforms which are identifiable on the basis of the metal ions present in the active site (i.e. copper, iron and manganese), the amino acid composition and distribution in organisms.

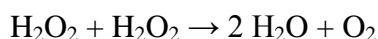
The genes encoding SOD derive from two ancestral genes, one derived from the group of Mn -SOD and Fe -SOD spread among all aerobic organisms from bacteria to plants to humans, the other, from the family of Cu / Zn -SOD, which is distributed exclusively among eukaryotic organisms (Rahaman, 2007).

In humans there are three isoforms of SOD: (SOD-1, SOD-2 and SOD-3) and all have the characteristic of having a transition metal redox active in their catalytic site necessary to catalyze the dismutation reaction (Culotta VC et al.,2006).

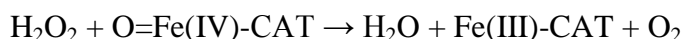
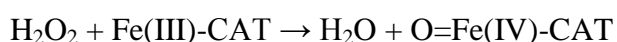
The different isoforms of the enzyme SOD are also characterized by the different localization; a Cu SOD (SOD1) distributed into the cytoplasm and in the intermembrane space, a Mn SOD (SOD2), mainly present in the mitochondrial matrix and a Fe -SOD (SOD-3) localized in the extracellular space.

Catalase

The degradation of H_2O_2 takes place via two families of enzymes, catalase and glutathione peroxidase, present in all aerobic organisms (Izawa et al.,1996) The catalases (CAT) are metalloproteins with tetrameric structure containing porphyrin in the active site, whose prosthetic group is represented by iron; they are localized in peroxisomes of eukaryotic cells (Izawa et al.,1996) These enzymes have the ability to protect tissues from peroxides. The catalase catalyzes the dismutation of H_2O_2 (at high concentrations) to H_2O and molecular O_2 according to the following reaction (Valko et al., 2006):



It is thought that the above reaction occurs in two steps:



CAT have a high speed turn-over: a single molecule can convert every minute approximately 6 million molecules of H_2O_2 to H_2O and O_2 (Rahaman.2007).

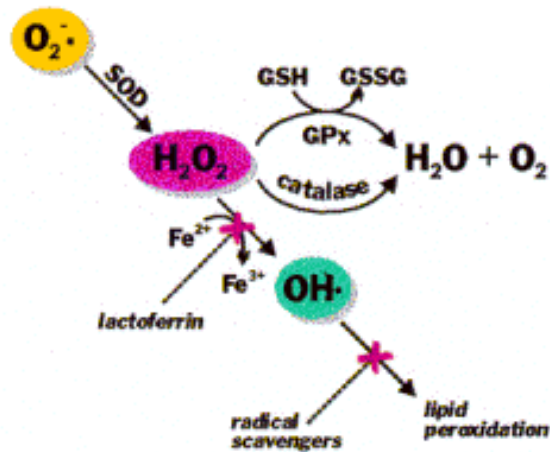


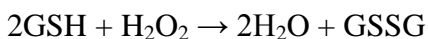
Fig.2.3. Antioxidants enzymatic

Glutathione peroxidase and glutathione reductase

When the levels of hydrogen peroxide are too low to activate the catalase its decomposition is carried out by the activation of glutathione peroxidase (Iorio et al., 2007). The enzyme is present in two different forms; a selenium-dependent (GPx) and a selenium-independent (glutathione-S-transferase (GST) enzyme. The differences between the two enzymes are due to the number of subunits, the catalytic mechanisms and the binding of selenium in the active site (Valko et al.,2006; Rahaman.2007).

In mammals there are five different types of GPx, which differ for the cellular localization and tissue specificity and have the function of reducing the peroxides.

GPx acts in association with glutathione: a molecule present at high concentrations in cells which is one of the most important endogenous mechanisms of detoxification by free radicals. GPx uses H₂O₂ or an organic peroxide (ROOH) as substrate and catalyzes the conversion of peroxides to water or alcohol through the oxidation of reduced glutathione (GSH) (Valko et al., 2006; and Rahaman. 2007):



Property	GPX1	GPX2	GPX3	GPX4	GPX5
Cellular location	Cytosol and mitochondria	Cytosol	Extracellular space and cytosol	Membrane-bound nuclei and mitochondria	Extracellular and membrane bound
Subunit	Tetrameric	Tetrameric	Tetrameric	Monomeric	Dimeric
Molecular mass, kDa	21	22	22.5	19	24
Tissue location	All tissues	Stomach, intestine	All tissues	Testes, spermatozoa, heart, brain	Epididymis, spermatozoa, liver, kidney

Fig.2.4 Different GPx isoenzymes

In these reactions, GPx catalyzes the reduction of H₂O₂ to H₂O and that of organic peroxides to the corresponding stable alcohols (ROH) using glutathione as the source of reducing equivalents. Furthermore GPx is a very important enzyme in preventing lipid peroxidation and then maintain the structure and function of biological membranes (McCord, 2000). Another enzyme involved in the detoxification of oxidized substrates is the Glutathione S transferase (GST) that catalyzes the conjugation of oxidized GSH directly to substrates which are then eliminated from the body. In humans and mammals seven different classes of glutathione S-transferase, belonging to a single family of cytosolic and soluble enzymes, have been identified and characterized. Recently, two other families of enzymes in the microsomal and in the mitochondrial locations have been identified (Hayes 2005).

GPX1 alters the cellular content of GSSG; in order to keep the ratio GSH/GSSG constant, GSSG is released from the cell into the extracellular environment and degraded or converted back to GSH. GSH can be regenerated by de novo synthesis or by reduction of the oxidized form GSSG by glutathione reductase (GR). GR is a flavoprotein that converts GSSG to GSH using NADPH as a reducing agent.

GSH can be synthesized de novo through two sequential reactions: the first one is ATP-dependent and catalyzed by γ -glutamylcysteina synthetase (γ GCS), the activity of which limits the speed of synthesis; the second is catalyzed by glutathione synthetase (*Figure 2.5*).

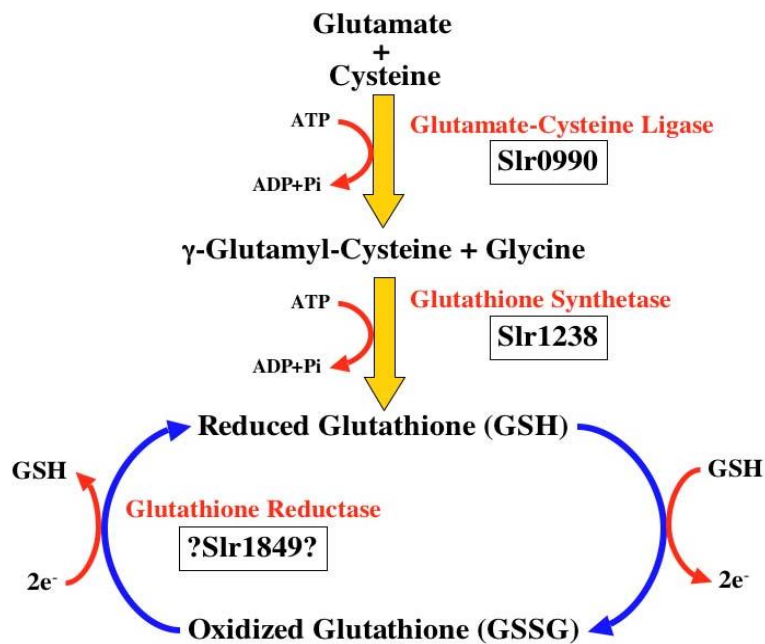
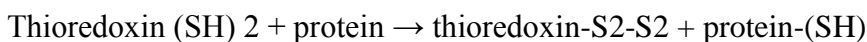


Fig.2.5 Biosynthesis and Regeneration of Glutathione

Thioredoxin (TRX)

The thiol antioxidant thioredoxin (TRX) is a protein with oxidoreductase activity which is present in eukaryotic and in prokaryotic cells (Rahman, 2007). In its catalytic site there are two cysteine residues that reduce disulfide bonds (SS) of other proteins that have been the targets of the action of oxygen free radicals.

In its reduced form, the TRX contains two adjacent SH groups which are converted into a disulfide units in the oxidized TRX when it undergoes redox reactions with multiple proteins in the following reaction (Valko et al., 2006)



TRX1 is present in the cytoplasm and is easily inducible by many types of stress (i.e. ROS, UV rays).

Non-Enzymatic or secondary antioxidants

Thiols are important non-enzymatic antioxidants. Thiol groups (-SH) are essential for the protection of the harmful effects of ROS (Valko et al., 2006). The most important thiol antioxidant is reduced glutathione (GSH), a tripeptide composed of cysteine, glycine and glutamate. GSH is among the most effective antioxidants products at the intracellular level, besides being a substrate for GPX and GST enzymes. It can act directly as a free radical scavenger during the process of detoxification of hydrogen peroxide and lipid hydroperoxides. GSH is very abundant in the cytosol (1-11 mM), in the nuclei (3-15 mM) and in mitochondria (5-11 mM) and is considered the major soluble antioxidant in these cellular compartments (Valko et al., 2006). Antioxidant capacity of the thiol compounds is due to the sulfur atom which can easily facilitate the loss of a single electron. The life of the radical species generated in this way as radical thiol (GS⁻) can be significantly longer than many other radicals generated during oxidative stress (Valko et al., 2006).

Another thiol antioxidant is the α -lipoic acid (ALA). It is a disulfide derivative by octanoic acid which can be either soluble that water-soluble. ALA is widely distributed in cell membranes and in the cytosol of eukaryotic and prokaryotic cells. ALA is rapidly absorbed from the diet and converted to its reduced form, dihydrolipoic acid (DHLA) (Valko et al., 2006). Both forms are potent antioxidants and exert their action as "scavengers" of free radicals and chelators of metal ions; they also act in the recycle of antioxidants and in the repair of proteins damaged by oxidative stress. Other molecules involved in the process of detoxification of free radicals are melatonin, carotenoids and flavonoids. Melatonin is a hormone synthesized mainly by the pineal gland and has many effects on a large number of pathophysiological functions. It is a strong antioxidant that can easily cross cell membranes and the blood-brain barrier (Reiter et al., 1997). The main function of melatonin is to counteract the free radicals produced during the metabolism of oxygen (Burrows et al., 2000). Carotenoids are a class of pigments found in plants and in different microorganisms, can physically remove the singlet oxygen reacting chemically to the free radicals and can eliminate peroxides, thus preventing damage at the level of lipophilic compartments (Rahaman 2007) Flavonoids are polyphenolic compounds and secondary metabolites of plants. (Valko et al., 2006). The flavonoids are of particular interest for their antioxidant properties and for their ability to chelate metals and potential role in the prevention of chronic diseases (Rahaman 2007). Flavonoids are extensively studied for their protective properties against oxidative stress. These compounds are also ideal scavengers of peroxides and are effective inhibitors of lipid peroxidation, able to chelate metal ions and thus to prevent the lipid breaks caused from hydrogen peroxide. However, under

certain conditions the flavonoids can also behave as pro-oxidants, according to the number of their hydroxyl groups (Valko et al., 2006).

Another non-enzymatic antioxidant is coenzyme Q, which carries out its antioxidant action in the mitochondrial electron transport chain. Moreover, vitamins A, E, and C are considered to be non-enzymatic antioxidants and are taken with the diet. Vitamin E is a potent lipid-soluble antioxidant which in humans is present in different forms; the most active is the α -tocopherol (Valko et al., 2006). Vitamin C is a water-soluble molecule that can be present in two forms, a reduced (ascorbic acid) and an oxidized (dehydroascorbic acid). Vitamin C is involved in the regeneration of the non-radical form of vitamin E, after it has reacted with a free radical.

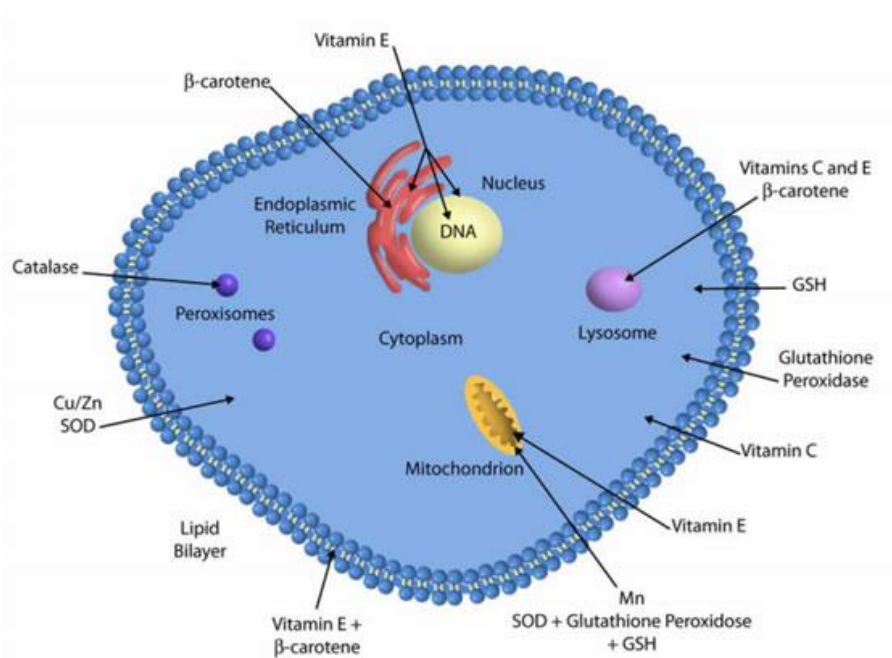


Fig.2.6 Summary of enzymatic and non-enzymatic antioxidant systems

2.4 Oxidative Stress and Biomarkers of Oxidative Stress

The word oxidative stress has been introduced for the first time in 1989 by Sies to describe an imbalance between the production of reactive oxygen species (ROS) and antioxidant defense systems. In physiological conditions, the cell maintains its internal reduced state by means of enzymes and molecules that counteract the production of ROS. Dysfunctions of the normal redox state can cause toxic effects through the production of reactive chemical species that damage cell components including proteins, lipids and nucleic acids (Siciliano et al., 2007).

ROS and other reactive species are constantly produced by the body through various biochemical processes (Uttara et al., 2009). If the generation of ROS exceeds the antioxidant capacity of the cell or an imbalance of detoxification mechanisms occurs, a condition of "oxidative stress" is established (Sompol et al., 2009). This condition has an important role in many diseases such as cancer, ischemia and neurodegenerative diseases (Butterfield et al., 2007), but also plays a crucial role during the physiological aging process (Jha et al., 2009). Recently, there has been a growing interest in understanding the role of oxidative stress in the pathogenesis of neurological disorders (Markesbery, 1996). Different tissues have different susceptibility to oxidative stress; it is now known that the central nervous system (CNS) is particularly vulnerable to damage by free radicals for several reasons that include a limited effectiveness of the antioxidant system and a high consumption of oxygen to produce energy. Direct analysis of ROS is extremely difficult because of their high reactivity and short half-life (10^{-5} , 10^{-6} , 10^{-9} sec for the superoxide radical, singlet oxygen and the hydroxyl radical, respectively) (Tarpey et al., 2004). The study of oxidative stress is based on methods that detect induced alterations of proteins, lipids and DNA. Additionally, the decrease of the molecules with antioxidant capacity is considered an indirect marker of oxidative stress, although this is more susceptible to interference of the diet.

Biomarkers of protein oxidation

The process of oxidation of proteins involves the introduction of new functional groups that can alter their function and metabolism (Dean et al., 1997). Studies on the oxidative modifications of proteins have shown a series of irreversible changes, including fragmentation, alteration of the three-dimensional structure and aggregation, all resulting in a loss of function (Dean et al., 1997 and Davies et al., 1999). These damaged proteins are degraded by the proteasome or by lysosomes, but

in some cases they can form aggregates that accumulate inside or outside the cell and are insensitive to degradation. The amino acid residues most sensitive to oxidation are those containing aromatic groups or thiol, but also aliphatic residues, that following oxidation generate the carbonyl groups. Carbonyl groups and the products of oxidation of tyrosine are the main biomarkers of protein oxidation. The carbonyl groups are a generic product of oxidation of proteins and can be generated by direct oxidation of the amino acids (i.e. proline, arginine, lysine, and threonine) by free radicals or in consequence of lipoperoxidation (LPO) or glycation / glycoxidation phenomena (Stadtman et al., 1997 Burcham et al., 1996 , Vlassara et al.,1994). The formation of carbonyl groups on proteins is considered a marker of severe oxidative stress (Stadtman et al., 2003). The measurement of total protein carbonyls can be carried out in plasma, serum, cell lysates and purified proteins. Accumulation of protein carbonyls has been demonstrated in cellular aging, in ischemia/reperfusion injury, chronic inflammation (Dalle-Donne et al., 2003). Protein aggregation is a frequent consequence of the phenomena of oxidation, and it could contribute to the formation of Tyr dimers; however, some authors have demonstrated that the formation of the dimer is significant only in the metal-proteins, in which the intermediate radical reaction is stabilized by association with metal ion associated (Wilks 1992).

Biomarkers of lipid oxidation

The membrane phospholipids and the triglycerides of low density lipoproteins (LDL) are particularly susceptible to radical attack. The process of lipid peroxidation (LPO) begins with the subtraction of a hydrogen atom from an ethylene group adjacent to a double bond of a polyunsaturated fatty acid (PUFA) of lipids, thus forming a radical centered on a carbon atom. By the rearrangement of the double bond, they forms a conjugated diene, while the molecular oxygen reacts with the carbon-centered radical forming a peroxy radical, which in turn reacts with another PUFA forming a hydroperoxide and a new carbon-centered radical. Lipid hydroperoxides can further react and form cyclic peroxides, cyclic endoperoxides, aldehydes, α , β - unsaturated aldehydes, such as 4 -hydroxy- nonenal (4-HNE), acrolein, and malondialdehyde (MDA). One of the methods most frequently used to assess the degree of LPO in vivo is the quantification of MDA in plasma or urine and the quantification of the 4 -hydroxy- nonenal (4-HNE) which is the main aldehyde generated following the attack of free radicals of n-6 PUFAs (i.e. arachidonic acid , linoleic acid, linolenic acid). The 4-HNE reacts readily with proteins, peptides, nucleic acids and phospholipids to form stable adducts that involve the introduction of new carbonyl groups (Uchida,

2003). Adducts of lysine (HEL) are formed by the oxidation of omega 6 fatty acids such as linoleic acid or arachidonic acid and are considered to be early biomarkers of lipid peroxidation. Specific classes of compounds generated during LPO dependent to arachidonic acid are isoprostanes. Isoprostanes are initially formed as fatty acids esterified to phospholipids affected by radical attack, then are released into the circulation by the action of membrane phospholipases (Roberts et al., 2000). In particular, the F2- isoprostanes are the most studied class as a marker of LPO (Morrow, 2005).

Biomarkers of DNA oxidation

The attack of ROS, in particular the hydroxyl radical on nucleic acids can cause mutations of specific bases and even breakage of the double helix. The most used marker of oxidative damage to DNA is 8-hydroxy-2'-deoxyguanosine (8-oxo-dG), for which competitive ELISA methods for its quantification in tissue extracts or biological fluids are also available (Griffiths et al. 2002 and Collins et al. 2004). During the process of DNA repair, the 8 - OXO -dG is free and secreted in the urine as single base and also included in the DNA oligomers without further modification (Lindahl 2001). Given its stability and specificity, the concentration of 8 -oxo -dG in the urine is one of the most reliable markers to assess the degree of systemic oxidative stress. However, the 8-OXO-dG may also derive from the degradation of the deoxynucleotide dGTP. 8-OXO-dG is considered a partial measure of DNA damage, relative only to guanine residues and its precursors (Dizdaroglu et al., 2002) .

2.5 Role of Oxidative Stress in Friedreich's Ataxia

Oxidative stress caused by deficiency of frataxin plays a pivotal role in the pathogenesis of FRDA. However, the precise sequences of molecular events that underlie oxidative stress in FRDA are still debated. Studies in humans and in different eukaryotic organisms have confirmed that the frataxin deficiency causes an increase of oxidative stress (Schulz et al., 2000; Bulteau et al., 2007 and Armstrong et al., 2010). Biomarkers of oxidative stress have been detected in the urine and blood of FRDA patients; the levels of 8-hydroxy-2'-deoxyguanosine, a marker of oxidative DNA damage (Schulz et al., 2000), and of malondialdehyde, a product of lipid peroxidation (Edmond et al., 2000), were higher in the urine and plasma of patients compared to healthy controls. However, in other studies no differences were found between the levels of 8-hydroxy-2'-deoxyguanosine (Di Prospero et al., 2007) and of F₂-isoprostanes between patients and controls (Myers et al., 2008). However, it has been reported that the loss of frataxin causes an impairment of cellular enzymatic anti-oxidant defenses, which in turn results in accumulation of ROS and oxidative stress. Indeed, in the blood of patients both a reduction in the levels of free glutathione (about 15 fold) and a significant increase of glutathione bound to hemoglobin (approximately 2-fold) were observed (Piemonte et al., 2001). The glutathione-dependent redox state has been studied in detail in yeast (Auchère et al., 2008). In yeast cells $\Delta yfh1$ mutant for the gene encoding frataxin, the concentration of total glutathione and the ratio GSH/GSSG were significantly reduced. Also, the GPX was more active than the wild-type. In contrast, there were no significant changes in the expression of genes involved in the glutathione-dependent system between mutant cells and controls. These results suggest that the deficiency of frataxin in yeast leads both to a remodeling of the defense system as glutathione-dependent adaptation of the cells to a state of chronic oxidative stress (Auchère et al., 2008). In addition, Paupe and co-workers (2009) have shown that the Nuclear factor (erythroid-derived 2)-like 2 (Nrf2) is compromised in frataxin-deficient fibroblasts. Nrf2 is a transcription factor that responds to oxidative stress by binding to the antioxidant response element (ARE) in the promoter of genes coding for antioxidant enzymes. (Dassa et al., 2008). In normal conditions, the activity of the transcription factor Nrf-2 is regulated by the actin-associated with the protein Kelch-like ECH-associated protein 1 (Keap1), which binds NRF2 sequestering it in the cytoplasm and promoting its degradation via ubiquitination. Under conditions of stress, this interaction is lacking, and the transcription factor Nrf-2 is translocated into the nucleus, where it binds to DNA sequences of the "cis-acting ARE" (antioxidant-responsive element), thus activating the expression of anti-oxidants phase II genes such as SOD, catalase, glutathione-S-transferase and quinone oxidoreductase

NADH8 (Zhu et al., 2005 and Young et al., 2005). In FRDA fibroblasts treated with oligomycin and TBHQ (tert-butylhydroquinone), the NRF2 is unable to translocate into the nucleus, and none of the previously named genes is induced. The authors have shown a disorganization of actin filaments in fibroblasts of patients and the consequent dissociation of Keap1 and Nrf2 from actin. This alteration of the cytoskeleton can be explained by changes in the pools of glutathione in the absence of frataxin. This causes an increase in glutathionylation and alterations in the actin cytoskeleton dynamics, with the consequent impairment of the pathways of anti-oxidant defense by Nrf2 pathway. Cortopassi and co-workers (2014) through a drug discovery program that screened a library of clinically-approved drugs, has identified several compounds that act as Nrf2 activators and rescue biochemical and cellular deficits related to frataxin deficiency.

As already said, oxidative stress due to frataxin deficiency is frequently associated with the accumulation of iron deposits into mitochondria (Richardson et al. 2010). Mitochondria are important organelles present in every cell type, but are especially important in the nervous system. Mitochondrial functions are essential for neuronal development and maintenance, where they participate in energy production, calcium homeostasis, maintenance of membrane potential, folding of proteins by chaperones, axonal and dendritic transport, and the release and reuse of neurotransmitters in the synapses. The main function of mitochondria is energy production through oxidative phosphorylation (OXPHOS). OXPHOS includes two steps, the electronic transport chain (ETC) that generates a gradient of protons, which is then used to produce ATP by oxidative phosphorylation. OXPHOS is the primary source of endogenous ROS, which are produced as toxic products of respiration (Gonzàles-Cabo and Palau, 2013). The importance of deficit in mitochondrial bioenergetics in FRDA is derived by the fact that the frataxin has an essential role in the biosynthesis of Fe-S clusters which constitute the complexes of the electron transport chain. Therefore, in FRDA patients, the deficit of frataxin and consequently the incomplete activity of Fe-S clusters could cause the increase of electron leakage and increase of ROS levels and oxidative stress. In contrast, Bayot and colleagues (2011) have proposed an alternative hypothesis concerning the generation of oxidative stress in the cells of FRDA patients and derived from studies in which the frataxin depletion was not found to be associated with decreased activity of ISC. Indeed, it has been shown that in different cell lines depleted of frataxin, no decrease in ISP containing enzyme was found (Rotting et al., 1997). Based on this results, it was hypothesized that in frataxin-depleted cells, deficient signaling of antioxidant defences sensitizes the frataxin-free iron-sulphur clusters to reactive oxygen species. This hypothesis is supported by the fact that in FRDA patients there is a differential pathological pattern in specific organs and tissues that appears to be related to different

sensitivity to oxidative damage. Therefore, further studies are needed to elucidate the precise events that occur in the establishment of the oxidative stress in FRDA.

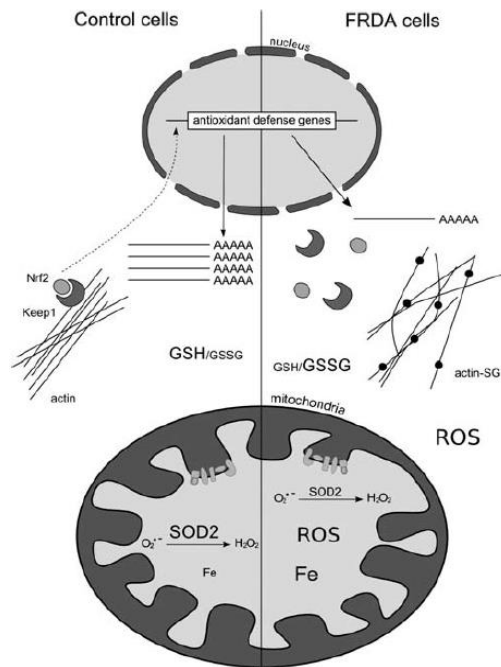


Fig.2.7 Dysregulation of Antioxidant defenses in FRDA cells

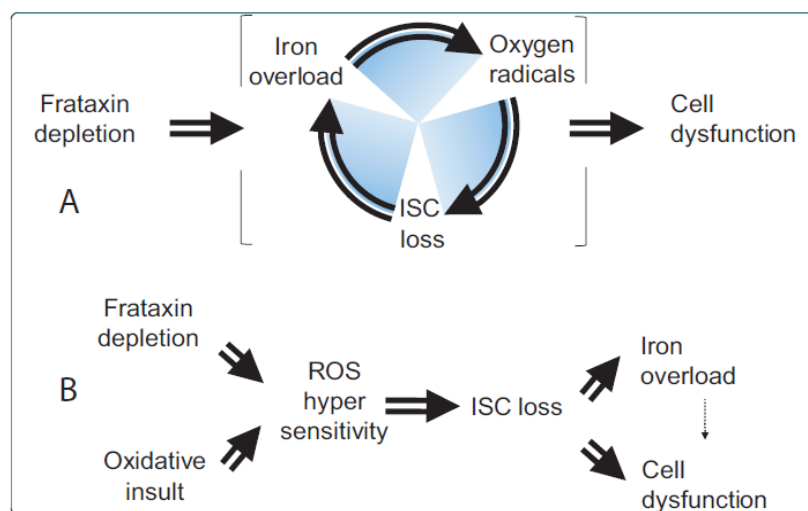


Fig.2.8 The vicious circle hypothesis revisited in Frda

Chapter III

Research Project

Part I: Aims

Oxidative stress appears to play a pivotal role in the pathogenetic mechanism of FRDA. For this reason, treatment with natural compounds with antioxidant activities may be useful to decrease the harmful effects due to free radicals in FRDA. The encouraging data relating to the beneficial effects observed in Friedreich's Ataxia patients treated with tocotrienol in an earlier study, has led our research group to investigate the potential therapeutic role of tocotrienol in counteracting the oxidative stress in FRDA patients. The first aim of my research project was to identify and evaluate a wide array of biochemical and molecular parameters related to oxidative stress in five young FRDA patients before and after two months of treatment with low dose of tocotrienol (5mg/kgbodyweight/day), and from five young healthy subjects chosen as controls. Patients were taking idebenone and did not discontinue it during the experimentation. We studied the following biochemical parameters related to oxidative stress: white blood cell gene expression of antioxidant enzymes (SOD-1, SOD-2, Catalase, GPX-1, GSR and GSTM-1), plasma content of GSH and GSSG; plasma Oxygen Radical Absorbance Capacity; plasma protein carbonyl groups; lipid composition of erythrocyte membranes to elucidate the molecular mechanisms underlying the tocotrienol antioxidant activity. These same parameters were measured following two month-treatment with tocotrienol, in order to evaluate the variation of the oxidative stress parameters. Moreover, literature reports the efficacy of tocotrienol in increasing the transcription of a gene whose mutation leads to Familial dysautonomia, a neurodegenerative disorder (Anderson et al., 2003). The authors reported that in vivo supplementation with tocotrienol resulted in an increase of both gene expression and protein IKBAP, the protein responsible for familial dysautonomia. Furthermore, other studies showed that FRDA patients treated with antioxidants such as coenzyme Q10 and vitamin E showed an increase in mRNA frataxin expression (Lodi et al., 2005). On the basis of these findings, the second aim of this work was to determine whether and how the treatment of patients with tocotrienol is able to modulate the transcription of the frataxin (FXN) gene. To this purpose, we evaluated the gene expression of frataxin isoform splice variants (FXN-1, FXN-2 and FXN-3) in blood mononuclear cells derived from patients before and after two months of treatment with low dose of tocotrienol and from of healthy subjects chosen as control. Moreover, since a small but significant increase in FXN-3 mRNA was found, we examined whether the less

expressed FXN-2 and FXN-3 isoforms may have a possible role in the cell; this was accomplished by bioinformatics means, building a 3D-model of both isoforms and carrying out a docking study between FXN-2 or FXN-3 and the human complex NFS1/ISCU.

Part II: Aims

In FRDA, the trinucleotide repeat expansion (GAA •TTC) of FXN gene has leads to gene silencing by epigenetic changes However, the study of the pathogenesis of FRDA is limited by the lack of availability of cellular models able to reproduce the molecular and epigenetic mechanisms of gene silencing. Recently, in the laboratory of Professor Gottesfeld (The Scripps Research Institute, La Jolla, CA), it has been demonstrated that human fibroblasts derived from subjects suffering from neurodegenerative diseases caused by trinucleotide expansions of triplets can be reprogrammed to induced pluripotent stem cells (hiPSCs) by the transduction of four defined transcription factors (Yamanaka et al.,2007). hiPSCs tecnology represent a good model to study the molecular and epigenetic mechanisms related to instability of (GAA)_n expansions (Ku et al. , 2010). For this purpose, the third year of my PhD project was carried out in the laboratory of Professor Gottesfeld, with the aim to generate hiPSCs-derived fibroblast from FRDA patients and healthy subjects. Furthermore, in the laboratory of Prof. Gottesfeld 298 DNA samples (obtained from Dr. David Lynch, of Children's Hospital of Philadelphia (CHOP) extracted from FRDA patients were analyzed by Sequenom MassARRAY platform, in order to identify single nucleotide polymorphisms (SNPs) non synonyms in the encoding regions of the genes for histone deacetylases, sirtuins, histone acetyltransferases, and other chromatin binding and modifying proteins, as potential secondary genetic modifiers of FRDA disease severity. From the analysis of various SNPs, using the Sequenom MassArray technology platform, only 5 SNPs were found to be polymorphic in this group of FRDA patients. Furthermore, Lynch and co-workers have used the DNA repository and clinical database of the Collaborative Clinical Research Network in FRDA to assess the effect of SNP polymorphisms on clinical features of FRDA The majority of SNPs assessed did not predict outcomes. In contrast, a specific amino acid changing polymorphism (rs352493) in Sirtuin 6 predicted FARS, with Z2 and Z3 (neurological outcome measures) scores with high significance This SNP changed the amino-acid Asn46 to Ser46. Therefore, the aim of my research project was to generate hiPSCs from fibroblasts derived from FRDA patients carrying heterozygous SNP (Asn46/Ser46) or omozygous for the prevalent Asn46 allele, and fibroblasts

derived from healthy subjects chosen as controls (Asn46/Asn6), and to study the role of Sirtuin 6 in order to investigate the molecular mechanisms that underlie the better outcome in individuals harboring the SNP (Asn46/Ser46).

Chapter IV

Role of Oxidative Stress in the Freidreich's Ataxia

Materials and Methods (Part I)

Patients and Healthy Subjects

Five FRDA patients and five healthy volunteers were enrolled after signing an informed consent form. The Child Neurology and Psychiatry Unit, IRCCS Institute of Neurological Sciences of Bologna, Bologna, Italy, enrolled all subjects in this study. This study was approved by the Ethical Committee of Regional Health Service (number 1635-08092011). FRDA was diagnosed according to Harding 123 diagnostic criteria. Patients regularly assumed idebenone (5mg/kg body weight/day, which was not discontinued during the study). Healthy volunteers, used as control, were age and sex matched with the FRDA patients; they were not affected by any neurological or psychiatric disease and were not under pharmacological treatment of any type nor were assuming food integrators.

Tocotrienol

Tocotrienol dose used in this study (5mg/kgbodyweight/day) was much lower than that estimated as no observed adverse effect level (NOEAL) in rats or humans (Osakada et al; 2004 and Khanna et al; 2005). Neither, FRDA patients, or healthy controls noticed adverse effects due to tocotrienol consumption. The tocotrienol mixture was designed by Ambrosialab s.r.l. a spin-off company of the University of Ferrara, Italy. It is a Palm Oil (*Elaeis Guineensis*) phytocomplex, prepared for the purposes of the study, as soft gel capsule formulation and labeled as OXI-3 (internal reference name ALAB103). It is composed by tocotrienols and tocopherols in the enantiomerically pure natural form (total tocotrienol and tocopherol: 256mg/g, of which D-tocotrienol is 197 mg/g and D-tocopherol is 59mg/g). (For details see the table 2 in the supplementary materials part I).

Blood sample

Venous blood (15 ml) was collected in Na-EDTA vacutainers. One ml whole blood was set apart for lipidomics evaluation (see below). The remaining was centrifuged (10 min. at 1000 x g) in order to separate the plasma, which was frozen at -20°C in 1 ml eppendorf sterile tubes. After diluting (1:1) the cell suspension with sterile Phosphate Buffered Saline (PBS), mononuclear white blood cells were separated from red cells by Ficoll (Histopaque 1077, Sigma, St.Louis, MO) density gradient centrifugation. Cells were suspended in 1 ml Trizol[®] Reagent (Invitrogen, Milan, Italy) and stored at -80°C before performing the RNA separation.

Urine sample

Spot urine samples (10 mL) from healthy and patient subjects were collected. Proteinuria and creatinine determinations were carried out by laboratory techniques. The remaining urine was centrifuged at 1200 g for 10 min in order to remove insoluble materials. Five mL of clear urine were aliquoted and stored at 280uC for hexanoyl-lysine adduct (HEL) and 8-isoprostane evaluations. The remaining urine was filtered with 0.45 mm filter, supplemented with 0.05% sodium azide and stored at -80 C° for 8-hydroxy-29-deoxyguanosine (8-oxo-dG) analysis.

GSH /GSSG ratio determination

Plasmatic glutathione (GSH) and glutathione disulphide (GSSG) were determined by High-Performance Capillary Electrophoresis using an automated Agilent^{3D} CE Instruments (Palo Alto, Ca) electrophoresis system equipped with a DAD detector (operated at 200 nm) and interfaced with a CoolerMaster PC. Briefly, patient plasma samples were measured with transient pseudo-isotachophoresis after deproteinization with acetonitrile. A 20 cm effective length x 75 µm uncoated fused silica capillary with 300 µM phosphate buffer at pH 7.4 was used for the analysis. The voltage for the separation was at 10 kV. Samples were introduced by pressure injection for 40 s., so the sample length can reach 25% of the effective capillary length and the sensitivity increases 15-20 fold.

Carbonyl groups Analysis

Albumin and IgG depletion from plasma samples

The deep frozen crude plasma samples were defrozen to 4°C. Using the commercially available ion exchange based Blue Albumin and IgG Depletion kit (PROTBA-1KT, Sigma-Aldrich, France), 50 µL of crude plasma was diluted with 150 µL of equilibration buffer (kit reagent) before application to the column. The protocol was performed as described in the Blue Albumin and IgG Depletion Kit user guide. The flow-through fraction contained the albumin/IgG depleted plasma and was stored at -20°C until use. Protein concentration was determined by the standard Bradford method (Bio-Rad Laboratories, Hercules, CA).

Derivatization of protein carbonyls and DNP immunostaining

After plasma sample IEF, the IPG strips used for carbonylation analysis (oxyblot) were placed in 10mL tubes and incubated in 2 N HCl with 10 mM DNPH (2,4-dinitrophenylhydrazine, Sigma-Aldrich, France) at 25°C for 20 min. Following the incubation enabling protein-bound carbonyl derivatization, the marked IPG strips were washed with 6M Urea, 20% Glycerol, 1% SDS, 150mM Tris-HCl pH 6.8. The marked IPG strips were then prepared for the second dimension, followed by protein blotting to a PVDF membrane as described previously (Korolainen et al., 2007 and Reinheckel et al., 2000). The PVDF membranes were incubated overnight at 4°C for immunostaining with the primary antibody solution consisting of a 1:10,000 dilution of the anti-DNP IgG antibody (Sigma-Aldrich, France) in the phosphate-buffered saline (PBS) containing 3% non-fat dry milk (Bio-Rad Laboratories). Next, the oxyblots were washed with PBS, 20% Tween and incubated with the goat anti-rabbit IgG/HRP conjugate (1:3000 dilution in PBS/Milk) for 1 h at room temperature. An enhanced chemiluminescence kit (Immobilon Western Chemiluminescent AP substrate, Millipore) was used for detection.

Urinary 8-oxo-dG.

Urinary 8-hydroxy-29-deoxyguanosine (8-oxo-dG) was measured using the HT 8-oxo-dG ELISA Kit (Trevigen Inc. Gaithersburg, MD, USA) according to the manufacturer's instructions. Briefly, filtered urine was diluted 1:20 with a buffer provided by the kit and added to a plate prebound

with 8-oxo-dG. Bound and sample 8-oxo-dG competes for binding to the anti-8-oxo-dG which was then added to the plate; the antibody fraction captured by the immobilized 8-oxo-dG in the plate was then detected by means of a HRP-conjugated secondary antibody. The assay was developed with tetramethylbenzidine substrate (TMB) and the absorbance was measured in a microplate reader at 450 nm. The 8-oxo-dG concentration was expressed in ng per milligram of creatinine.

Urinary 8-isoprostane

Urinary 8-isoprostane (also known as 8-epi-PGF_{2a}, 8-iso-PGF_{2a} or 15-isoprostane F_{2t}) was determined by the use of a competitive ELISA kit (Oxford Biomedical Research Inc., Oxford, MI, USA). As suggested by the manufacturer, urine samples are diluted 1:5 with a buffer provided in the kit. The 15- isoprostane F_{2t} in the samples competes with 15- isoprostane F_{2t} conjugated to horseradish peroxidase (HRP) for binding to a polyclonal antibody specific for 15-isoprostane F_{2t} coated on the microplate. A substrate was added and the absorbance was measured at 450 nm in a microplate reader. The 15-isoprostane F_{2t} concentration was expressed in ng per milligram of creatinine.

Hexanoyl-lysine adducts (HEL)

(HEL) concentration was measured by a competitive ELISA kit (JaICA, Fukuroi, Shizuoka, Japan) in unfiltered urine of healthy and FRDA patients. According to the manufacturer's instructions, the urine samples were diluted five times with PBS. Some urine samples containing proteins were treated with 14 mg/mL alphachymotrypsin in PBS (pH 7.4) and incubated at 37°C O.N. Samples were filtered using ultra filters with cut-off molecular weight 10 kDa (Amicon Ultra, Millipore, Cork, Ireland). The absorbance was measured at 450 nm using a microplate reader. The HEL concentration was expressed in nmol per milligram of creatinine (nmol/mg creatinine).

Oxygen Radical Absorbance Capacity

The ORAC assay was carried out on a Fluoroskan FL® ascent (Thermo Fisher Scientific, Inc. Waltham, MA) with fluorescent filters (excitation wavelength: 485 nm; emission filter: 538 nm) following a modified protocol. Briefly, in the final assay mixture (0.2 mL total volume), fluorescein

sodium salt (85 nM) was used as a target of free radical attack with 2,2'-azobis(2-amidino-propane) dihydrochloride (AAPH) as a peroxy radical generator. Trolox, a water-soluble analogue of vitamin E, was used as a standard control: a calibration curve was carried out with 10, 20, 30, 40, 50 μ M solution. The fluorescence measurements, carried out at 37 °C, were recorded at 5 min intervals up to 30 min after the addition of AAPH. The ORAC values, calculated as difference of the areas under the quenching curves of fluoresceine between the blank and the sample, were expressed as Trolox equivalents (TE), pH = 7.4. All the experiments were performed with three replicates.

Lipidomic analysis

Lipidomic analysis was carried out as previously described (Viviani Alsemi et al., 2010). Briefly, whole blood was centrifuged to remove plasma, then erythrocytes were lysed and membranes were separated by centrifugation. Phospholipids were extracted according to the method of Bligh and Dyer. The total phospholipids fraction was treated with KOH/MeOH solution (0.5 M) for 10 min at room temperature, and fatty acid methyl esters were subsequently extracted with n-hexane. GC analysis of released fatty acids showed separation of all fatty acids and their isomers. This was confirmed by comparison with commercially available references and with a library of geometrical trans MUFA and PUFA obtained by thiyl radical-catalysed reaction of naturally occurring lipids (Ferreri et al., 2005). The content of individual fatty acids in erythrocyte membranes was expressed as percentages of the total fatty acids identified. Specifically, we correlated the percentages of the main saturated and unsaturated residues of membrane phospholipids together with the sums of saturated (SFA), monounsaturated (MUFA) and polyunsaturated (PUFA n-3 and PUFA n-6) fatty acid residues, and some indicative ratios (SFA/MUFA; Palmitoleic acid-C16:1/ Palmitic acid-C16:0; Oleic acid-C18:1/ Stearic acid-C18:0).

The Peroxidation Index (PI) was determined from the percentages of monoenoic, dienoic, trienoic, tetraenoic, pentaenoic and hexaenoic fatty acids according to the following formula:

$$\text{PI} = (\% \text{ Monoenoic} \times 0.025) + (\% \text{ Dienoic} \times 1) + (\% \text{ Trienoic} \times 2) + (\% \text{ Tetraenoic} \times 4) + (\% \text{ Pentaenoic} \times 6) + (\% \text{ Hexaenoic} \times 8).$$

The unsaturation index (UI), also known as the index of hydrogen deficiency, was calculated from number of double bonds per number of unsaturation of each fatty acid. It was given by equation:

$$\text{UI} = (\% \text{ Monoenoic} \times 1) + (\% \text{ Dienoic} \times 2) + (\% \text{ Trienoic} \times 3) + (\% \text{ Tetraenoic} \times 4) \\ + (\% \text{ Pentaenoic} \times 5) + (\% \text{ Hexaenoic} \times 6).$$

RNA Extraction and cDNA Synthesis

Total RNA was extracted from Trizol suspension following the manufacturer's instructions (Invitrogen, Milan, Italy). RNA quality and cDNA synthesis was assessed as previously described Abruzzo et al; 2010. Briefly, RNA quality was measured by evaluation of 28S and 18S rRNA band sharpness after denaturing electrophoresis. Genomic DNA contamination was removed by digestion with RNase-free Deoxyribonuclease I (DNase I) (Amplification Grade DNase I, Sigma Aldrich, St. Louis, MO), and its absence was assessed by PCR analysis using specific primers for HSP70 promoter (left primer: cgccatggagaccaacaccc; right primer: gcggttcctgctctctgctc). RNA purity and concentration were measured by spectrophotometer (Ultrospec 3000, Pharmacia Biotech, Cambridge, UK). Equal amounts of total RNA were reverse transcribed using the iScript cDNA Synthesis Kit (Bio-Rad, Hercules CA) following the manufacturer's instructions. The cDNA thus obtained was stored at 20 °C and used for PCR and qRT-PCRs.

Primer FXN Isoforms Design

Specific primer sequences for frataxin isoforms, for PPARG, and for two housekeeping genes, beta actin and GAPDH, were designed with the help of two freely available software tools Primers3 and Amplify. In order to discriminate between *FXN-1* and *FXN-2* isoforms, the primer pairs shared the left primer, while the right primer was designed in the precise site where the two isoforms differ (i.e., in the region where the *FXN-2* isoform has 8 bp insertion). *FXN-3* primers were designed in the cDNA region following nucleotide 702. Primer sequences summarized in Table 4 (see Supplementary Materials Part I). PCR products were subjected to both agarose gel electrophoresis and melting curve analysis. Moreover, *FXN-1* and *FXN-2* primer specificity were evaluated by enzymatic digestion of PCR products obtained with semi-quantitative PCR.

PCR

PCR analysis was performed using a Taq PCR core kit. (Qiagen, Milan, Italy) in according to manufacturer's instructions, PCR conditions were as follows: a denaturing state at 95°C for 5 min, 40 cycles at 95°C for 50 s, 62.5°C for 50 s, 72°C for 10 min and a final stage extension at 72°C for 10 min, PCR products were analyzed on 2.5% agarose gel stained with ethidium bromide at 0.5mg/ml and after one h of running at 70mV.

Enzymatic Digestion of FXN-1 and FXN-2 PCR Products

FXN-1 and FXN-2 PCR products, 126 bp and 133 bp, respectively were digested with BstNI endonuclease (New England Biolabs, Milan, Italy), taking into account that its restriction site (5' CCWGG '3 and 3' GGWCC '5) is found exclusively in the FXN-2 PCR product. To this purpose, FXN-1 and FXN-2 PCR products were incubated with 1 X NEB Buffer 2, 1mM BSA, and 1X BstNI in a final reaction volume of 20 μ l. The digestion was carried out at 60°C for 90 min. The digested fragments were separated by electrophoresis on 10 % polyacrylamide gel along with undigested samples and were visualized by ethidium bromide staining.

Quantitative RT-PCR Analysis and Statistical Analysis

Quantitative RT-PCR was performed in a Bio-Rad CFX96 real-time thermal cycler using the SsoFast EvaGreen Supermix (Bio-Rad Laboratories, Hercules, CA). The primer sequences for antioxidant genes and housekeeping genes (β Actin and GAPDH) are listed in Table 3 (See Supplementary materials (Part I)). Data were normalized to the housekeeping genes Beta-Actin and GAPDH. Primers were designed with *PRIMER3* and *AMPLIFY* software and whenever possible, were designed so as to span an exon-exon junction (Sigma-Aldrich, France- Software CFX Manager Software (Bio-Rad Laboratories, Hercules, CA) and qbaseplus (<http://www.biogazelle.com/>) was used to date calculation. Data were analyzed with the $2^{-\Delta\Delta CT}$ method (Livak et al; 2001) taking into account the efficiency of the real-time PCR reaction between 95% and 105% (Pfaffl et al; 2001) Quantitative RT-PCR evaluations were repeated at least twice. Data were evaluated by ANOVA test.

Modelling of Human FXN-2 and FXN-3 and of the Human NFS1/ISCU Complex

In order to build the 3D model of the on each ligand, consisting of 126 points (XYZ) and spacing of 0.475 ° A that allows an unconstrained roto-translation of the ligand. For each isoform, twenty five independent jobs were submitted by the Lamarckian genetic algorithm, with an initial population of 150 conformations, a cut off of 27,000generations, and with rates of mutation and crossover set to 0.02 and 0.8, respectively. The final solution was characterized by the lowest binding energy.

Statistical analysis

Data were evaluated by ANOVA by using ORIGIN 6.0 (Microcal Software, Inc.). Differences were considered to be statistically significant when $0.01 < p \leq 0.05$ and highly significant when $p \leq 0.01$.

Supplementary materials (Part I)

Table 1. Phenotypic and genotypic features of FRDA patients

Gender	Age at time of study	Age of disease onset	Length GAA Repeats	Total ICARS Score
F	13	9	830	20
M	29	16	360	37
M	24	11	625	81
F	18	8	621	19
F	27	3	560	59

Table 2 Composition of OXI-3 by Ambrosialab, University of Ferrara (Italy)

TOTAL TOCOTRIENOL AND TOCOPHEROL	MINIMUM 250 mg/g (25%)	
	RANGE	TYPICAL VALUE
Total D-Tocotrienol in the mix	Min. 190 mg/g	197.5 mg/g
Total D-Tocopherol in the mix	Min. 51 mg/g	59 mg/g

Table 3; Primer sequence for antioxidant and housekeeping genes studied with qRT-PCR.

Unigene accession no.	Gene	Left Primer	Right Primer	Amplicon length (bp)
Hs.520640	<i>Beta Actin</i> *	TGTGGCATCCACGAAACTAC	TGATCTTGATCTTCATTGTGC T	175
Hs.544577	<i>GADPH</i> *	GGCCTCCAAGGAGTAAGACC	CTGTGAGGAGGGGAGATTCA	130
Hs.530227	<i>HSF1</i> **	CGCCATGGAGACCAACACCC	GCGGTTCCCTGCTCTCTGTC	488
Hs.443914	SOD-1	GGTGTGGCCGATGTGTCTAT	CACCTTTGCCCAAGTCATCT	112
Hs.487046	SOD-2	GGAAGCCATCAAACGTGACT	CTGATTGGACAAGCAGCAA	148
Hs.502302	catalase	GTGCAAATGCAAGCTAGTGG	TCCAATCATCCGTCAAAACA	150
Hs.76686	GPX-1	CTCTTCGAGAAGTGCGAGGT	AGGCTCGATGTCAATGGTCT	240
Hs.433951	GPX-4	AAGGAC CTGCCCCACTATTT	GGTGCACGCTGGATTTTC	145
Hs.271510	GSR	CCCGATGTATCACGCAGTTA	AAACCCTGCAGCATTTCATC	129
Hs.301961	GSTM-1	TCATTACCCTTCCTGCACT	ACCAGTCAATGCTGCTCCTT	146
Hs.527078	PGC1-alpha	TTGCTGCTCTTGAAAATGGA	TTACCTGCGCAAGCTTCTCT	212

*Beta-Actin and GADPH genes were used as reference genes for normalization purposes. **The promoter of HSF1 (*HSF1 heat shock transcription factor 1*) was used to exclude the presence of genomic DNA in the RNA preparation before carrying out the reverse transcription.

Table 4: Primer sequence for FXN -1, FXN-2 and FXN-3 isforms and PPARG genes studied with qRT-PCR.

Unigene	Gene	left	Right	Amplicon
Hs.20685	<i>FXN-1</i>	GATGTCTCCTTTGGGAGTGG	ACGCTTAGGTCCACTGGATG	126
Hs.20685	<i>FXN-2</i>	GATGTCTCCTTTGGGAGTGG	CGCTTAGGTCCACTACATACCTG	133
Hs.20685	<i>FXN-3</i>	CCTTGCAGACAAGCCATACA	CTTCGTTGCTCACTTGCTGA	275
Hs.162646	<i>PPARG</i>	CATAAAGTCCTTCCCGCTGA	ACCTCTTTGCTCTCCTCCTG	165

Results (Part I)

GSH/GSSG ratio

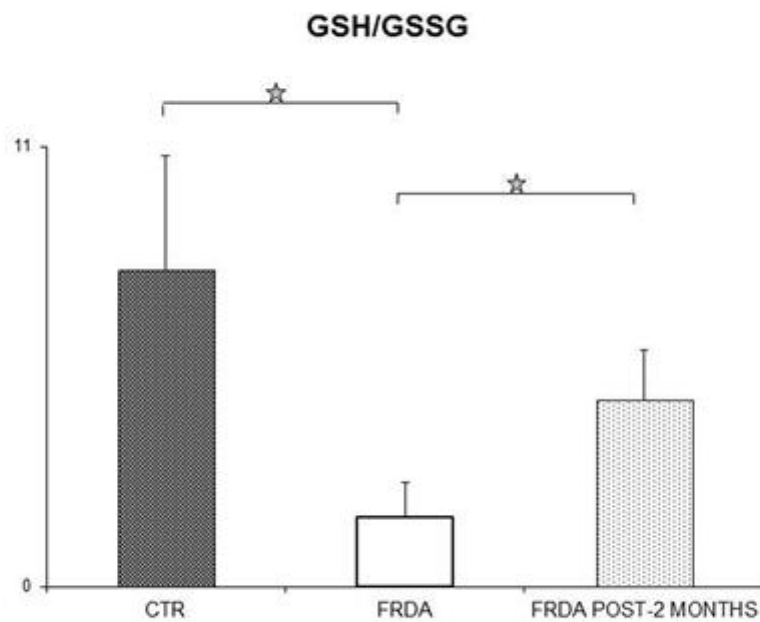


Fig.1 GSH/GSSG ratio values (Mean \pm SD) of plasma from normal age-matched controls and from FRDA patients before the two-month add-on tocotrienol supplementation; FRDA-POST, FRDA patients at the end of the two-month add-on tocotrienol supplementation. Star, $0.01 \leq p \leq 0.05$ by ANOVA.

Carbonyl groups Analysis

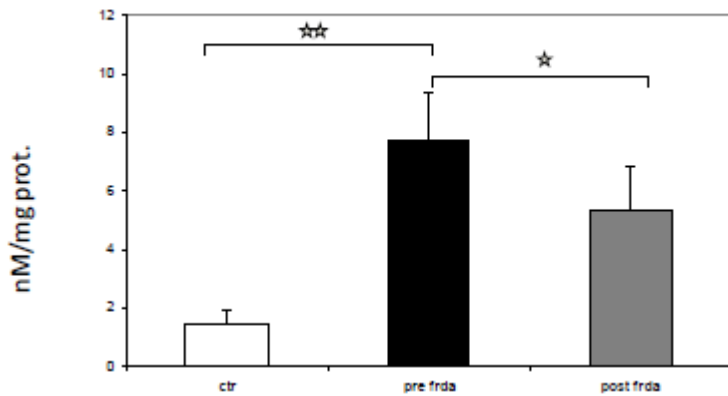


Fig. 2 Level of plasma protein carbonylation (nM/mg proteins). Values represent the Mean \pm SD of percentage oxyblot spot volumes normalized to the Coomassie-stained spot volumes (%V, where V = integration of OD over the spot area and where % V = V single spot / V total spots) in plasma derived from FRDA patients before and after the two-month add-on tocotrienol supplementation and in healthy subjects. Star, $0.01 \leq p \leq 0.05$; two stars, $p \leq 0.01$ by ANOVA.

Lipidomics Analysis

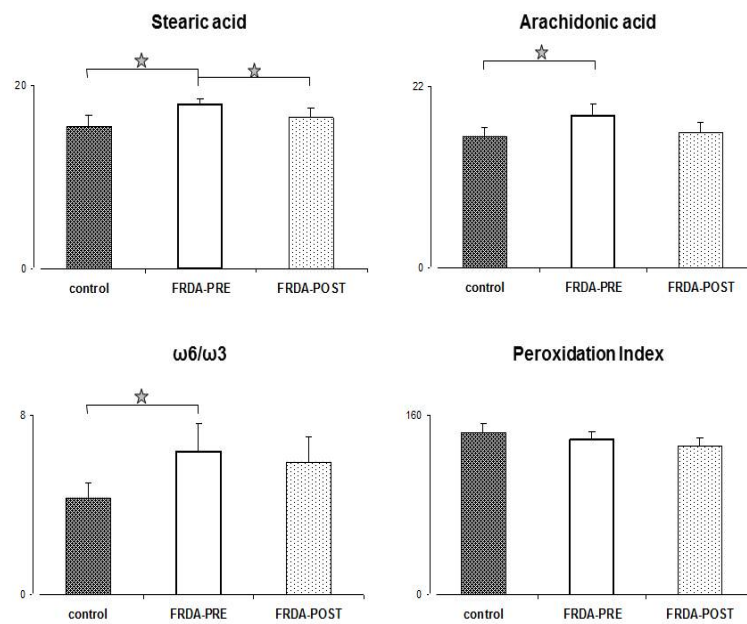
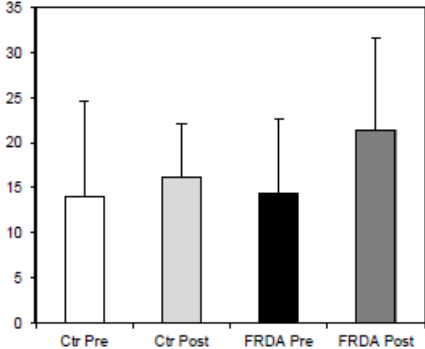


Fig. 3 Relevant lipidomics parameters from normal age-matched controls and from FRDA patients (Mean \pm SD). CTR, normal age-matched controls. FRDA patients before and after the two-month add-on tocotrienol supplementation. Star, $0.01 \leq p \leq 0.05$ by ANOVA. The content of individual fatty acids in erythrocyte membranes is expressed as percentages of the total fatty acids identified.

Urinary Oxidative Markers

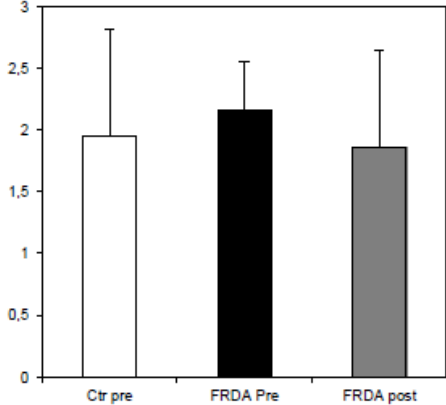
(A)

8-OXO-dG



(B)

Isoprostane



(C)

Hexanoyl -Lysine Adducts (HEL)

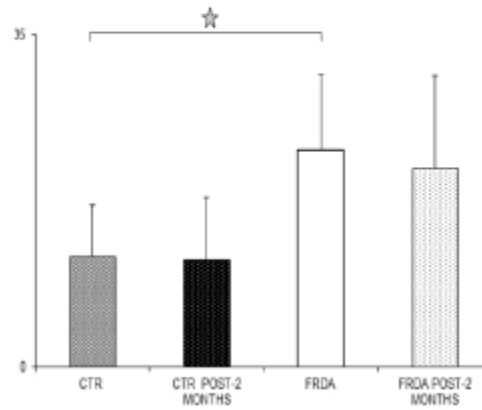


Fig.4 Analysis Urinary Oxidative Markers of urine from normal age-matched controls and from FRDA patients. (A) 8-hydroxy-29-deoxyguanosine (8-OXO-dG) levels measured using the HT 8-oxo-dG ELISA Kit. The 8-oxo-dG concentration was expressed in ng/ mg of creatinine. (B) 8-isoprostane was determined by the use of a competitive ELISA kit. 8-isoprostane concentration was expressed in ng per mg/ creatinine. Controls were evaluated both before (CTR) and following (CTR-POST) a two-month tocotrienol supplementation. FRDA patients were evaluated both before (FRDA-PRE-2 months) and following (FRDA-POST-2 months) a two-month add-on tocotrienol supplementation. Data are expressed as (Mean \pm SD). Star, $0.01 \leq p \leq 0.05$ by ANOVA. (C) (HEL) concentration was measured by a competitive ELISA kit. The concentration was expressed in nmoli/ mg of creatinine.

Oxygen Radical Absorbance Capacity (ORAC)

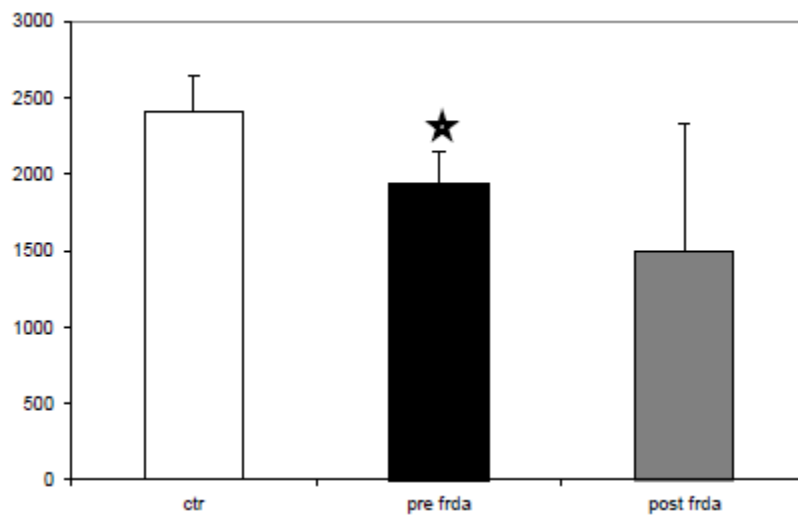


Fig. 5 Oxygen Radical Absorbance Capacity (ORAC) of plasma from normal age-matched controls and from FRDA patients. FRDA patients were evaluated both before (FRDA-PRE-2 months) and following (FRDA-POST-2 months) a two-month add-on tocotrienol supplementation. Data are expressed as $\mu\text{M Trolox/L}$ (Mean \pm SD). Star, $0.01 \leq p \leq 0.05$ by ANOVA.

qRT-PCR Antioxidant genes expressions

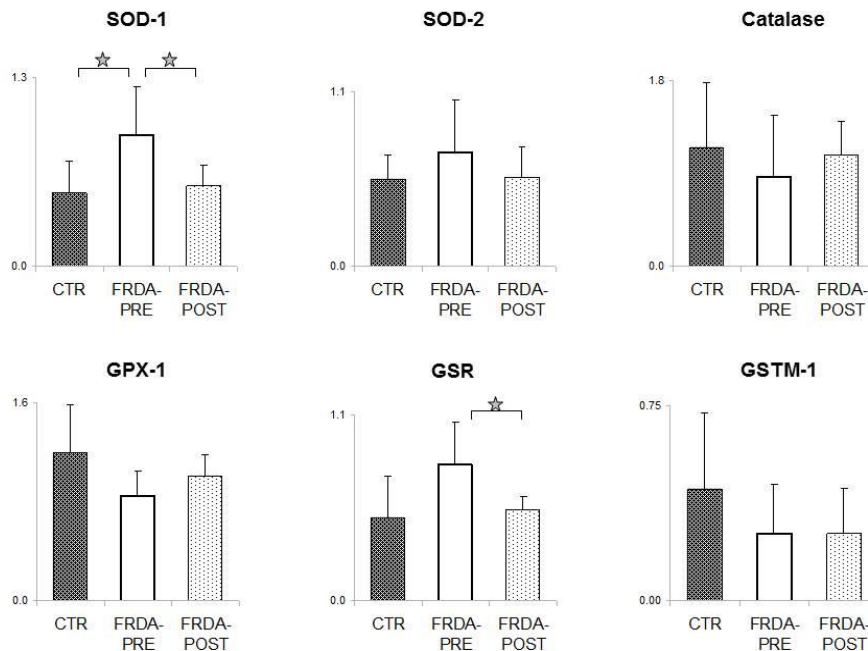
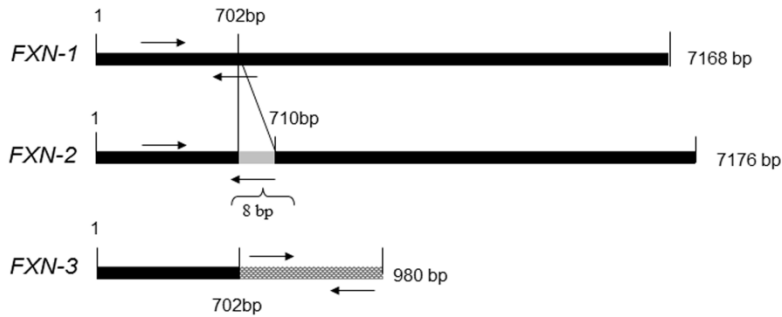


Fig. 6 Gene expression study by qRT-PCR of oxidative stress enzymes in leukocyte extracts of the five FRDA patients examined, before (FRDA, open columns) and after (FRDA-POST, light grey columns) two months of tocotrienol treatment. The same genes were studied also in five age-and-sex-matched controls (CTR, dark grey columns). Data were normalized for two housekeeping genes and are expressed in arbitrary units as Mean \pm SD. SOD-1, Superoxide Dismutase-1; SOD-2, Superoxide Dismutase-2; catalase; GPX-1, Glutathione Peroxidase-1; GSR, Glutathione Reductase; GSTM-1, Glutathione-S-Methyl-Transferase-1. Star, $0.01 \leq p \leq 0.05$ by ANOVA.

Enzymatic digestion of *FXN-1* and *FXN-2* PCR products.

(A) Frataxin isoform cDNAs and primer sequences



(B) Enzymatic digestion of *FXN-1* and *FXN-2* PCR products

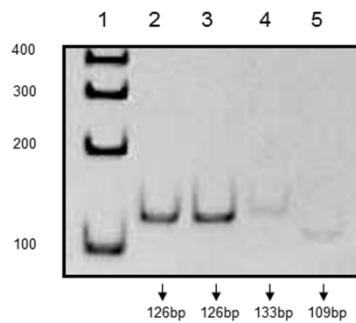


Fig. 7: (A) A representative scheme of frataxin isoform cDNAs and primer sequences. Frataxin isoform 1 (*FXN-1*) and isoform 2 (*FXN-2*) share the left primer sequence, while the right primer was specific for each isoform. Frataxin isoform 3 (*FXN-3*) right primer sequence was designed in the region downstream the 702 base pair. (B) Enzymatic digestion of *FXN-1* and *FXN-2* PCR products. A representative polyacrylamide gel electrophoresis (10%) of *FXN-1* and *FXN-2* PCR products digested or undigested with *Bst*NI restriction enzyme. Lane 1: DNA ladder; lane 2: undigested *FXN-1* PCR product; Lane 3: *Bst*NI digested *FXN-1* PCR product; lane 4: undigested *FXN-2* PCR product; lane 5: *Bst*NI digested-*FXN-2* PCR product.

PCR analysis of frataxin isoforms in a healthy subject

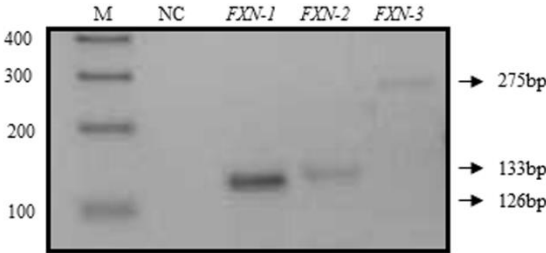


Fig. 8: Semiquantitative PCR analysis of frataxin isoforms in a healthy subject. Equal amount of a control subject cDNA was used for *FXN-1*, *FXN-2*, and *FXN-3* semiquantitative PCR analysis. PCR products were run in an agarose gel electrophoresis (2.5%). M: DNA ladder; NC: negative control.

qRT-PCR expression of frataxin isoforms

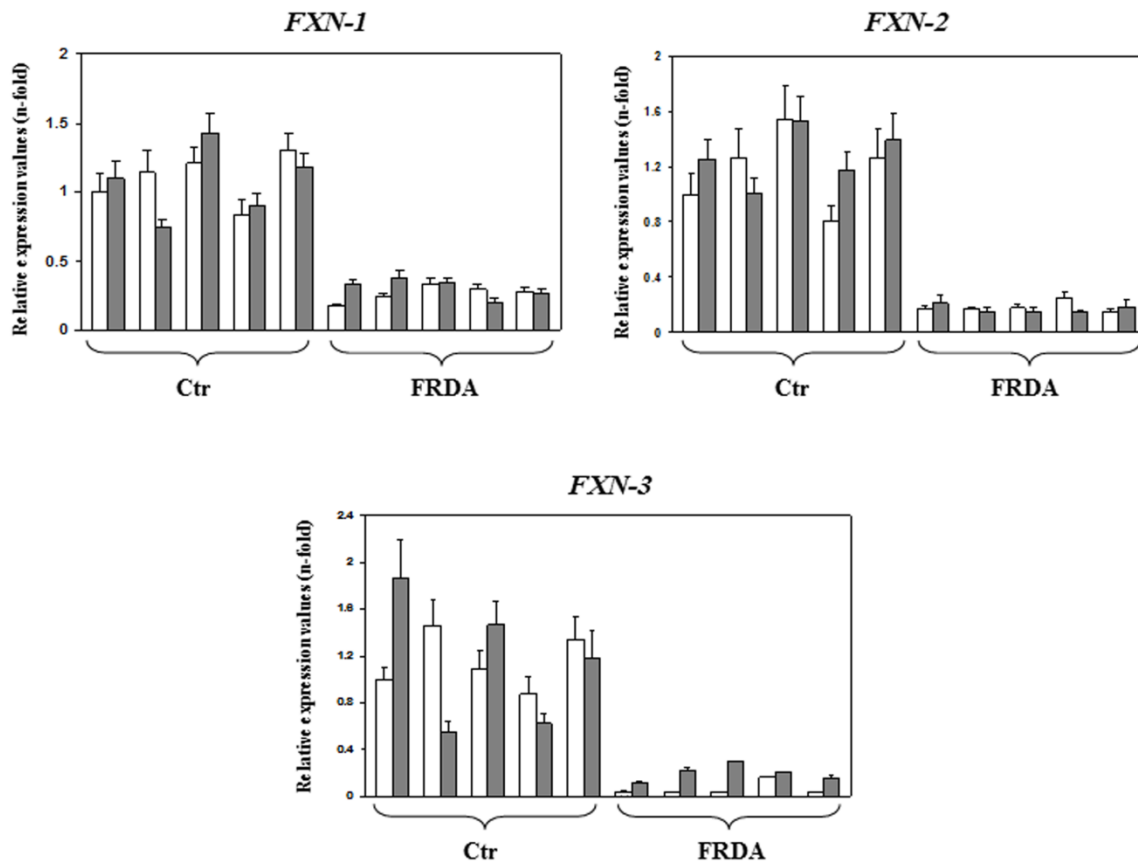


Fig. 9 qRT-PCR expression of frataxin isoforms. Frataxin isoform mRNA expression was analyzed by qRT-PCR in five healthy subjects (Ctr) and in five FRDA patients before (white columns) and after (grey columns) two-month tocotrienol supplementation. Data were normalized for two housekeeping genes, beta-actin and GAPDH; for each gene target, the normalized expression value of one control subject arbitrarily chosen was set to 1, and all other gene expression data were reported to that sample. Data are expressed as mean of technical triplicates } SD and analyzed by ANOVA. Following tocotrienol supplementation, *FXN-3* mRNA increased 3.49-fold in FRDA patients ($p \leq 0.00000000342$).

qRT-PCR expression of *PPARG*

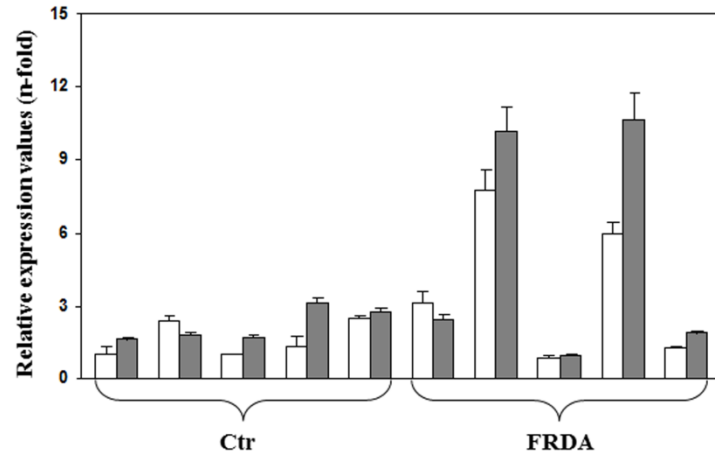


Fig. 10: qRT-PCR expression of *PPARG*. Peroxisome proliferator-activated receptors- γ (*PPARG*) mRNA expression was analyzed by qRT-PCR in five healthy subjects (Ctr) and in five FRDA patients before (white columns) and after (grey columns) two months tocotrienol supplementation. Data were normalized for two housekeeping genes, beta-actin and GAPDH; for each gene target, the normalized expression value of one control subject arbitrarily chosen was set to 1, and all other gene expression data were reported to that sample. Data are expressed as mean of technical triplicates \pm SD and analyzed by ANOVA.

Structural comparison of human FXN-1 with FXN-2 and FXN-3.

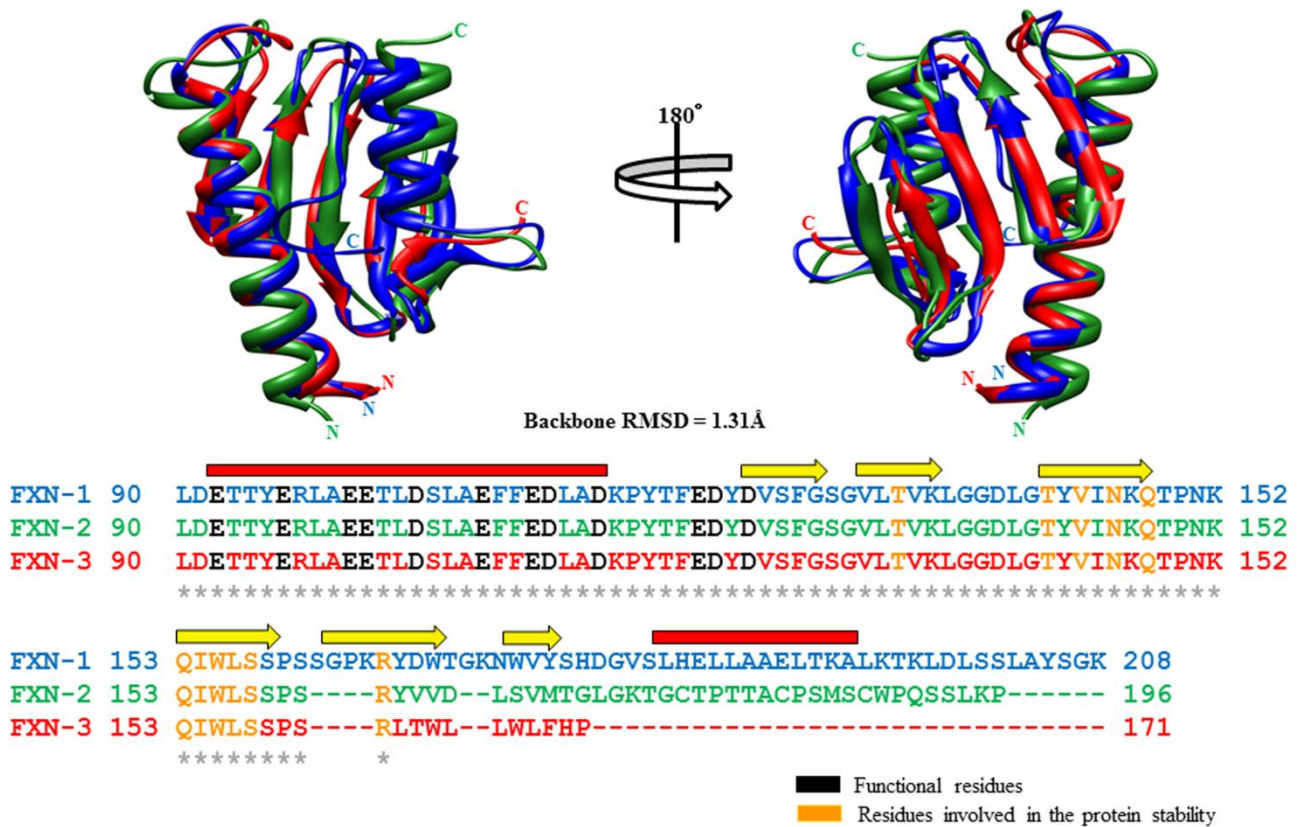


Fig. 11: Structural comparison of human FXN-1 with FXN-2 and FXN-3. Sequence and structural alignment of FXN-1 (1EKG, depicted in blue) with the computed 3D models of FXN-2 and FXN-3 (colored in green and red, resp.). The secondary structure of FXN-1 is also reported along the structural alignment (helices: red line; beta sheets: yellow arrow). Functional residues of the anionic patch and residues involved in protein stability are highlighted in black and orange, respectively, and are conserved in all the isoforms.

Docking of human FXN-1, FXN-2, and FXN-3

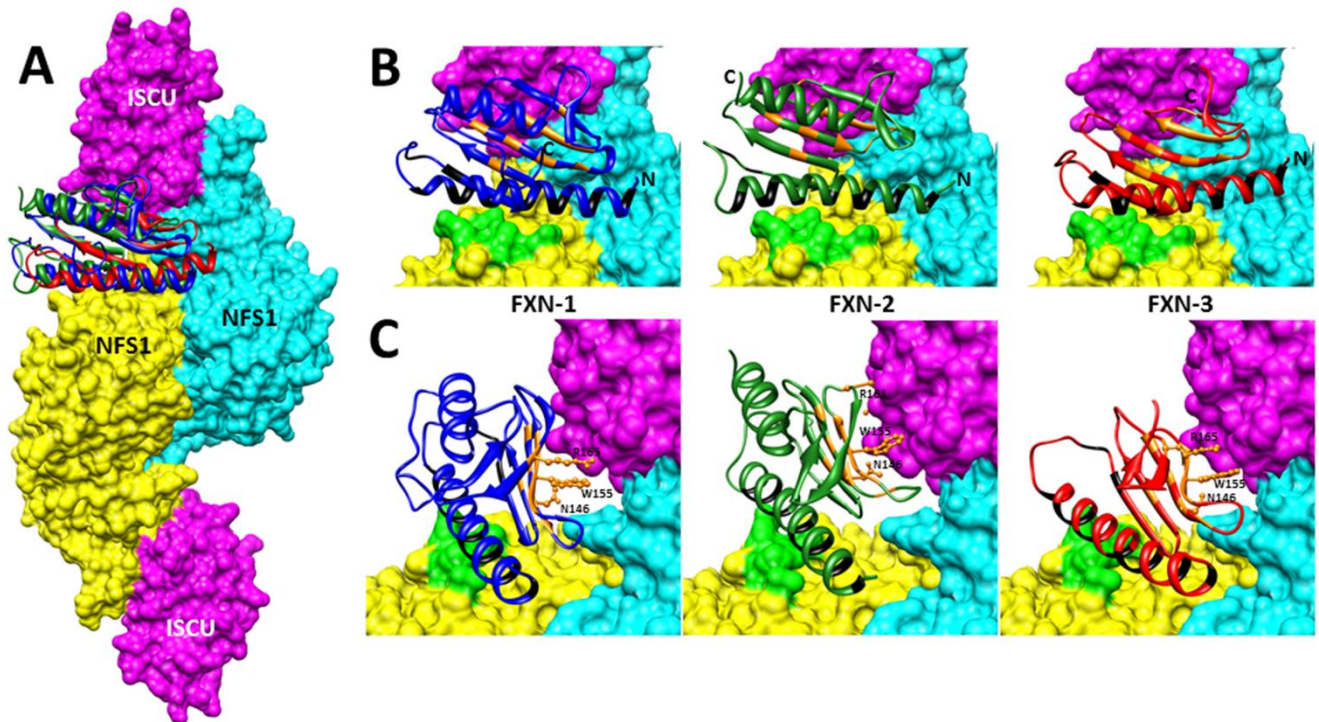


Fig. 12: Docking of human FXN-1, FXN-2, and FXN-3 on the human tetrameric NFS1/ISCU complex. (a) The human iron-sulfur assembly complex was modeled adopting the *E. coli* counterpart as a template (PDB code: 3LVL). The NFS1/ISCU complex includes two copies of ISCU (surface representation in purple) and two copies of NFS1 (surface in cyan and yellow, resp.). The backbone of the three frataxin isoforms is depicted in blue (FXN-1), in green (FXN-2), and in red (FXN-3). The three backbones overlap with a pairwise root mean square deviation (RMSD) of about 1.3 \AA . (b) Important residues essential for functional interaction are conserved in all isoforms and highlighted in black. Relevant interactions on the complex are highlighted in orange. Basic residues of NFS1 involved in the interaction with the anionic patch of frataxin (R218, R219, R221, and R223) are colored in light green. (c) Zooming on conserved residues among human frataxins was experimentally proven in yeast and humans to play a critical role in the interaction with the ISCU complex: W155 N146 and R165 (R161 in FXN-2 and FXN-3).

Discussion and Conclusions

Part I

Data obtained in the first part of my research project are the results of a small-scale trial involving five young FRDA patients who were treated for two months with a low dose of tocotrienol. Notwithstanding the limited number of examined subjects, our results show that most oxidative stress parameters studied gave clear indications that FRDA patients still suffered of oxidative stress; despite chronic idebenone treatment. The expression of all antioxidant enzyme transcripts in FRDA patients circulating mononuclear cells differed from that of healthy controls, thus suggesting *per se* an unbalance in anti-oxidant defenses of FRDA patients, despite their being treated with idebenone. Moreover, the expression level of most antioxidant genes was consistently modified upon the two-month tocotrienol add-on treatment, resembling that of healthy controls. Patients had an increased transcription of SOD-1, SOD-2 and GSR genes, which is consistent with the fact that these genes are known to be induced by reactive oxygen species (ROS) (Bubici et al., 2006 and Bernadt et al., 2007) and that chronic oxidative stress in FRDA patients' fibroblasts has been shown to increase the level of basal SOD enzymatic activity (Paupe et al., 2009). Catalase and GPX-1 both reacting with peroxides had a reduced mRNA expression in FRDA patients, as already seen in FRDA fibroblasts (Kemp et al., 2001) We showed that, upon tocotrienol treatment, the patients' relative abundance of five out of six examined mRNAs (with the sole exception of GSTM-1) tended to resemble that of normal controls. We also showed that the plasmatic GSH/GSSG ratio tended to normal values following treatment. It should be stressed that the GSH/GSSG ratio values are considered to be a more feasible measure of the plasma redox capacity than the absolute amount of GSH and GSSG (Jones et al., 2006). Carbonyl groups (*i.e.* aldehyde or ketone groups) result from the oxidation of some amino acids (Stadtman et al., 2000) and serve as useful markers for metal-catalyzed protein oxidation that occurs under conditions of oxidative stress. The evaluation of this relevant marker in plasma proteins leads to the same conclusions reached by examining the other parameters discussed above, FRDA patients were found to display clear signs of oxidative stress, which was relieved by tocotrienol. Moreover, we found a baseline difference in urinary HEL levels between FRDA patients and healthy controls. Hexanoyl-Lysine (HEL) adducts formation results from the reaction of linoleic or arachidonic acid hydroperoxide or of 4-hydroxy-nonenal with Lysine residues. It is an oxidative stress marker (Kato et al., 1999) which may be evaluated also in urine. However, no differences are observed in the levels of urinary markers 8-OXO-dG and Isoprostane.

Plasmatic ORAC (Oxygen Radical Absorbance Capacity) values clearly show that FRDA patients' have a reduced plasma antioxidant capacity whereas no change is apparent upon two month treatment only. ORAC is the only oxidation index obtained from plasma that does not change upon two month tocotrienol treatment, so that it may be suggested that it is not a very sensitive indicator of the tissue oxidative stress. The evaluation of oxidative stress has been here approached also by lipidomics. The analysis of lipidic profile allows to assess changes of metabolic pathways that occur at the expense of the membrane in response to stressful cellular events. (Chatgililoglu et al., 2008). Fatty acid membrane composition of erythrocytes is representative of that of relevant tissues, such as liver, heart and kidney (Zambonin et al., 2006) and is affected by a number of pathological conditions, in particular by inflammation and oxidative stress. It is worth mentioning that peroxidation index gives an estimation of PUFA index prone to peroxidation, whereas the occurrence of oxidative stress is linked to an inflammatory status which in turn is correlated with the arachidonic acid content. The global lipidomics approach allowed us to track the presence of lipid peroxidation in FRDA patients based on the combined reduction in membrane $\omega 3$ and the increase in stearic acid content. In fact, peroxidation of polyunsaturated fatty acids (such as $\omega 3$) induces a higher rate of membrane fatty acid turnover, hence an increased stearic acid content. Noteworthy, stearic acid is associated with the induction of TNF- α , a mediator of inflammatory processes (de Lima Salgado et al., 2011). Also associated with a pro-inflammatory profile of FRDA patients is the increased content in arachidonic acid and the high $\omega 6/\omega 3$ ratio (Wall et al., 2010). The increased of arachidonic acid found in erythrocyte membranes from FRDA patients is confirmed by the increased formation of fatty acid peroxides-lysine adduct we measured. It is thus encouraging that two-month tocotrienol treatment led towards a decrease of both stearic and arachidonic acid and somehow also of the $\omega 6/\omega 3$ ratio; in fact it may be hypothesized that protracting further the anti-oxidant treatment might result into the normalization of the patients' lipid membrane profile. In conclusion, our data has demonstrated that tocotrienol supplementation is able to considerably abate oxidative stress even when administered at very low doses (5 mg/kg body weight/day) and for two months only; moreover, there is evidence that a longer tocotrienol treatment may be even more effective. Recently, was pointed out the striking similarities of the symptoms in vitamin E deficiency and Frataxin deficiency (Di donato et al., 2010). The remarkable efficacy of tocotrienol supplementation in abating oxidative stress indexes in FRDA patients suggests that FRDA patients are actually lacking of antioxidant power at the membrane level. However, due to the impaired ability of FRDA cells to cope with ROS, the association of more than one antioxidant may be even more effective. Future work will be addressed at the evaluation of the

effects of a cocktail of antioxidants, both in FRDA cell cultures and in the patients, exploiting the model here developed to investigate the efficacy of the approaches for oxidative stress damage protection.

This encouraging results, (*Marini et al., submitted*) prompted us to investigate whether tocotrienol could modulate the expression of the different isoforms of frataxin mRNA. Here we report for the first time that tocotrienol induces, exclusively in FRDA patients, a significant 3.49 fold increase of the *FXN-3* isoform mRNA. Such increase is specific, since it does not affect *FXN-1* or *FXN-2*. Although, we are aware that the increase in *FXN-3* gene expression should be confirmed by an analysis of protein expression, at present, it is not possible to measure protein expression of the *FXN-3* isoform because a specific antibody it is not available. Marmolino and co-workers showed that peroxisome proliferator-activated receptors- γ (PPARG) is involved in the up-regulation of mRNA and protein frataxin expression in cell lines from FRDA patients. Tocotrienols both increase mRNA expression of PPAR receptors α , γ , and δ and, by directly binding their LBDs, induce an increase of their transcriptional activities (Fang et al., 2010). *PPARG* gene expression was measured in both treated and untreated subjects in order to evaluate whether tocotrienol enhancement of *FXN-3* was mediated by an increase in *PPARG* expression. The high variability in *PPARG* expression among subjects did not allow a significant conclusion to be reached; however, as already pointed out, tocotrienol may activate *PPARG* transcriptional activities in a way that is independent of its increase (Fang et al., 2010). On the other hand, tocotrienol may promote *FXN-3* mRNA expression through signalling pathways alternative to *PPARG*, as tocotrienols are able to modulate different targets at transcription, translation and post-translation levels (Aggarwal et al., 2010). Whether the tocotrienol-induced increase in *FXN-3* expression is biologically relevant obviously depends on the ability of the *FXN-3* isoform to perform its tasks. To our knowledge, no functional and structural studies have been carried out for the *FXN-3* isoform, therefore we performed a structural analysis by means of bioinformatics tools. *FXN-3* and *FXN-1* share a 93% protein sequence identity; from the comparison of their sequences, the residues known to be correlated with protein function (Dhe-Paganon et al., 2000) and with stability (Leidgens et al., 2010) were found to be well conserved in sequence, secondary and tertiary structures. By modeling of the iron-sulphur assembly complex from *E. coli* and computing from it the 3D structure of the human tetrameric complex, we found that all relevant interactions are conserved between *FXN-1*, *FXN-2* and *FXN-3*), with comparable docking binding energy. Despite the partial or total lack of the C-terminus alpha helix, these data show that both *FXN-2* and *FXN-3* not only have an identity of structure compared to *FXN-1* but

also have the same ability to interact with NFS1/ISCU. These bioinformatics data show for the first time that both FXN-2 and FXN-3 may have a biological function and can be considered a starting point for future studies aimed at confirming the function of both FXN-2 and FXN-3 isoforms by using the purified protein. In conclusions, our results demonstrate, for the first time, i) that tocotrienol induces in FRDA patients the up-regulation of the *FXN-3* mRNA isoform; ii) that FXN-3 and FXN-2 proteins share the same 3D structure as FXN-1 and are apparently able to complex with NFS1/ISCU, thus suggesting that they may play the same functions. Since basal level of *FXN-3* is very low, its 3.49 fold increase in tocotrienol-treated patients was not enough to reach frataxin mRNA amounts enabling normal cellular functions (Gellera et al., 2007). The mechanism by which tocotrienol enhances *FXN-3* mRNA levels should be further investigated. In fact, it has been reported that SRF and TFAP2 iron-dependent transcription factors regulate frataxin expression (Li et al., 2010) and that tocotrienol stimulates PPARG activity dose-dependently (Fang et al., 2010). Therefore, we are planning to evaluate in FRDA cell lines whether higher tocotrienol concentrations could further enhance frataxin mRNA levels, in PPARG dependent or independent manner. Cell culture studies will also allow the evaluation of variations in frataxin protein levels, which is almost impossible to perform in mononuclear cells, which are poor frataxin producers. This will hopefully enable the use of tocotrienol not only as antioxidant therapy but also as inducer of frataxin expression.

Chapter V

Generation of human induced Pluripotent Stem Cells (hiPSCs) from Friedreich's Ataxia (FRDA) patients

Materials and Methods (Part II)

Cells lines

Fibroblasts, human induced pluripotent stem cells (hiPSCs), neurospheres, neurons, and HEK293T cells were grown at 37 °C and 5% CO₂. Fibroblasts were cultured with 10% FBS in minimal essential medium, 2 mM glutamine, 1% non-essential amino acids, 20 mM HEPES, and 1% antibiotic/antimycotic (Invitrogen). iPSCs were grown on irradiated mouse embryonic fibroblasts (GlobalStem, Rockville, MD) in DMEM/F-12 with 20% KnockOut serum replacement, 1 mM glutamine, 1% nonessential amino acids, 1% antibiotic/antimycotic, 0.1 mM Beta-mercaptoethanol (Invitrogen), and 20 ng/ml basic FGF (Stemgent, San Diego, CA) and passaged manually every 7 or 8 days. Neurospheres were grown in Neurobasal-A medium with 2% B-27 supplement, 1% N-2 supplement, 2 mM glutamine, 1% antibiotic/antimycotic, 10 mM HEPES, 20 ng/ml basic FGF, and 20 ng/ml EGF (R&D Systems). Neuronal cells were grown on matrigel in Neurobasal-A medium with 2% B-27 supplement, 1% N-2 supplement, 2 mM glutamine, 1% antibiotic/antimycotic, and 10 mM HEPES. HEK293T cells were grown with 10% FBS in DMEM, 2 mM glutamine, 20 mM HEPES, 1% nonessential amino acids, and 1% antibiotic/antimycotic.

Isolation of primary fibroblasts

Dermal explant cultures were established from dispase-treated skin biopsies on fibronectin underneath a glass coverslip with fibroblast media after 5–7 days. After establishment, primary dermal fibroblasts were cultured as described above. Biopsies were performed under an approved Human Subjects Protocol. (For phenotypic and genotypic features of fibroblasts see the supplementary materials Part II, Table 1 and Table 2)

Retrovirus production

Retroviruses were packaged via Phoenix cells and Lipofectamine (Invitrogen). The four reprogramming vectors (Yamanaka et al., 2007) (<http://www.addgene.org>) were packaged individually and pseudotyped with VSV-G.

Derivation of iPSCs

Donor fibroblasts were transduced daily for 3 consecutive days, and 4 to 6 days after the last transduction, cells were replated onto MEFs. Beginning 1 day following, cells were given ESC media daily. Colonies were picked between 21 and 28 days after transduction.

Derivation of Neurospheres and Neural Differentiation

iPSC colonies were passaged onto high-density-irradiated mouse embryonic fibroblasts (at 60×10^3 cells/cm²) with ROCK inhibitor (10 μ M; Stemgent). Induction was performed with either LDN (0.5 μ g/ml; PeproTech Inc., Rocky Hill, NJ) or (5 μ M; P5499, Sigma-Aldrich) and SB431542 (10 μ M; 040010, Stemgent) in ESC medium. During induction, FRDA iPSCs were maintained for 2 weeks without passage. Subsequently, induced colonies were dissected and transferred to suspension culture as neurospheres in neurobasal-A medium with EGF (20 ng/ml) and basic FGF (20 ng/ml). Neurospheres were maintained as a suspension culture and passaged manually every 4–5 days. Neural differentiation was performed by dissociating neurospheres with Accutase (Invitrogen) and replating onto matrigel-coated plates at the density of 100,000 cells. Neurons were maintained in Neurobasal-A medium without EGF or FGF for 7 or 8 days after replating.

Characterization of Neurons

iPSCs-neurons derived, were grown on poly-lysine coated six-well plates. Monoclonal anti-neuron-specific class III β -tubulin (TuJ1) antibody (MMS-435P) (Covance Inc) (1:1000 dilution) was used as a neuronal marker. Fluorescent secondary antibody (goat-anti mouse IgG) was obtained from Santa Cruz Biotechnology and used at 1:1000 dilutions. Nuclei were stained with 1 μ g/ml DAPI for 20 min. The images were obtained with a Leica microscope.

Transfection HEK293 cells with pcDNA3.1 Flag Asn46 and pcDNA3.1 Flag tagged Ser46

HEK293T cells were seeded at a density of 0.3×10^6 /ml in DMEM medium without antibiotics and transfected with the carrier pcDNA3.1.Flag tagged fusion protein (Addgene). The Ser46 version of Sirt6 was derive by site directed mutagenesis by the Asn46 version available from Addgene, which is cloned in the FLAG-tagged mammalian expression vector pcDNA3.1 (see <http://www.addgene.org/13817/>). Both, the prevalent Sirt 6 version Asn46 or the rare Ser46 allelic variant are cloned as FLAG-tagged fusion proteins in HEK293 cells. The transfection was performed using Lipofectamine (Life Technologies) and in accordance with the instructions provided by the company.

Identification of Sirt6 SNP status by PCR amplification and direct sequencing

A standard PCR was performed to amplify the sequence corresponding to the Sirtuin 6. 20ng of DNA were used with 50 μ M primer SIRT6 (GAC ACA TCC AGG AAA GC) and cycled making use the following: denaturation at 98 ° C for 5 minutes, 98 ° C 5 seconds, annealing at 62 ° C for 15 sec, extension at 72 ° C for 15 sec, for 40 cycles. Subsequently, the band corresponding to Sirt6 was separated by electrophoresis on agarose gel and extracted using Qiaquick Gel kit extraction kit (Qiagen) genotyping was performed by facilities Eton Bioscience (San Diego California).

Nucleic Acid Purification

Total RNA was purified with the RNeasy Plus Mini kit (QIAGEN) according to the manufacturer. Genomic DNA was purified by isopropanol precipitation of cell lysates prepared in total cell lysis buffer (100 mM Tris, 5 mM EDTA, 0.2% SDS, 0.2 M NaCl, 200 mg/mL proteinase K [pH 8]).

PCR and Quantitative RT-PCR

For GAA•TTC triplet-repeat length conventional PCRs, Phusion polymerase (New England Biolabs, Ipswich, MA) was used according to the manufacturer. 20 ng of genomic DNA and 0.1 μM primers GAA-104F and GAA-629R were used in 20 μl of reactions cycled through the following conditions: denaturation at 98 °C for 5 s, annealing at 70 °C for 15 s, and extension at 72 °C for 90 s for 40 cycles with a 5-min initial denaturation and a 5-min final extension. Quantitation of PCR band size was performed using an inverse power function directly correlating gel migration of a molecular weight ladder to its known sizes. Quantitative RT-PCR analysis was done with the qScript One-Step SYBRGreen qRT-PCR kit (Quanta Biosciences) according to the manufacturer. All primers for pluripotency markers and FXN, SirT6, Beta Actin and GAPDH genes are described in Supplementary materials (Table 3 and Table 4, Part II). Analysis of relative qRT data was performed via $2^{-\Delta\Delta CT}$ method (Livak et al; 2001)

Western Blot Analysis

Whole cell extracts (in 50 mM Tris [pH 7.4], 150 mM NaCl, 10% glycerol, 0.5% Triton X-100, protease inhibitor; Roche) were electrophoresed in polyacrylamide gels and transferred onto nitrocellulose membranes. Primary antibodies were incubated overnight, and secondary antibodies were incubated 1 hr at room temperature. Antibody incubation was performed in 3% BSA in TBS containing 0.1% Tween 20. Anti-αLN 13 (2765S) and anti-GAPDH (9484) antibodies were obtained from (Cell Signaling) and used at 1:2000 and 1:1000 dilutions, respectively. Anti-SirT6 (2590S) and Anti-SirT6 (62739) and antibodies were obtained from Cell Signaling and abcam, respectively, and used at 1:250 dilutions. IRDye 680LT-conjugated goat anti-mouse IgG (H +L; 926-68020) and IRDye 800CW-conjugated goat anti-rabbit IgG (H+L; 926-32211) secondary antibodies were obtained from LI-COR Bioscience and used at a dilution of 1:5000.

Immunocytochemistry

Cells were fixed in 4% paraformaldehyde and permeabilized with PBS 1X and 0.1% Triton X-100. Primary antibodies Oct4, Tra1-81, Tra1-61, SSEA4, were obtained from Millipore (MAB4305,

MAB4381, MAB4303, and MAB4304) and were all used at 1:50 dilution and incubated at 4 °C overnight. Fluorescent secondary antibodies were obtained from Santa Cruz Biotechnology (anti-mouse Texas Red conjugate, anti-mouse FITC conjugate, anti-rat 8 Texas Red conjugate, and anti-rat FITC conjugate). All secondary antibodies were used at 1:100 dilutions and incubated at room temperature for one hour followed by nuclear staining with DAPI.

Supplementary materials (Part II)

Table 1; Phenotypic and Genotypic data of Healthy and FRDA patients

Sample ID	Gender	Age	GAA Repeat Lengths
GM08333	Male	5MO	/
GM04078	Male	30	541-420
GM03816	Female	36	330-380

Table 2; Phenotypic and Genotypic data of FRDA patients harboring Sirt6 Asn 46/Ser46

Sample ID	Gender	Age	Age of Onset	GAA Repeat Lengths
FA50	Male	31	15	454- 777
FA272	Male	22	14	566-866
FA78	Female	60	43	41-696
FA71	Male	36	18	229-1043

Table 3; Primer sequences of the genes studied with RT-PCR

Gene	Left	Right
Frataxin	CTG GGT GGA GAT CTA GGA ACC	TTT CCC AGT CCA GTC ATAACG
Sirtuin6	GTC TCC TGG TCA GCC AGA	CTT GGC ACA TTC TTC CAC AA
YWHAZ	ACT TTT GGT ACA TTG TGG CTT CAA	CCG CCA GGA CAA ACC AGT AT
Beta Actin	TGC GTG ACA TTA AGG AGA AG	GTG AGG CAG CTC GTA GCT CT
GAPDH	GAG GTC AAT GAA GGG GTC AT	GAG TCA ACG GAT TTG GTC GT

Table 4; Primer sequences of the pluripotency genes studied with RT-PCR

Gene	Left	Right
OCT-4	CCT CAC TTC ACT GCA CTG TA	CAG GTT TTC TT CCC TAG CT
SOX-2	CCC AGC AGA CTT CAC ATG T	CCT CCC ATT TCC CTG GTT TT
NANOG	TGA ACC TCA GTC ACA AAC AG	TGG TGG TAG GAA GAG TAA AG
REX-1	AAA GCA TCT CCT CAT TCA TGG T	TGG GCT TTC AGG TTA TTT GAC T
TERT-1	TGT GCA CCA ACA TCT ACA AG	GCG TTC TTG GTC TTC AGG AT
GDF-3	AAAA TGT TTG TGT TGC GGT CA	TCT GGC ACA GGT GTC TTC AG
FOXD3	AAG CCC AAG AAC AG C CTA GTG A	GGG TCC AGG GTC CAG TAG TTC
GAPDH	GAG TCA ACG GAT TTG GTC GT	GAG GTC AAT GAA GGG GTC AT

Chapter V: Generation of human induced Pluripotent Stem Cells (hiPSCs) from Friedreich's Ataxia (FRDA) patients

Results Part II

Correlation SNPs and disease severity outcome measures

SNP	GENE	Age of onset	Z2	Z3	9HPT (1/x)	T25W (1/x)	FARS	LCLA
rs34402301	HDAC10	0.12	0.99	0.26	0.91	0.96	0.40	0.04
rs228757	HDAC5	0.92	0.79	0.96	0.89	0.56	0.35	0.57
rs1045288	SIRT3	0.24	0.66	0.37	0.34	0.67	0.40	0.42
rs34162626	SIRT5	0.69	0.88	0.34	0.94	0.35	0.79	0.15
rs352493	SIRT6	0.88	0.0016	0.0008	0.0014	0.0064	0.011	0.69

Tab. 1 p-values for the correlation of SNPs and disease severity outcome measures derived by clinical database of the Collaborative Clinical Research Network in FRDA to assess the effect of SNP polymorphisms on clinical features of FRDA including age of onset, FARS score, performance measures and composites Z2 and Z3, and presence of diabetes, cardiomyopathy or scoliosis. Data was analyzed by assessing the ability of individual SNPs to predict phenotype in regression analysis of specific outcomes measures (e.g., FARS), accounting for the confounding effects of GAA repeat length, sex and age. The majority of SNPs assessed did not predict outcomes. In contrast, a specific amino acid changing polymorphism (rs352493) in *SIRT6* predicted FARS, Z2 and Z3 scores with high significance (P=0.0016;P=0.0008;P=0.0014, respectively).

Western Blot analysis of HEK293 Cells Sirt6 (Asn46+) and (Ser46+)

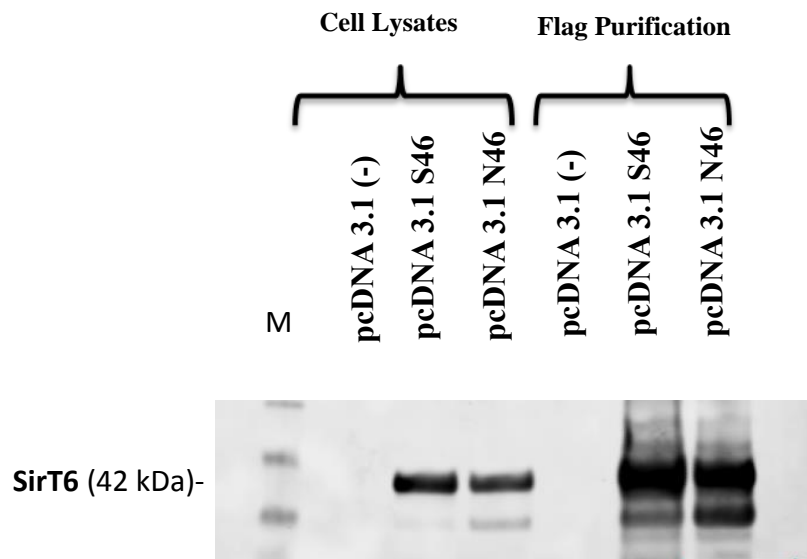
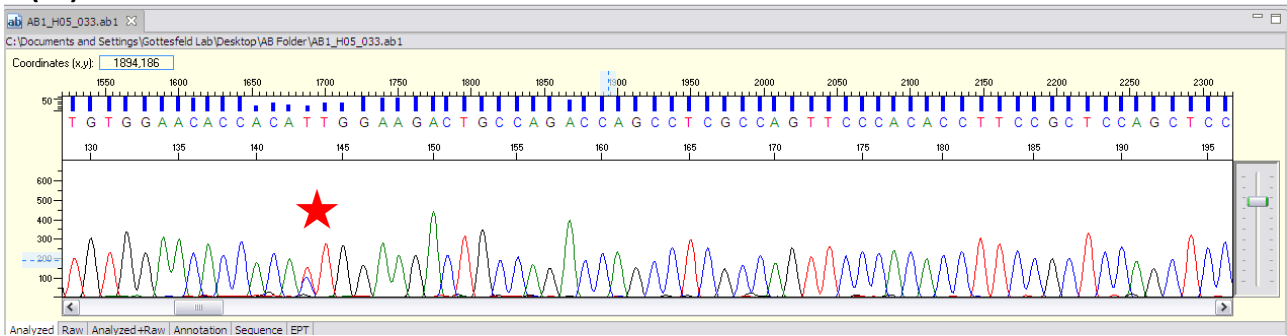


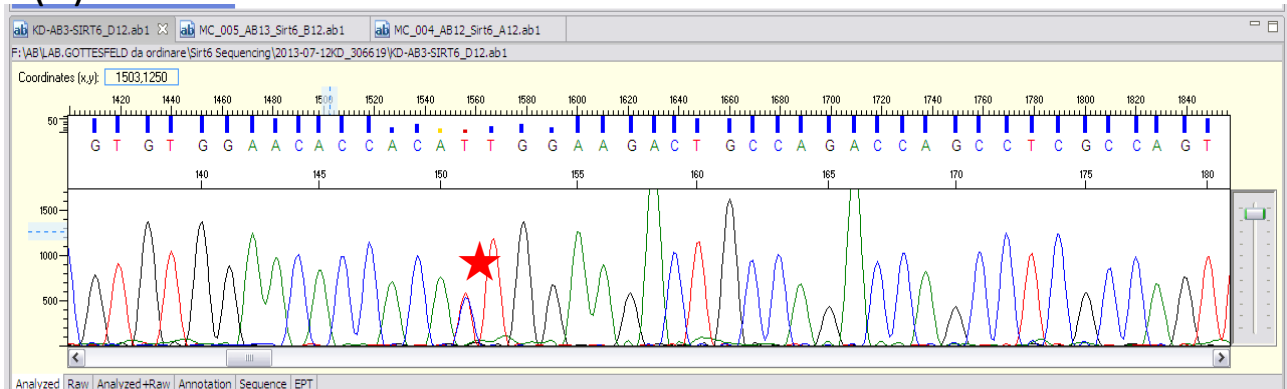
Fig.1 Western blots results for Sirt6 (42 kDa) protein in HEK293 cells transfected with FLAG-tagged mammalian expression vector. From left, pcDNA 3.1.pcDNA 3.1(-) is empty vector, pcDNA 3.1 S46 expressing the rare Ser46 version and pcDNA 3.1 N46 expressing the prevalent Asn46 version.

Genotyping SirT6 SNP [Asn46/Ser46] of FRDA Fibroblasts

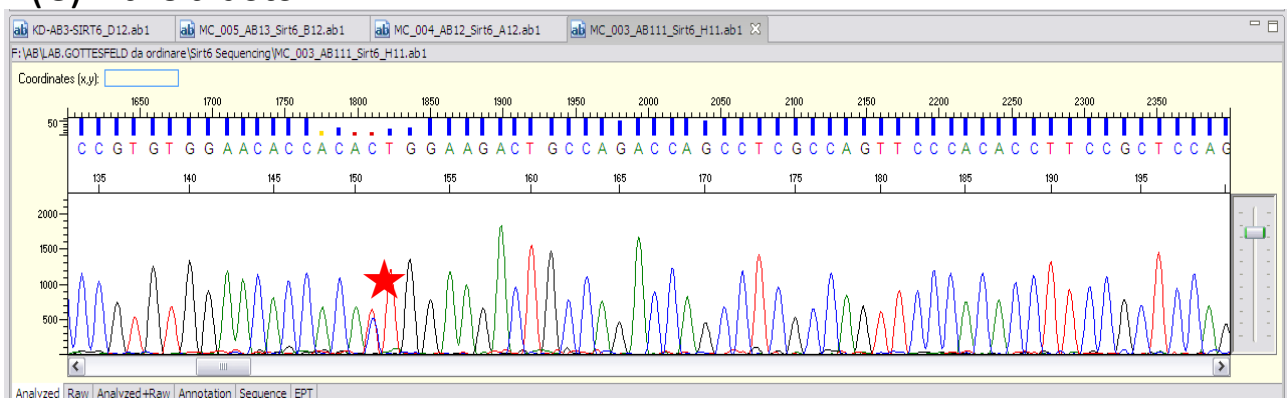
(A) Fibroblast FA50



(B) Fibroblasts FA272



(C) Fibroblasts FA71



(D) Fibroblasts FA78

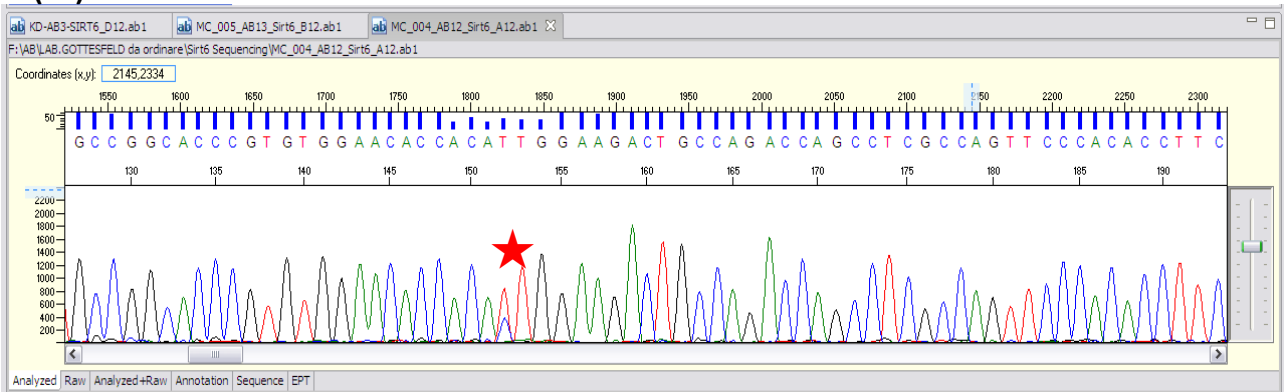
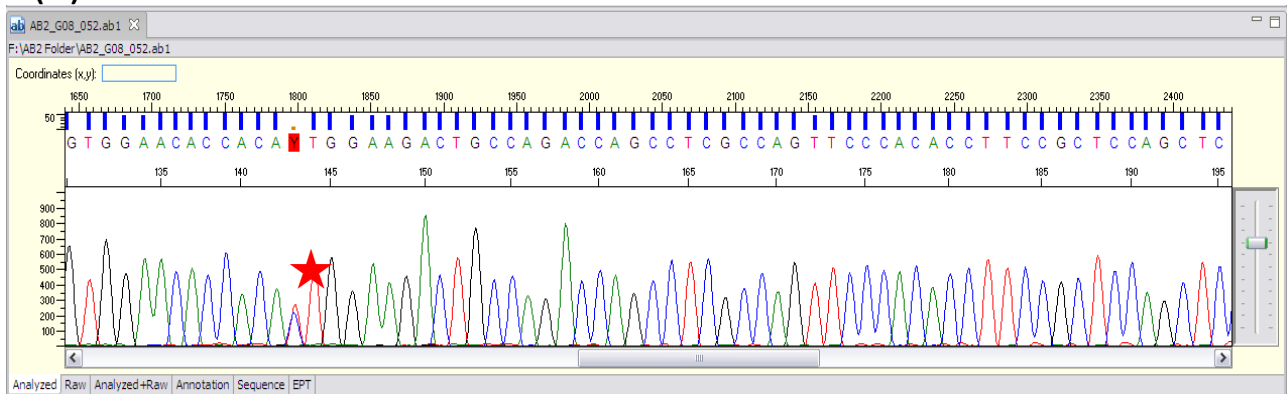


Fig.2 Genotyping of fibroblasts cell lines derived from FRDA patients harboring of Sirt6 SNP (Asn 46/Ser46). The results were obtained from all fibroblast lines by PCR amplification and direct sequencing to check the Sirt6 SNP status.

Genotyping SirT6 SNP [Asn46/Ser46] of FRDA iPSCs

(E) iPSCs FA50



(F) iPSCs FA272

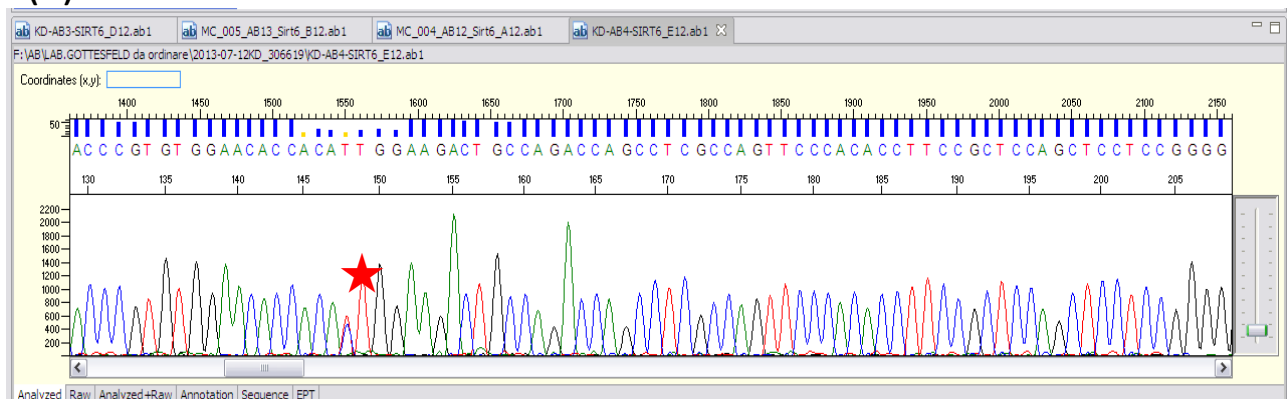


Fig.3 Genotyping of iPSCs derived from fibroblasts FRDA patients harboring of Sirt6 SNP (Asn 46/Ser46). The results were obtained by PCR amplification and direct sequencing confirmed the Sirt6 SNP (Asn46/Ser46).

PCR GAA•TTC repeat length

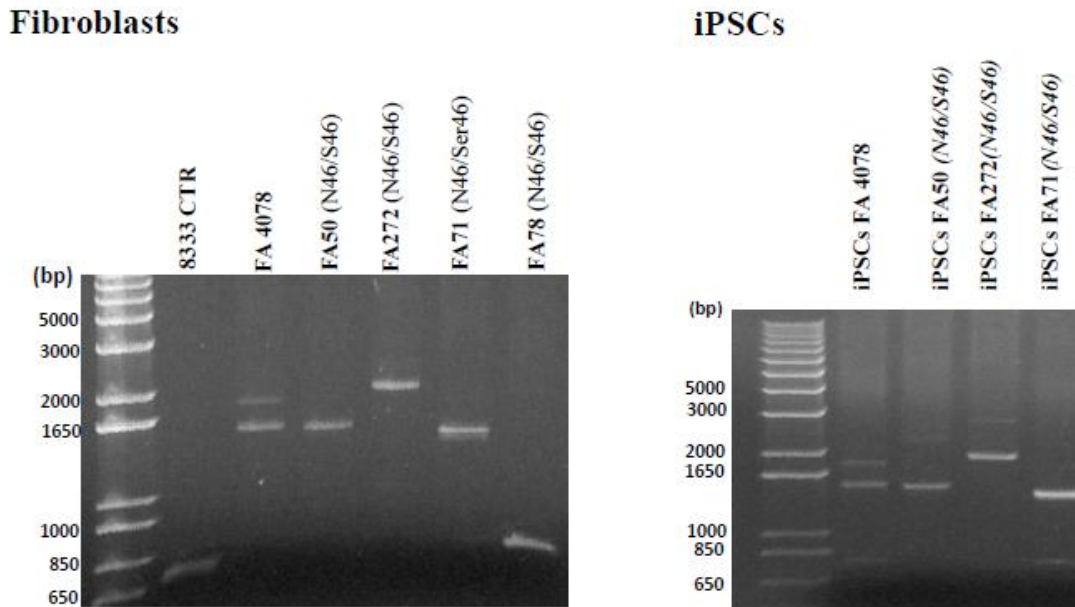


Fig 4 GAA-TTC triplet-repeat expansion analysis in fibroblasts and FRDA iPSCs. From *left to right* gel analysis of PCR products from genomic DNA obtained from fibroblasts and iPSCs FRDA.

Characterization of FRDA iPSCs

qRT PCR Real time pluripotency genes

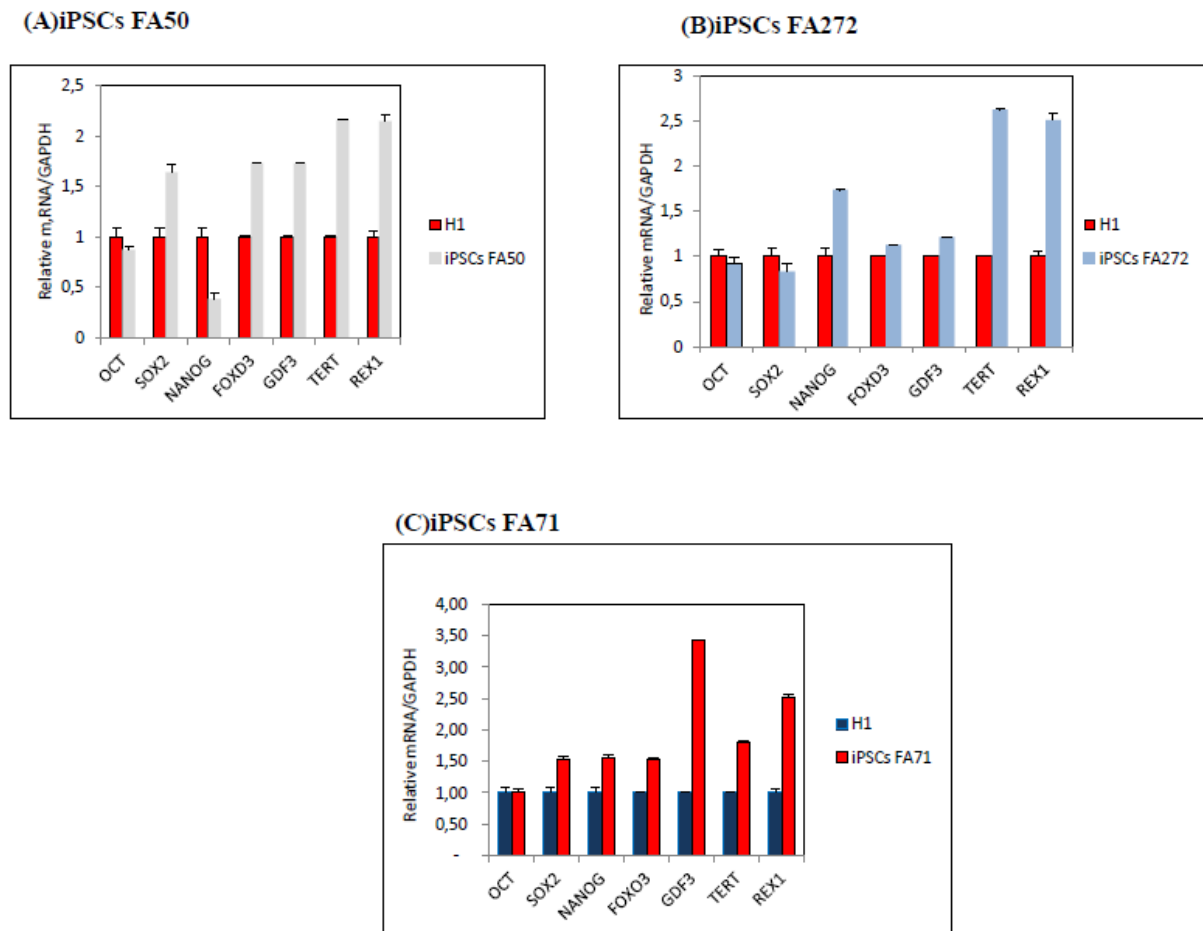


Fig.5 Analysis of pluripotency genes expression in three iPSCs lines derived from fibroblasts of FRDA patients harboring the Sirt6 SNP (Asn46/Ser46) (A) iPSCs FA50, iPSCs (B) and (C) iPSCs FA71 by quantitative real time PCR. All iPSCs cells line shows similar expression of pluripotency mRNAs compared to H1 hESCs. mRNA levels are normalized to GAPDH. Error bars indicate SEM of triplicate measurements.

Immunostaining pluripotency markers.

iPSCs FA50

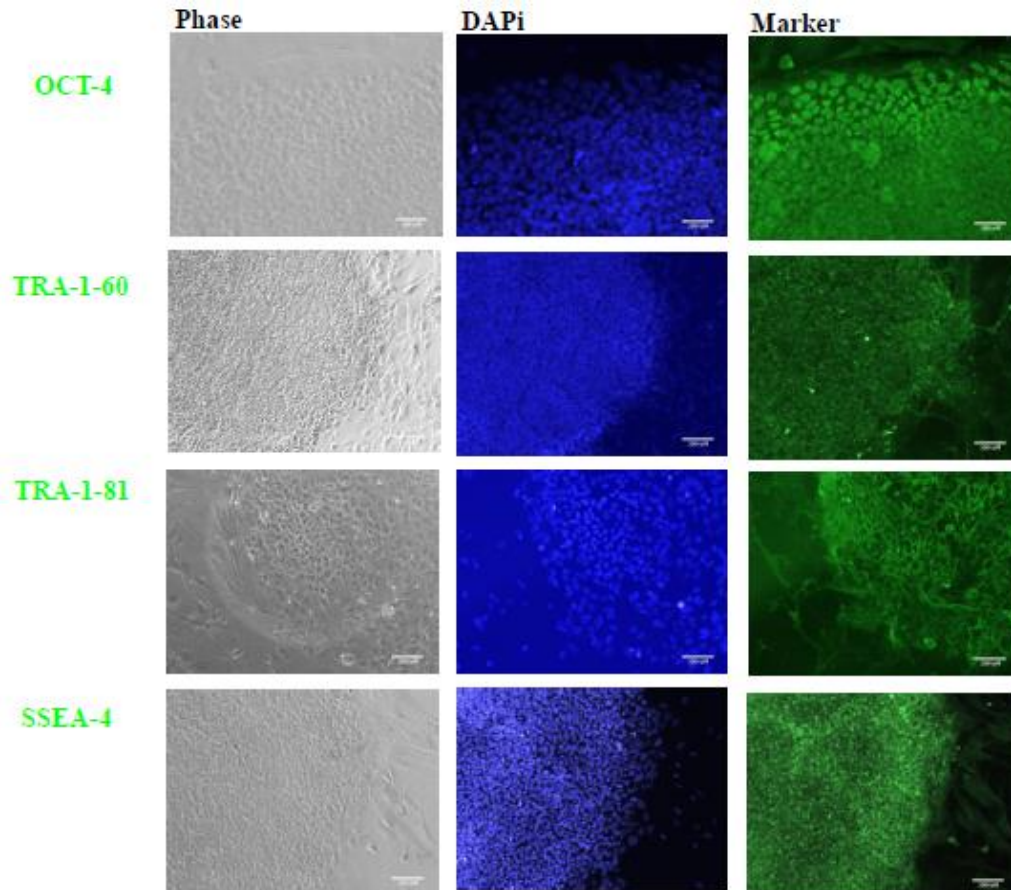


Fig. 6 iPSCs FA50 Immunostaining of pluripotency markers. Phase contrast (gray); nuclear staining (blue); pluripotency markers staining (green) is as denoted by the colored text labels. Tra1-60 and Tra1-81, surface markers; SSEA-4, stage-specific embryonic antigens; Oct4, transcription factor. Scale bars represent 100 mm.

iPSCs FA272

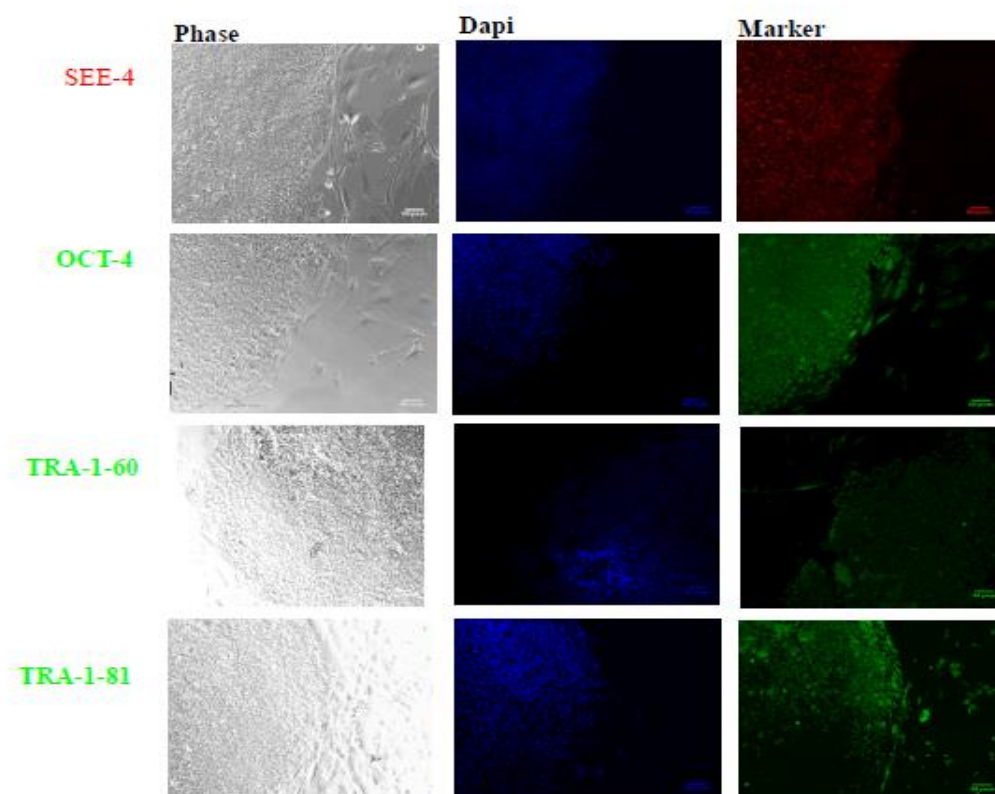


Fig. 7 iPSCs FA272 Immunostaining of pluripotency markers. Phase contrast (gray); nuclear staining (blue); pluripotency markers staining (green and red) is as denoted by the colored text labels. Tra1-60 and Tra1-81, surface markers; SSEA-4, stage-specific embryonic antigens; Oct4, transcription factor. Scale bars represent 100 μ m.

iPSCs FA71

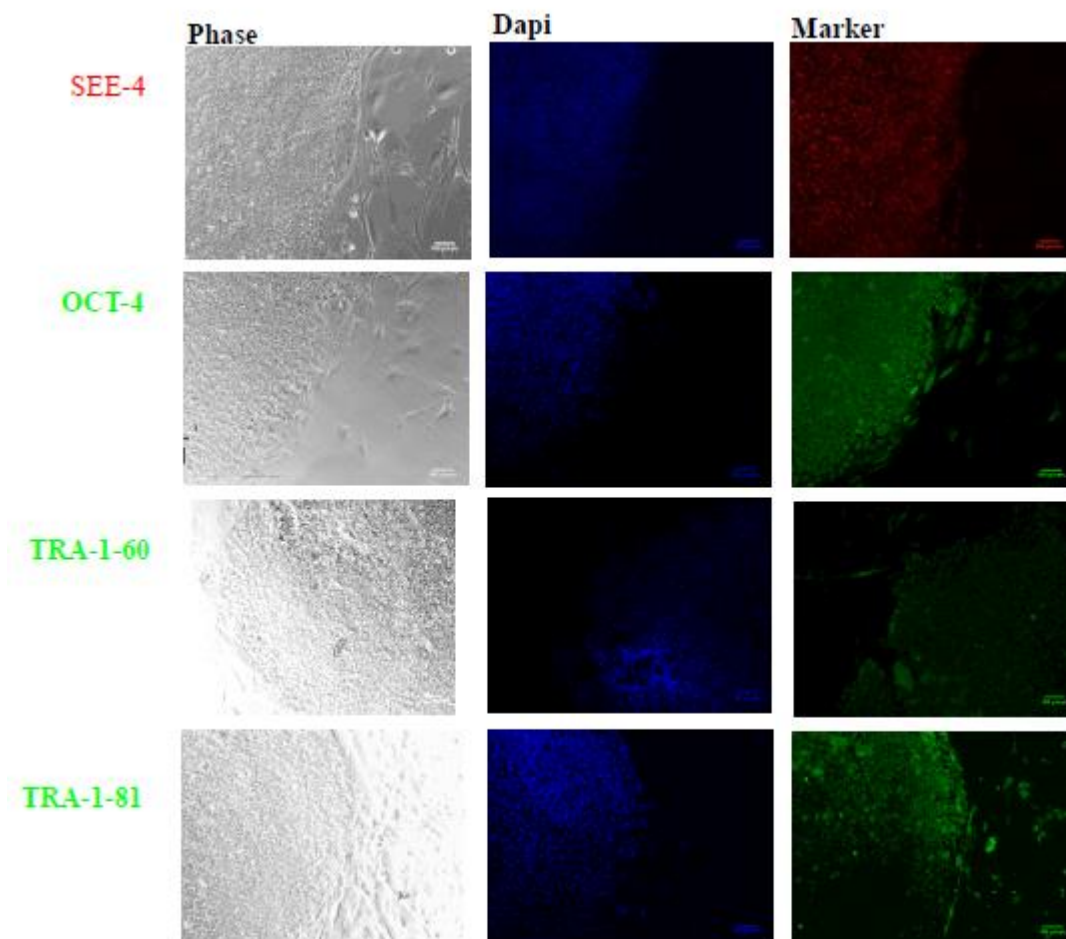
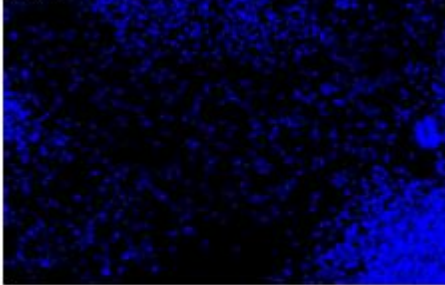


Fig.8. iPSCs FA71 immunostaining of pluripotency markers. Phase contrast (gray); nuclear staining (blue); pluripotency markers staining (green and red) is as denoted by the colored text labels. Tra1-60 and Tra1-81, surface markers; SSEA-4, stage-specific embryonic antigens; Oct4, transcription factor. Scale bars represent 100 μ m.

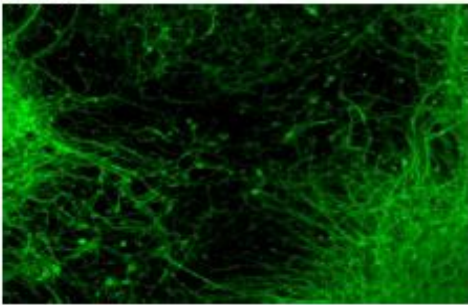
Characterization of FA50 Neurons

Immunostaining neuronal marker (TUJ-1)

Dapi



Marker



TUJ-1 (+)

Fig. 9 Characterization of FA50 iPSCs-derived neurons from patients harboring SNP Sirt6 (ASN46/Ser 46) with antibody against to neurons specific class III β -tubulin (β III), TUJ-1.

qRT PCR Real time analysis FXN and SirT6 expression in FRDA fibroblasts

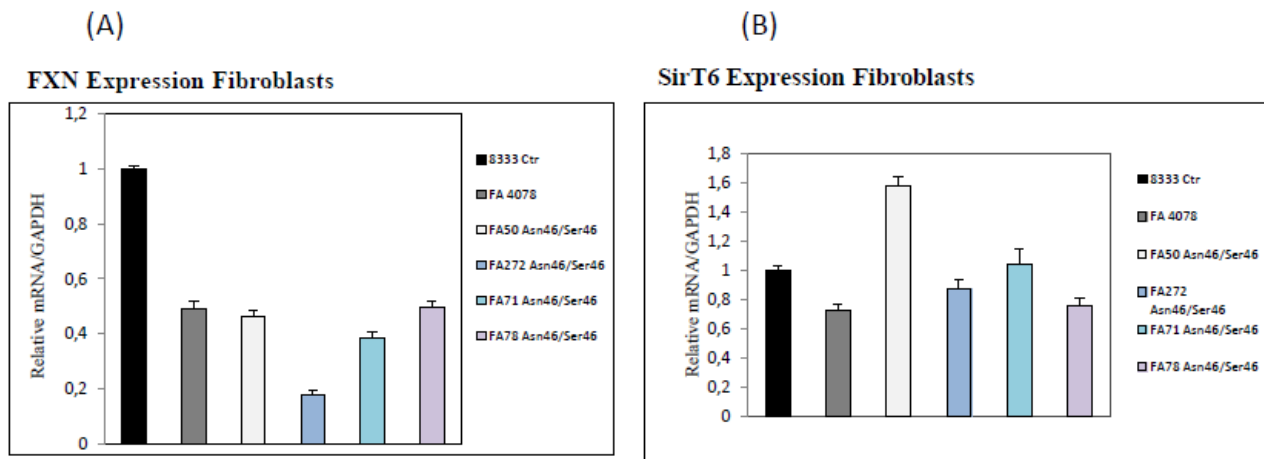


Fig. 10 Gene expression study by qRT-PCR of frataxin (FXN) (Fig. A) and Sirtuin 6 (SirT6) (Fig. B) in fibroblasts control (GM08333), FRDA patients (GM04078) and in FRDA Sirt6 arboring SNP (Asn46/Ser 46) (FA50, FA272, FA71, FA78). Data were normalized for GAPDH housekeeping gene and are expressed in arbitrary units as Mean \pm SD.

qRT PCR Real time analysis FXN and SirT6 expression in FRDA NSCs

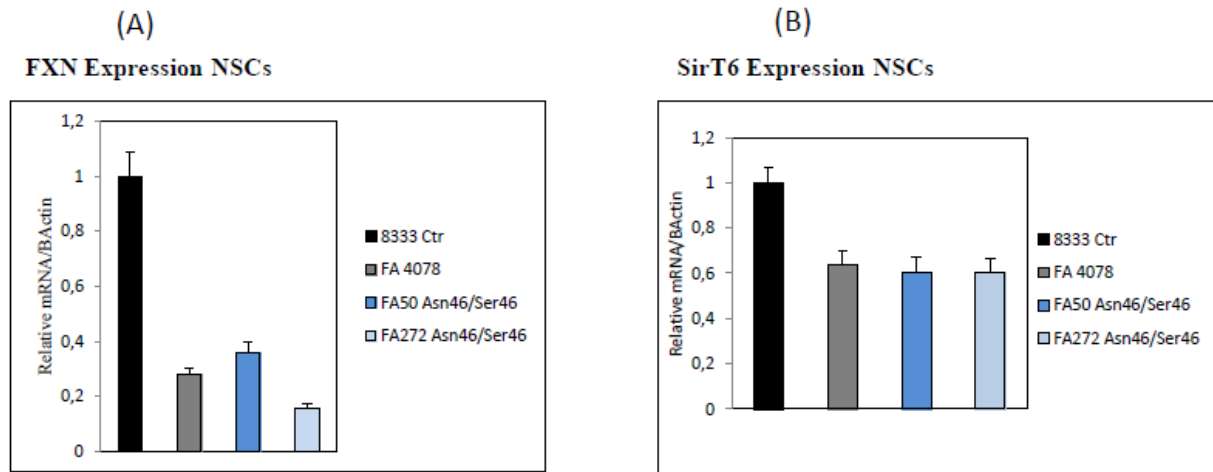


Fig. 11 Gene expression study by qRT-PCR of frataxin (FXN) (Fig. A) and Sirtuin 6 (SirT6) (Fig. B) in neural stem cell (NSCs) control (GM08333), FRDA patients (GM04078) and in FRDA harboring SNP SirT6 (Asn46/Ser46) (FA50, FA272). Data were normalized for GAPDH housekeeping gene and are expressed in arbitrary units as Mean \pm SD.

qRT PCR Real time analysis FXN and SirT6 expression in FRDA Neurons

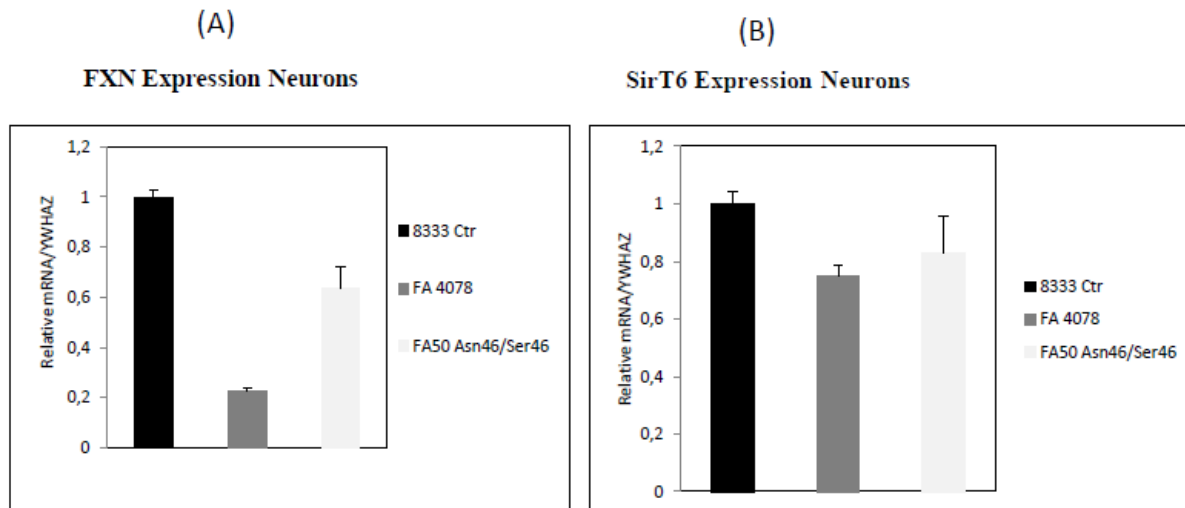


Fig. 12 Gene expression study by qRT-PCR of frataxin (FXN) (Fig. A) and Sirtuin 6 (SirT6) (Fig. B) in neurons control (GM08333), FRDA patients (GM04078) and in FRDA harboring SNP Sirt6 (Asn46/Ser46) (FA50, FA272). Data were normalized for GAPDH housekeeping gene and are expressed in arbitrary units as Mean \pm SD.

Western Blot Analysis of Sirt6 in Fibroblasts derive from FRDA patients (I)

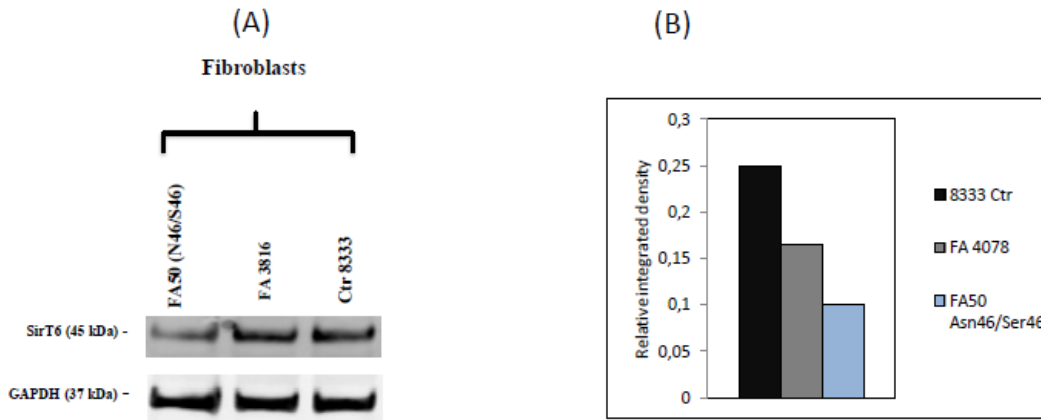


Fig.13 (A). Western blot of Sirtuin 6 protein (42 kDa) and loading control GAPDH (37 kDa) in fibroblasts from healthy subject and FRDA patients. From Left to right: FA50(Asn46/Ser46) FRDA patients harboring SNP Sirt6 (Asn46/Ser46), GM04078 FRDA patients (Asn46/Asn46), GM08333 healthy subjects (Asn46/Asn46) (B) Densitometric analysis of Sirt6 protein normalized to GAPDH.

Western Blot Analysis of Sirt6 in Fibroblasts derive from FRDA patients (II)

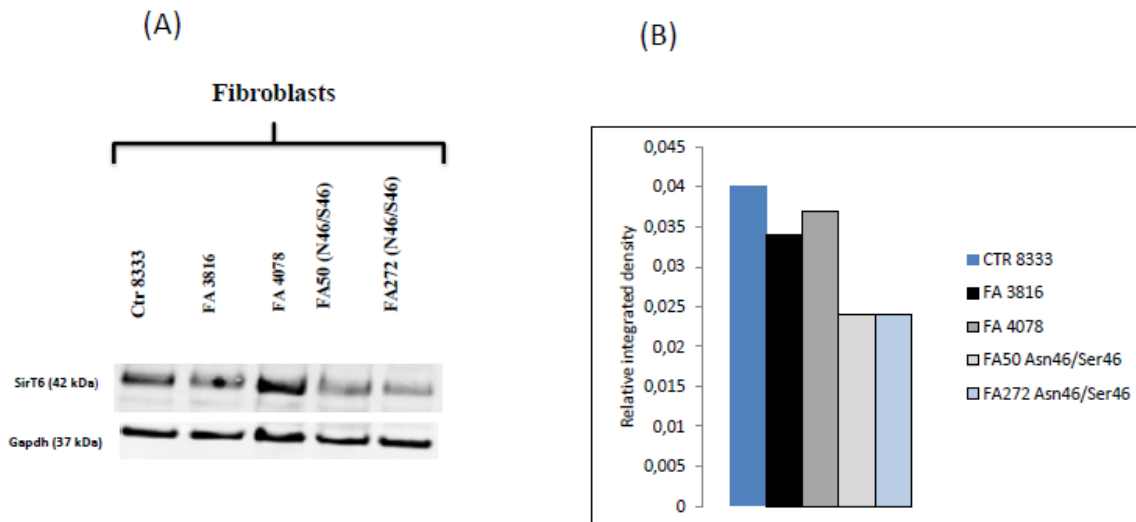
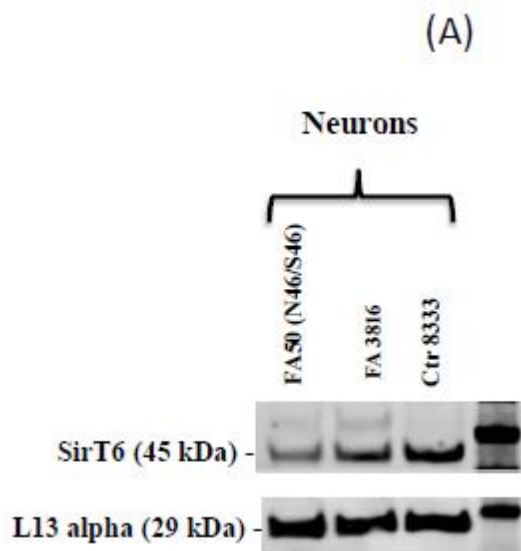


Fig.14 (A). Western blot of Sirtuin 6 protein(42 kDa) and loading control GAPDH (37 kDa) in fibroblasts from healthy subjects and FRDA patients. Left to right: GM08333 healthy subject (Asn46/Asn46), GM03816 FRDA patients (Asn46/Asn46), GM04078 FRDA patients (Asn46/Asn46), FA50 and FA272 (Asn46/Ser46) FRDA patients harboring SNP SirT6 (Asn46/Ser46) (B) Densitometric analysis of Sirt6 protein normalized to GAPDH.

Western Blot Analysis Sirt6 in Neurons FRDA



(B)

Neurons

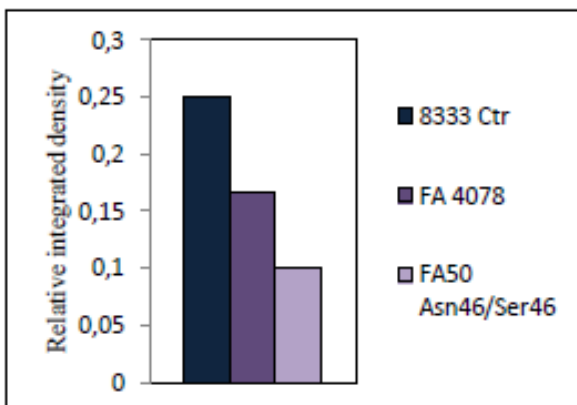


Fig. 15 (A) Western blot of Sirtuin 6 protein (42 kDa) and loading control LN13 alpha (29 kDa) in Neurons from healthy subjects and FRDA patients. Left to right: FA50(Asn46/Ser46) FRDA patients harboring SNP Sirt6 (Asn46/Se46)neurons, GM03816 FRDA patients (Asn46/Asn46) neurons, GM08333 control (Asn46/Asn46) neurons; (B) Densiometric analysis of Sirt6 protein in neurons normalized to GAPDH.

Discussion and Conclusions

Part II

Results obtained by a screening of genetic modifiers of disease severity, have highlighted the potential role of a specific Sirtuin, Sirt6, in FRDA pathogenesis. Individuals who harbors a single nucleotide polymorphism (SNP) in the gene encoding Sirt6 (Asn46/Ser46) show a better outcome as identified by standard neurological measures. In order to understand the molecular mechanisms underlying the better outcome of FRDA patients harboring of rare variant Asn46/Ser46, as first step we expressed both the prevalent Asn46 version of Sirt6 or the rare Ser46 version of Sirt6 proteins in HEK293 cells. For this purpose, we used site-directed mutagenesis to derive the Asn46 version of Sirt6 from the Ser46 version available from Addgene, which is cloned in the FLAG-tagged mammalian expression vector pcDNA3.1. Western blot analysis of protein lysates derived from HEK293 cells expressing (+Asn46) and expressing the rare variant (+Ser46) of Sirt6 show that the Ser46 version appeared to be partially degraded in these cells, compared to the Asn46 version. We found, also that two fibroblast cell lines derived from FRDA heterozygous for the rare variant (Asn46/Ser46) have a reduced amount of Sirt6 protein compared to fibroblasts from FRDA patients who are homozygous (Asn46/Asn46) of the prevalent variant. Subsequently, we generated the induced pluripotent stem cells (iPSCs) from fibroblasts of FRDA patients with the prevalent variant (Asn46/Asn46) and the rare variant (Asn/Ser46) of SIRT6 SNP by retroviral transduction (Yamanaka et al., 2007). Both fibroblasts and iPSCs cell lines were genotyped by direct sequencing in order to confirm the status of heterozygosity Asn46/Ser46 or the status of homozygosity (Asn46/Ser46). Also, the presence of trinucleotide repeats (GAA)_n were verified by standard PCR. Furthermore, the iPSCs were characterized using standard methods (immunostaining of pluripotency markers expression and expression of pluripotency genes by qRT PCR). Subsequently, the neurons were derived from iPSCs by induction with small molecules. In iPSCs derived-neurons (Asn46/Ser46), we found that, similarly to the fibroblasts, also these cells had decreased levels of Sirt6 compared to neurons from iPSCs (Asn46/Asn46). However, no significant differences in frataxin mRNA were observed between Sirt6 Asn46/Asn46 and Sirt6 Asn46/Ser 46 fibroblasts or iPSCs derived neurons by qRT PCR, analysis. These data suggest that the Ser46 allele affects some other aspect of FRDA pathology other than FXN gene expression. In conclusions, our results suggest that the Ser46 variant of Sirt6 is unstable and subject to rapid turnover in fibroblasts and neurons FRDA harboring of the rare variant (Asn46/Ser46) and provide new preliminary information on the role of Sirt6 in FRDA pathogenesis. Recently, some experimental studies have

revealed that some members belonging to the family of Sirtuin proteins have proved to be functional and therapeutic targets in FRDA. Indeed, Chan and colleagues have shown that the Nicotidammide (Vitamin B3), a generic inhibitor of Sirtuins, is able to restore the frataxin expression in lymphocytes derived from FRDA patients. On the other hand, Resveratrol, a compound known as an activator of sirtuins, is able to increase the levels of mRNA of frataxin in fibroblasts and lymphocytes FRDA (Li et al., 2013). Therefore, further studies are needed to understand the role that sirtuins have in the modulation of gene expression of Frataxin with the aim of identifying specific chemical modulators as potential therapeutic agents in the treatment of FRDA.

References

Abruzzo PM, di Tullio S, Marchionni C, Belia S, Fanó G, Zampieri S, Carraro U, Kern H, Sgarbi G, Lenaz G, Marini M. Oxidative stress in the denervated muscle. *Free Radical Research*. 2010 vol. 44, no. 5, pp. 563–576.

Acquaviva F., Castaldo I., Filla A., Giacchetti M., Marmolino D., Monticelli A., Pinelli M., Sacca F. and Coccozza S. Recombinant human erythropoietin increases frataxin protein expression without increasing mRNA expression. *Cerebellum*. 2008. 7,360–365.

Adinolfi S., Trifuoggi M. Politou Martin A.S., and Pastore A. A structural approach to understanding the iron binding properties of phylogenetically different frataxins. *Hum. Mol. Genet*. 2002. 11: 1865–1877.

Aggarwal B. B., Sundaram C., Prasad S., Kannappan R. Tocotrienols, the vitamin E of the 21st century: It potential against cancer and other chronic diseases *Biochemical Pharmacology* 2010 80 1613–1631.

Al-Mahdawi S., Pinto R. M., Ismail O., Varshney D., Lymperi S., Sandi C., Trabzuni D. and Pook M. The Friedreich ataxia GAA repeat expansion mutation induces comparable epigenetic changes in human and transgenic mouse brain and heart tissues. *Hum. Mol. Genet*. 2008. 17, 735–746.

Anderson S. L., Qiu J., and Rubin B.Y., “Tocotrienols induce IKBKAP expression: a possible therapy for familial dysautonomia,” *Biochemical and Biophysical Research Communications*. 2003. 306, no. 1, pp. 303–309, 2003.

Armstrong J. S., Khmour O. and Hecht M. S. “Does oxidative stress contribute to the pathology of Friedreich's ataxia? A radical question,” *FASEB Journal* 2010.vol. 24, no. 7, pp. 2152-2163.

- Auchère F., Santos R., Planamente S., Lesuisse E., and Camadro J. Glutathione- dependent redox status of frataxindeficient cells in a yeast model of Friedreich's ataxia. *Hum Mol Genet* 2008.17: 2790–2802,
- Babcock, M., de Silva, D., Oaks R., Davis-Kaplan S., Jiralerspong S., Montermini, L., Pandolfo M. and Kaplan J. Regulation of mitochondrial iron accumulation by Yfh1p, a putative homolog of frataxin. *Science*. 1997 276, 1997. 1709–1712.
- Bayot A., Santos R., Camadro J. M.,Rustin P. Friedreich's ataxia: the vicious circle hypothesis revisited. *BMC Medicine* 2011; 9:112.
- Bentinger M., Dallner G., Chojnacki T. and Swiezewska E. Distribution and breakdown of labeled coenzyme Q10 in rat. *Free Radic. Biol. Med.* 2003. 34, 563–575.
- Berndt C., Lillig CH., Holmgren A. Thiol-based mechanisms of the thioredoxin and glutaredoxin systems: implications for diseases in the cardiovascular system. *Am J Physiol Heart Circ Physiol* 2007; 292:H1227-36.
- Bligh EG, Dyer WJ. A rapid method of total lipid extraction and purification. *Can J Biochem Physiol.*, 1959; 37:911-7.
- Byrd T.F., Horwitz M.A. Regulation of transferrin receptor expression and ferritin content in human mononuclear phagocytes.Coordinate upregulation by iron transferrin and downregulation by interferon γ . *J. Clin. Invest.*1993;91:969–976.
- Boddaert N. Le Quan Sang K. Rötig A., Leroy-Willig A. Gallet S. Brunelle F et al. Selective iron chelation in Friedreich ataxia: biologic and clinical implications. *Blood* 2007.110(1):401–408
- Boesch S. Sturm B. Hering S. Goldenberg H. Poewe W. Scheiber-Mojdehkar B. Friedreich's ataxia: clinical pilot trial with recombinant human erythropoietin. *Ann Neurol* 2007; 62(5):521–524

Bonizzi G, Piette J, Merville M.P., Bours V. Cell type-specific role for reactive oxygen species in nuclear factor kB activation by interleukin-1. *Biochem Pharmacol* 2000.59: 7–11,

Bradley J.L, Homayoun S, Hart PE, Schapira AH, and Cooper JM. Role of oxidative damage in Friedreich's ataxia. *Neurochem Res.* 2004.29: 561–567,

Brines M. L., Ghezzi P., Keenan S., Agnello D., de Lanerolle N. C., Cerami C., Itri L. M. and Cerami A. Erythropoietin crosses the blood-brain barrier to protect against experimental brain injury. *Proc. Natl Acad. Sci.* 2000 USA 97. 10526–10531

Bubici C, Papa S, Pham CG, et al. The NF-kappaB-mediated control of ROS and JNK signaling. *Histol Histopathol* 2006; 21:69-80.

Burnett R., Melander C., Puckett J.W., Son L.S., Wells R.D., Dervan P.B., Gottesfeld J.M. DNA sequence-specific polyamides alleviate transcription inhibition associated with long GAA.TTC repeats in Friedreich's ataxia. *Proc Natl Acad Sci U S A.*2006 103(31):11497-502

Bradley J.L., Blake, J.C., Chamberlain, S., Thomas, P.K., Cooper, J.M. and Schapira, A.H. Clinical, biochemical and molecular genetic correlations in Friedreich's ataxia. *Hum. Mol. Genet.* 2000 9, 275–282.

Branda S.S, Cavadini P., Adamec J., Kalousek F., Taroni F. and Isaya G. Yeast and human frataxin are processed to mature form in two sequential steps by the mitochondrial processing peptidase. *J. Biol. Chem.*1999. 274: 22763–22769.

Burcham P.C, Kuhan Y.T. Introduction of carbonyl groups into proteins by the lipid peroxidation product malondialdehyde. *Biochem. Biophys. Res. Commun.* 1996; 220:996-1001 423:57-65.

Butterfield D.A., Reed T., Newman S.F., Sultana R. Roles of Amyloid-Peptide-Associated Oxidative Stress and Brain Protein Modifications in the Pathogenesis of Alzheimer's Disease and Mild Cognitive Impairment. *Free Radic Biol Med.* 2007; 43(5): 658–677.

Branda S.S, Cavadini P., Adamec J., Kalousek F., Taroni F., and Isaya G. Yeast and human frataxin are processed to mature form in two sequential steps by the mitochondrial processing peptidase. *J. Biol. Chem.* 1999 274: 22763–22769.

Bürk K., Schulz S.R., and Schulz J.B. Monitoring progression in Friedreich ataxia (FRDA): the use of clinical scales. *Journal of Neurochemistry.* 2013, 126 (118-124).

Calapai G., Marciano M. C., Corica F., Allegra A., Parisi A., Frisina N., Caputi A. P. and Buemi M. Erythropoietin protects against brain ischemic injury by inhibition of nitric oxide formation. *Eur. J. Pharmacol.* 2000 401, 349–356

Campuzano V., Montermini L., Moltò M.D., Pianese L., Cossee M., Cavalcanti F., Monros E., Rodius F., Duclos F., Monticelli A., Zara F., Cañizares J., Koutnikova H., Bidichandani S.I, Gellera C., Brice A., Trouillas P., De Michele G., Filla A., De Frutos R., Palau F., Patel P.I, Di Donato S., Mandel J.L, Coccozza S., Koenig M., Pandolfo M. Friedreich's ataxia: Autosomal recessive disease caused by an intronic GAA triplet repeat expansion. *Science* 1996; 271: 1423-1427.

Chan P. K., Torres R., Yandim C. et al. Heterochromatinization induced by GAA-repeat hyperexpansion in Friedreich's ataxia can be reduced upon HDAC inhibition by vitamin B3. *Hum. Mol. Genet.* 2013. [Epub ahead of print].

Chatgililoglu, C, Ferreri C, Hermetter A, et al. Lipidomics and free radical modifications of lipids. *Chimia* 2008; 62:713-20.

Cho S.J, Lee M.G, Yang J.K, Lee J.Y, Song H.K, and Suh S.W. Crystal structure of *Escherichia coli* CyaY protein reveals a previously unidentified fold for the evolutionarily conserved frataxin family. *Proc Natl Acad Sci U S A.* 2000. 97: 8932–8937.

Christodoulou K, Deymeer F, Serdaroglu P, Ozdemir C, Poda M, Georgiou DM, Ioannou, P, Tsingis M, Zamba E, Middleton LT. Mapping of the second Friedreich's ataxia (FRDA2) locus to chromosome 9p23-p11: evidence for further locus heterogeneity. *Neurogenetics* 2001 3: 127-132

Cnop M, Igoillo-Esteve M, Rai M, Begu A, Serroukh Y, Depondt C, Musuaya AE, Marhfour I, Ladrière L, Moles Lopez X, Lefkaditis D, Moore F, Brion JP, Cooper JM, Schapira AH, Clark A, Koeppen AH, Marchetti P, Pandolfo M, Eizirik DL, Féry F. Central role and mechanisms of B cell dysfunction and death in Friedreich ataxia associated diabetes. *Ann. Neurol.* 2012 72, 971–982

Collins AR, Cadet J, Moller L, et al. Are we sure we know how to measure 8-oxo-7, 8-dihydroguanine in DNA from human cells? *Arch. Biochem. Biophys.* 2004; 423:57-65

Condò I, Ventura N., Malisan F., Rufini A., Tomassini B. and Testi R. In vivo maturation of human frataxin. *Hum. Mol. Genet.* 2007. 16, 1534–1540

Coppola G., Marmolino D., Lu D., Wang Q., Cnop M., Rai M., Acquaviva F., Coccozza S., Pandolfo M. and Geschwind D. H. Functional genomic analysis of frataxin deficiency reveals tissue-specific alterations and identifies the PPAR γ pathway as a therapeutic target in Friedreich's ataxia. *Hum. Mol. Genet.* 2009 18. 2452–2461.

Castaldo I., Pinelli M., Monticelli A. et al. (2008) DNA methylation in intron 1 of the frataxin gene is related to GAA repeat length and age of onset in Friedreich ataxia patients. *J. Med. Genet.* 2008 45, 808–812.

Cavadini P., Adamec J., Taroni F., Gakh O., and Isaya G. Two-step processing of human frataxin by mitochondrial processing peptidase: precursor and intermediate forms are cleaved at different rates. *J. Biol. Chem.* 2000 275: 41469–41475.

Cossée M., Puccio H., Gansmuller A., Koutnikova H., Dierich A., LeMeur M., Fischbeck K., Dollé P, Koenig M. Inactivation of the Friedreich ataxia mouse gene leads to early embryonic lethality without iron accumulation. *Hum. Mol. Genet.* 2000 9: 1219-1226,

Culotta VC, Yang M, O'Halloran TV. Activation of superoxide dismutases: putting the metal to the pedal. *Biochim Biophys Acta* 2006. 1763: 747–758.

Dalle Donne I, Aldini G., Carini M., Colombo R., Rossi R. and Milzani A. Davies K.J.A. Protein damage and degradation by oxygen radicals. I. General aspects. *J. Biol. Chem* 1987. 262: 9895-9901.

Dalle-Donne I, Rossi R, Colombo R, et al. Biomarkers of oxidative damage in human disease. *Clin Chem*. 2006; 52:601-23

Dassa EP, Paupe V, Goncalves S, Rustin P. The mtDNA NARP mutation activates the actin-Nrf2 signaling of antioxidant defenses. *Biochem. Biophys. Res. Commun.* 2008. 368: 620–4.

Davis KL, Martin E, Turko IV, Murad F. Novel effects of nitric oxide. *Annu. Rev. Pharmacol. Toxicol.* 2001;41:203-36.

Davies KJ, Quintanilha AT, Brooks GA, Packer L. Free radicals and tissue damage produced by exercise. *Biochem. Biophys. Res. Commun.* 1982. 107(4):1198-205.

Davies MJ, Fu S, Wang H, Dean RT. Stable markers of oxidant damage to proteins and their application in the study of human disease. *Free Radic Biol Med.* 1999; 27:1151-63

Dean RT, Fu S, Stocker R, Davies MJ. Biochemistry and pathology of radical-mediated protein oxidation. *Biochem J.* 1997; 324:1-18

De Biase I., Rasmussen A., Endres D., Al-Mahdawi S., Monticelli A., Coccozza S., Poo M., Bidichandani SI. Progressive GAA expansions in dorsal root ganglia of Friedreich's ataxia patients. *Ann Neurol* 61: 55-60, 2007.

De Biase I, Rasmussen A, Monticelli A, Al-Mahdawi S, Pook M, Coccozza S, Bidichandani SI. Somatic instability of the expanded GAA triplet-repeat sequence in Friedreich ataxia progresses throughout life. *Genomics* 2007 90: 1-5.

De Biase I., Chutake Y., K., Rindler P. M. and Bidichandani S. I. Epigenetic silencing in Friedreich ataxia is associated with depletion of CTCF (CCCTC-binding factor) and antisense transcription. *PLoS ONE*. 2009. 4, e7914.

Del Gaizo V., Payne R. A novel TAT-mitochondrial signal sequence fusion protein is processed, stays in mitochondria, and crosses the placenta. *Mol Ther* 2003; 7(6):720–730

Del Gaizo V., MacKenzie J., Payne R. Targeting proteins to mitochondria using TAT. *Mol Genet Metab* 2003;80 (1–2):170–180

De Michele G., Filla A., Cavalcanti F., Tammaro A., Monticelli A., Pianese L., Di Salle F., Perreti A., Santoro L., Caruso G., Coccozza S. Atypical Friedreich ataxia phenotype associated with a novel missense mutation in the X25 gene. *Neurology* 54: 496-499, 2000.

Dhe-Paganon S., Shigeta R., Chi Y.I., Ristow M., and Shoelson S.E. Crystal structure of human frataxin. *J Biol Chem* 2000. 275: 30753–30756.

Delatycki M., Paris D., Gardner R., Forshaw K., Nicholson G., Nassif N, Williamson R., Forrest S. Sperm DNA analysis in a Friedreich ataxia premutation carrier suggests both meiotic and mitotic expansion in the *FRDA* gene. *J Med Genet* 1998.35: 713-716,

Delatycki M.B. and Corben L. A. Clinical features of Friedreich ataxia. *J. Child Neurol.* 2012 27, 1133–1137.

de Lima-Salgado T.M, Alba-Loureiro T.C, do Nascimento C.S, et al. Molecular Mechanisms by Which Saturated Fatty Acids Modulate TNF-alpha Expression in Mouse Macrophage Lineage. *Cell Biochem Biophys* 2011; 59:89-97.

Di Donato I., Bianchi S., Federico A. Ataxia with vitamin E deficiency: update of molecular diagnosis. *Neurol Sci* 2010; 31:511-5.

Di Prospero N. A. and Fischbeck K. H. Therapeutics development for triplet repeat expansion diseases. *Nat. Rev. Genet.* 2005. 6, 756–765.

Di Prospero N.A, Baker A., Jeffries N., and Fischbeck K.H. Neurological effects of high-dose idebenone in patients with Friedreich's ataxia: a randomised, placebo-controlled trial. *Lancet Neurol.* 2007 6: 878–886.

Dizdaroglu M., Jaruga P., Birincioglu M., et al. Free radical-induced damage to DNA: mechanisms and measurement. *Free Radic Biol Med* 2002; 32:1102-15

Dolezal P., Dancis A., Embley M., Tachezy J. Functional frataxin homologue in hydrogenosomes of *Trichomonas vaginalis* *Journal of Eukaryotic Microbiology.* 2005.35S–38S,

Dröge.W. Free Radicals in the Physiological Control of Cell Function. *Physiol. Rev.* 82: 47–95, 2002;

Du J., Campau E., Soragni E., Ku S., Puckett J.W., Dervan P.B., and M.J. Gottesfeld M.J. Role of Mismatch Repair Enzymes in GAA_TTC Triplet-repeat Expansion in Friedreich Ataxia Induced Pluripotent Stem Cells. *The Journal of Biological Chemistry.* 2012 Vol. 287, 35: 29861–29872

Emond M., Lepage G., Vanasse M. and Pandolfo M. Increased levels of plasma malondialdehyde in Friedreich ataxia. *Neurology.* 2000. 55: 1752–1753.

Yandim C., Natisvili T. and R. Festenstein Gene regulation and epigenetics in Friedreich's ataxia. *Journal of Neurochemistry*. 2013. 126. 21-24.

Fang F., Kang Z., and Wong C, "Vitamin E tocotrienols improve insulin sensitivity through activating peroxisome proliferator-activated receptors," *Molecular Nutrition & Food Research*, 2010 vol. 54, no. 3, pp. 345-352.

Feelders R.A., Vreugdenhil G., Eggermont A.M., Kuiper-Kramer P.A., van Eijk H.G., Swaak A.J. Regulation of iron metabolism in the acute-phase response: interferon γ and tumor necrosis factor alpha induce hypoferraemia, ferritin production and a decrease in circulating transferrin receptors in cancer patients. *Eur. J. Clin. Invest.* 1998; 28:520–527.

Ferreri C, Kratzsch S, Brede O, et al. Trans lipid formation induced by thiols in human monocytic leukemia cells. *Free Rad Biol Med* 2005; 38:1180–7.

Festenstein R. Breaking the silence in Friedreich's ataxia. *Nat. Chem. Biol.* 2006. 2, 512–513.

Foury, F. Low iron concentration and aconitase deficiency in a yeast frataxin homologue deficient strain. *FEBS Lett.* 1999 456, 281–284

Foury F., Pastore A., Trincal M. Acidic residues of yeast frataxin have an essential role in Fe-S cluster assembly. *EMBO.* 2007. Rep 8:194–199

Fuchs J. *Oxidative Injury in Dermatology*. New York: Springer-Verlag, 1992.

Gakh, O., Adamec, J., Gacy, A.M., Twosten, R.D., Owen, W.G. and Isaya, G. Physical evidence that yeast frataxin is an iron storage protein. *Biochemistry*. 2002 41, 6798–67804.

Gellera C., Castellotti B., Mariotti C., et al., "Frataxin gene point mutations in Italian Friedreich ataxia patients," *Neurogenetics* 2007, vol. 8, no. 4, pp. 289-299.

Gibson TJ, Koonin EV, Musco G, Pastore A, Bork P. Friedreich's ataxia protein: phylogenetic evidence for mitochondrial dysfunction. *Trends Neurosci.* 1996 19: 465-468.

Gogvadze V., Orrenius S., Zhivotovsky B. Mitochondria in cancer cells: what is so special about them? *Trends Cell Biol.* 2008. 18(4):165-73.

Gomez-Sebastian S., Gimenez-Cassina A, Diaz-Nido J., Lim F., Wade-Martins R. Infectious delivery and expression of a 135 kb human FRDA genomic DNA locus complements Friedreich's ataxia deficiency in human cells. *Mol. Ther.* 2007; 15(2):248-254

Gordon D.M, Kogan M., Knight S.A., Dancis A., and Pain D. Distinct roles for two N-terminal cleaved domains in mitochondrial import of the yeast frataxin homolog, Yfh1p. *Hum Mol. Genet* 10: 259–269.

Geissler A., Krimmer T., Schönfisch B, Meijer M, and Rassow J. Biogenesis of the yeast frataxin homolog Yfh1p: Tim44-dependent transfer to mtHsp70 facilitates folding of newly imported proteins in mitochondria. *Eur. J Biochem.*2000 267: 3167–3180.

Gonzalez-Cabo P. and Palau F. Mitochondrial pathophysiology in Friedreich's. *Journal of Neurochemistry.* 2013. 126. 53-64.

Gottesfeld J. Small molecules affecting transcription in Friedreich ataxia. *Pharmacol. Ther.* 2007; 116(2):236–248

Gottesfeld J.M., Rusche J.R. and Pandolfo M. Increasing frataxin gene expression with histone deacetylase inhibitors as a therapeutic approach for Friedreich's ataxia. *Journal of Neurochemistry.* 2013. 126. 147-154.

Grabczyk E.D., Halabi A., Ditch S., Wang J. Human cells promotes GAA·TTC repeat expansion in DNA mismatch repair complex MutSbeta. *J. Biol. Chem.* 2012.

Greene E., Mahishi L., Entezam A., Kumari D., and Usdin K. Repeat-induced epigenetic changes in intron 1 of the frataxin gene and its consequences in Friedreich ataxia. *Nucleic Acids Res* 35: 3383–3390, 2007.

Griffiths HR, Møller L, Bartosz G, et al. Biomarkers. *Mol Aspects Med.* 2002; 23:101.

Gutteridge J.M. and Halliwell B. Free radicals and antioxidants in the year 2000. A historical look to the future. *Ann. NY Acad. Sci* 2000. 899: 136-147.

Halliwell, B. and Gutteridge, J. M. C. Antioxidant defenses; in *Free Radicals in Biology and Medicine*, pp. 105-244, 1999

Halliwell B. Effect of diet on cancer development: is oxidative DNA damage a biomarker? *Free Radic Biol Med* 2002; 32:968-74.

Hargreaves I. P. Ubiquinone: cholesterol's reclusive cousin. *Ann. Clin. Biochem.* 2003 40, 207–218

Harman D. The aging process. *Proc. Natl. Acad. Sci.* 1981. 78: 7124-7128.

Hart P.E, Lodi R., Rajagopalan B., Bradley J.L, Crilley J.G, Turner C., Blamire A.M, Manners D., Styles P., Schapira A.H, Cooper J.M. Antioxidant treatment of patients with Friedreich ataxia: four-year follow-up. *Arch Neurol.* 2005; 62(4):621-626.

Hayes J.D.; Flanagan, J.U.; Jowsey, I.R.; Glutathione transferases, *Ann. Rev. Pharmacol. Toxicol.*, 2005, 45, 51-88.

He Y., Alam S.L., Proteasa S.V., Zhang Y, Lesuisse E., Dancis A., and Stemmler T.L. Yeast frataxin solution structure, iron binding, and ferroxidase interaction. *Biochemistry*. 2004 43 16254–16262.

Herman D., Jenssen K., Burnett R., Soragni E., Perlman S., Gottesfeld J. Histone deacetylase inhibitors reverse gene silencing in Friedreich's ataxia. *Nat Chem Biol* 2006; 2 (10):551–558

Iorio E. L. Specie chimiche reattive e radicali liberi. Convegno “Radicali liberi e antiossidanti in medicina nello sport 2006

Isaya G., O'Neill H.A, Gakh O., Park S., Mantcheva R, Mooney SM. Functional studies of frataxin. *Acta Paediatr Suppl* 2004May; 93(445):68-71.

Izawa S, Inoue Y, Kimura A. Importance of catalase in the adaptive response to hydrogen peroxide: analysis of acatalasaemic *Saccharomyces cerevisiae*. *Biochem J*. Nov. 1996; 320 (Pt 1):61-7

Jha R., Rizvi S.I Age-dependent decline in erythrocyte acetylcholinesterase activity: correlation with oxidative stress. *Biomed pap Med*; 2009 .153(3): 195-198.

Ji L.L, Gomez-Cabrera M.C, Vina J. Exercise and hormesis: activation of cellular antioxidant signaling pathway. *Ann. N Y Acad. Sci.*2006. 1067:425-35.

Jiralerspong S., Liu Y., Montermini L., Stifani S., Pandolfo M. Frataxin shows developmentally regulated tissue-specific expression in the mouse embryo. *Neurobiol Dis* 4: 1997 103-113.

Kakkar P. and Singh B.K. Mitochondria: a hub of redox activities and cellular distress control. *Mol. Cell. Biochem*. 2007. 305: 235-53.

Kalinowski D., Richardson D. The evolution of iron chelators for the treatment of iron overload disease and cancer. *Pharmacol Rev* 2005 57(4):547–583.

Karlberg T., Schagerlo U., Gakh O., Park S., Ryde U., Lindahl M., Leath K., Garman E, Isaya G, and Al-Karadaghi S. The structures of frataxin oligomers reveal the mechanism for the delivery and detoxification of iron. *Structure*. 2006. 14: 1535–1546.

Karthikeyan G., Lewis L. K. and. Resnick M A. The mitochondrial protein frataxin prevents nuclear damage. *Human Molecular Genetics*, 2002, Vol. 11, No. 11 1351–1362.

Kato Y., Mori Y., Makino Y., et al. Formation of N ϵ (hexanonyl) lysine in protein exposed to lipid hydroperoxide. *J Biol Chem* 1999; 274: 20406-14.

Kawakami M., Sekiguchi M., Sato K., Kozaki S. and Takahashi M. Erythropoietin receptor-mediated inhibition of exocytotic glutamate release confers neuroprotection during chemical ischemia. *J. Biol. Chem.*2001. 276, 39469–39475.

Kemp K, Mallam E, Hares K, et al. Mesenchymal stem cells restore frataxin expression and increase hydrogen peroxide scavenging enzymes in Friedreich ataxia fibroblasts. *PLoS One* 2011; 6:e26098.

Kim S., Ponka P. Effects of interferon- γ and lipopolysaccharide on macrophage iron metabolism are mediated by nitric oxide-induced degradation of iron regulatory protein 2. *J. Biol. Chem.*2000; 275: 6220–6226.

Khanna S., Patel V., Rink C., et al. Delivery of orally supplemented alpha-tocotrienol to vital organs of rats and tocopherol-transport protein deficient mice. *Free Rad Biol Med* 2005; 39:1310-19.

Knight SAB, Sepuri NBV, Pain D, and Dancis A. Mt-Hsp70 homolog, Ssc2p, required for maturation of yeast frataxin and mitochondrial iron homeostasis. *J Biol Chem.*1998 273: 18389–18393

Koeppen A.H., Morral J.A., Davis A.N., J. Qian., S. V. Petrocine. M.D. Knutson. W.M. Gibson. M.J.Cusack., E.D.Li. The dorsal root ganglion in Friedreich's ataxia. *Act.Neuropathol.* 2009 118:763-776.

Koeppen A.H. Nikolaus Friedreich and degenerative atrophy of the dorsal columns of the spinal cord. *Journal of Neurochemistry.* 2013, 126 (4-10).

Koutnikova H., Campuzano V., and Koenig M. Maturation of wild-type and mutated frataxin by the mitochondrial processing peptidase. *Hum Mol Genet.*1998 7: 1485–1489.

Ku S., Soragni E. Campau E.. Thomas E.A., Altun G. Laurent L.C., Loring J.F., Napierala M., and Gottesfeld M.J. Friedreich's Ataxia Induced Pluripotent Stem Cells Model Intergenerational GAA•TTC Triplet Repeat Instability. *Cell Stem Cell.* 2010 November 5; 7(5): 631–637

Kumari D. and Usdin K.The distribution of repressive histone modifications on silenced FMR1 alleles provides clues to the mechanism of gene silencing in fragile X syndrome. *Hum. Mol.Genet.* 2010. 19, 4634–4642

Lagedrost S. J., Sutton M. S. J., Cohen M. S et al., “Idebenone in friedreich ataxia cardiomyopathy- results from a 6-month phase III study (IONIA),”*The American Heart Journal.* 2011- 161. 3, 639–645.

Lamarche, J.B., Cote, M. and Lemieux, B. The cardiomyopathy of Friedreich's ataxia morphological observations in 3 cases. *Can. J. Neurol. Sci.*, 1980. 7, 389–396.

Lee SP, Mar GY, Ng LT. Effects of tocotrienol-rich fraction on exercise endurance capacity and oxidative stress in forced swimming rats. *Eur J Appl Physiol* 2009 107:587–95.

Lenaz G., Fato R., Formiggini G. and Genova M. L. The role of coenzyme Q in mitochondrial electron transport. *Mitochondrion*. 2007. 7 (Suppl), S8–S33

LeProust E. M., Pearson C. E., Sinden R. R. and Gao X. Unexpected formation of parallel duplex in GAA and TTC trinucleotide repeats of Friedreich's ataxia. 2000 *J. Mol. Biol.* 302 1063–108

Li, L., Voullaire, L., Sandi, C., Pook, M.A., Ioannou, P.A., Delatycki, M.B., and Sarsero, J.P. Pharmacological screening using an FXN-EGFP cellular genomic reporter assay for the therapy of Friedreich ataxia. *PLoS One*. 2013 8, e55940.

Lim CK, Kalinowski DS, Richardson DR. Protection against hydrogen peroxide-mediated cytotoxicity in Friedreich's ataxia fibroblasts using novel iron chelators of the 2-pyridylcarboxaldehyde isonicotinoyl hydrazone class. *Mol Pharmacol*. 2008; 74(1):225-235

Lindahl T. Keynote: past, present, and future aspects of base excision repair. *Prog. Nucleic Acid. Res. Mol. Biol.* 68, XVII–XXX 2001.

Li K., Besse EK, Ha D., Kovtunovych G., Rouault T.A. Iron-dependent regulation of frataxin expression: implications for treatment of Friedreich ataxia. *Hum Mol Genet* 2008.17: 2265-2273.

Li K., Singh A., Crooks D., R. Dai X., Cong Z., Pan. L. Ha. D. Rouault T. A. Expression of Human Frataxin Is Regulated by Transcription Factors SRF and TFAP2 *PloS ONE* 2010 Vol. 5.8

Livak J.K, Schmittgen T.D. Analysis of relative gene expression data using real-time quantitative PCR and the 2- $\Delta\Delta$ CT method. *Methods* 2001;25:402-408.

Lynch D. R., Perlman S. L., and Meier T., “A phase 3, doubleblind, placebo-controlled trial of idebenone in friedreich ataxia,” *Archives of Neurology*,2010. 67, 8, 941–947.

McCord JM. (2000). The Evolution of Free Radicals and Oxidative Stress. *AmJ Med.*;108:652–659.

Markesbery W.R. Oxidative stress hypothesis in Alzheimer’s disease. *Free Radical Biology & Medicine*. 1996. Vol. 23, No. 1: 134–147.

Mariotti C., Solari A., Torta D., Marano L., Fiorentini C. and Di Donato S. Idebenone treatment in Friedreich patients: one-year-long randomized placebo-controlled trial. *Neurology*. 2002 60, 1676–1679

Marmolino, F. Acquaviva, M. Pinelli, et al., “PPAR-gamma agonist Azelaoyl PAF increases frataxin protein and mRNA expression: new implications for the Friedreich's ataxia therapy,” *Cerebellum*, 2009 vol. 8, no. 2, pp. 98-103.

Marmolino D., Acquaviva F., Pinelli M., Monticelli A., Castaldo I., Filla A. and Coccozza S. PPAR-gamma agonist Azelaoyl PAF increases frataxin protein and mRNA expression: new implications for the Friedreich’s ataxia therapy. *Cerebellum*. 2009. 8, 98–103.

Marmolino D., Manto M., Acquaviva F., Vergara P., Ravello A., Monticelli A. and Pandolfo M. PGC-1alpha downregulation affects the antioxidant response in Friedreich’s ataxia. *PLoS ONE* 2010 5, e10025.

Marmolino D., “Friedreich's ataxia: past, present and future,” *Brain Research Reviews*, vol. 67, no. 1-2, pp. 311-330, 2011.

Meier T and Buyse G., “Idebenone: an emerging therapy for friedreich ataxia,” *Journal of Neurology*, 2009 vol. 256, no. 1. 25–30.

Myers L.M, Lynch D.R, Farmer J.M, Friedman L.S, Lawson J.A, and Wilson R.B. Urinary isoprostanes in Friedreich ataxia: lack of correlation with disease features. *Mov Disord* 2008.23: 1920–1922,

Morrow J.D. Quantification of isoprostanes as indices of oxidant stress and the risk of atherosclerosis in humans. *Arterioscler Thromb Vasc Biol*. 2005; 25:279-86

Musco G., Stier G., Kolmerer B., Adinolfi S., Martin S., Frenkiel T., Gibson .T, and Pastore A. Towards a structural understanding of Friedreich’s ataxia: the solution structure of frataxin. *Structure* 2000. 8: 695–707.

Nair M, Adinolfi S, Pastore C, Kelly G, Temussi P, and Pastore A. Solution structure of the bacterial frataxin ortholog, CyaY: mapping the iron binding sites. *Structure*. 2004. 12: 2037–2048

Napoli E, Taroni F, and Cortopassi GA. Frataxin, ironsulfur clusters, heme, ROS, and aging. *Antioxid Redox Signal* 8: 506–516, 2006.

Ohshima K, Montermini L., Wells R. Pandolfo M. Inhibitory effects of expanded GAA.TTC triplet repeats from intron I of the Friedreich ataxia gene on transcription and replication in vivo. *J Biol Chem* 1998; 273(23):14588–14595.

Oktay Y., Dioum E., Matsuzaki S., Ding K., Yan L.J, Haller R.G, Szweda L.I, and Garcia J.A. Hypoxia-inducible factor 2a regulates expression of the mitochondrial aconitase chaperone protein frataxin. *J Biol Chem*. 2007.282: 11750–11756

Orsucci D., Mancuso M., Caldarazzo Ienco E., LoGerfo A. and Siciliano G. Targeting mitochondrial dysfunction and neurodegeneration by means of coenzyme Q10 and its analogues. *Curr. Med. Chem*.2011. 18, 4053–4064

Osakada F., Hashino A., Kume T., Katsuki H., Kaneko S., Akaike A. Alpha-tocotrienol provides the most potent neuroprotection among vitamin E analogs on cultured striatal neurons. *Neuropharmacology* 2004; 47:904-15.

Pastore A., Tozzi G., Gaeta L.M, Bertini E., Serafini V., Di Cesare S., Bonetto V., Casoni F., Carozzo R., Federici G., and Piemonte F. Actin glutathionylation increases in fibroblasts of patients with Friedreich's ataxia: a potential role in the pathogenesis of the disease *J Biol Chem* 2003.278: 42588–42595

Pastore A. and Helene Puccio H. Frataxin: a protein in search for a function. *Journal of Neurochemistry*.2013. 126. 43-52

Pandolfo M. Drug Insight: antioxidant therapy in inherited ataxias. *Nat Clin Pract Neurol*.2008 4: 86-96.

Parker R.A, Pearce B.C, Clark R.W, Gordon D.A, Wright J.J. Tocotrienols regulate cholesterol production in mammalian cells by post-transcriptional suppression of 3-hydroxy-3-methylglutaryl coenzyme A reductase. *J Biol Chem* 1993;268:11230–8.

Paupé V., Dassa E.P., Goncalves S. Auchère F., Lonn M. Holmgren A. Rustin P. Impaired Nuclear Nrf2 Translocation Undermines the Oxidative Stress Response in Friedreich Ataxia. *PLoS ONE*.2009. 4(1): e4253

Pearce B.C, Parker R.A, Deason M.E, Qureshi A.A, Wright J.J. Hypocholesterolemic activity of synthetic and natural tocotrienols. *J Med Chem* 1992; 35: 3595–606.

Pianese L., Tammara A., Turano M. de Biase, I.Monticelli A.and. Coccozza S. "Identification of a novel transcript of X25, the human gene involved in friedreich ataxia," *Neuroscience Letters*, 2002 vol. 320, no. 3, pp. 137–140.

Piemonte F, Pastore A, Tozzi G, Tagliacozzi D, Santorelli FM, Carrozzo R, Casali C, Damiano M, Federici G, and Bertini E. Glutathione in blood of patients with Friedreich's ataxia. *Eur J Clin Invest.* 2001. 31: 1007–1011

Pilger A., Rüdiger H.W. 8-Hydroxy-2'-deoxyguanosine as a marker of oxidative DNA damage related to occupational and environmental exposures. *Int Arch Occup Environ Health.* 2006; 80(1):1-15.

Pfaffl M.W. A new mathematical model for relative quantification in real-time RT-PCR. *Nucl Acids Res.* 2001; 29:e45.

Powers S.K, Jackson M.J. Exercise-induced oxidative stress: cellular mechanisms and impact on muscle force production. *Physiol Rev.* 2008. 88(4):1243-76.

Puccio H., Koeing M. Recent Advances in the molecular pathogenesis of Friedreich's Ataxia. *Human Molecular Genetics.* 2000; Vol.9 No. 6. (887-892)

Piyush M. V., W. J. Tomamichel, P. M., Pridel, C. M. Babbey, Q.Wang, J.Mercier, E. M. Martin and R. M. Payne. A TAT-Frataxin fusion protein increases lifespan and cardiac function in a conditional Friedreich's ataxia mouse model. *Hum.Mol. Gen.* 2011 21, 6, 1230-1247

Rahman K. Studies on free radicals, antioxidants, and co-factors. *Clinical Interventions in Aging;* 2007 2(2): 219–236.

Rai M., Soragni E., Jenssen K., Burnett R., Herman D., Coppola G., Geschwind D. H., Gottesfeld J. M. and Pandolfo M. HDAC inhibitors correct frataxin deficiency in a Friedreich ataxia mouse model. *PLoS ONE* 2008 3, e1958.

Rai M., Soragni E., Chou C. J., Barnes G., Jones S., Rusche J. R., Gottesfeld J. M. and Pandolfo M. Two new pimelic diphenylamide HDAC inhibitors induce sustained frataxin upregulation in cells from Friedreich's ataxia patients and in a mouse model. *PLoS ONE.* 2010. 5, e8825

Rance G., Ryan M. M., Carew P., Corben L. A., Yiu E., Tan J. and Delatycki M. B. Binaural speech processing in individuals with auditory neuropathy. *Neuroscience* 2012 226,227–235.

Reiter R.J, Carneiro R.C, Oh C.S. Melatonin in relation to cellular antioxidative defense mechanisms. *Horm Metab Res.* 1997 ;29(8):363-72

Ricci C., Pastukh V., Leonard J., Turrens J., Wilson G., Schaffer D., Schaffer S.W. Mitochondrial DNA damage triggers mitochondrial-superoxide generation and apoptosis. *Am J Physiol Cell Physiol.* 2008. 294(2):C413-22.

Richardson D., Mouralian C., Ponka P., Becker E. Development of potential iron chelators for the treatment of Friedreich's ataxia: ligands that mobilize mitochondrial iron. *Biochim Biophys Acta* 2001;1536(2–3):133–140

Richardson D. Friedreich's ataxia: iron chelators that target the mitochondrion as a therapeutic strategy? *Expert Opin Investig Drugs* 2003; 12(2):235–245

Roberts L.J and Morrow J.D. Measurement of F (2)-isoprostanes as an index of oxidative stress in vivo. *Free Radic Biol Med.* 2000; 28:505–13.

Rötig A., de Lonlay P., Chretien D., Foury F., Koenig M., Sidi D., Munnich A., Rustin P. Aconitase and mitochondrial iron-sulphur protein deficiency in Friedreich ataxia. *Nat Genet* 17: 215-217, 1997.

Santos R., Lefevre S., Sliwa D., Seguin A., Camadro J.M, Lesuisse E. Comprehensive invited review friedreich's ataxia: molecular mechanisms, redox considerations and therapeutic opportunities. *Antioxid Redox Signal.* 2010; Feb 16.1-135.

Sakamoto N., Ohshima K., Montermini L., Pandolfo M. and Wells R. D. Sticky DNA, a self-associated complex formed at long GAA*TTC repeats in intron 1 of the frataxin gene, inhibits transcription. *J. Biol. Chem.* 2001 276, 27171–27177.

Sakanaka M., Wen T., Matsuda S., Masuda S., Morishita E., Nagao M et al. In vivo evidence that erythropoietin protects neurons from ischemic damage. *Proc Natl Acad Sci.* 1998 U S A;95(8):4635–4640.

Saveliev A., Everett C., Sharpe T., Webster Z. and Festenstein R. DNA triplet repeats mediate heterochromatin-protein-1-sensitive variegated gene silencing. *Nature* 2003. 422, 909–913.

Schoenle E.J., Boltshauser E.J., Baekkeskov S., Landin Olsson M, Torresani T, von.Felten A. Preclinical and manifest diabetes mellitus in young patients with friedreich's ataxia: no evidence of immune process behind the islet cell destruction. *Dabetologia.* 1989, Volume 32, Issue 6, pp 378-381.

Schraufstatter I., Hyslop P.A., Jackson J.H. and Cochrane C.G. Oxidant-induced DNA damage of target cells. *J Clin Inves.* 1988. 82: 1040-1050.

Schmucker S., Argentini M., Carelle-Calmels N., Martelli A. and Puccio H. The in vivo mitochondrial two-step maturation of human frataxin. *Hum. Mol. Genet.* 2008 17, 3521–3531.

Schulz J.B, Dehmer T., Schöls L., Mende H., Hardt C., Vorgerd M., Bürk K., Matson W., Dichgans J, Beal MF, Bogdanov MB. Oxidative stress in patients with Friedreich ataxia. *Neurology.* 2000. 55: 1719-1721

Schulz T.J, Thierbach R., Voigt A., Drewes G., Mietzner B.H, Steinberg P., Pfeiffer A.F, Ristow M. Induction of oxidative metabolism by mitochondrial frataxin inhibits cancer growth: Otto Warburg revisited. *J Biol Chem.* 2006. 281: 977-981,

Sen C.K, Khanna S., Roy S., Packer L. Molecular basis of vitamin E action, tocotrienol potently inhibits glutamate-induced pp60(c-Src) kinase activation and death of HT4 neuronal cells. *J Biol Chem* 2000;275:13049–55.

Siciliano G., Piazza S., Carlesi C., et al. Antioxidant capacity and protein oxidation in cerebrospinal fluid of amyotrophic lateral sclerosis. *J Neurol*; 2007 254:575-80.

Sies H., Cadenas E. Oxidative stress: damage to intact cells and organs. *Philos Trans R Soc Lond B Biol Sci* 1985.311: 617–631.

Sirano D., Shigeta R., Chi Y., Ristow M., and Shoelson S. E. Crystal structure of human frataxin, *The Journal of Biological Chemistry*. 2000 vol. 275, no. 40, pp. 30753–30756,

Sohn Y.S., Breuer W., Munnich A. and Cabantchik Z. I. Redistribution of accumulated cell iron: a modality of chelation with therapeutic implications. *Blood*. 2008. 111, 1690–1699.

Soragni E., Herman D., Dent S. Y., Gottesfeld J. M., Wells R. D. and Napierala M. Long intronic GAA*TTC repeats induce epigenetic changes and reporter gene silencing in a molecular model of Friedreich ataxia. *Nucleic Acids Res*. 2008 36, 6056–6065.

Spiteller G.V. Peroxyl radicals: inductors of neurodegenerative and other inflammatory diseases. Their origin and how they transform cholesterol, phospholipids, plasmalogens, polyunsaturated fatty acids, sugars, and proteins into deleterious products. *Free Radic Biol Med*. 2006 Aug 1;41(3):362-87.

Stadtman E.R, Berlett B.S. Reactive oxygen-mediated protein oxidation in aging and disease. *Chem Res Toxicol*. 1997; 10:485-94

Stadtman E.R, Levine RL Protein oxidation. *Ann. N. Y. Acad. Sci.*2000; 899:191-208.

Stadtman E.R, Levine RL. Free radical-mediated oxidation of free amino acids and amino acid residues in proteins. *Amino Acids*. 2003 Dec;25(3-4):207-18. Epub 2003 Jul 29. Review.

Sturm B., Stupphann D., Kaun C., Boesch S., Schranzhofer M., Wojta J., Goldenberg H. and Scheiber-Mojdehkar B. Recombinant human erythropoietin: effects on frataxin expression in vitro. *Eur. J. Clin. Invest.* 2005. 35, 711–717.

Sturm B., Helminger M., Steinkellner H., Heidari M. M., Goldenberg H. and Scheiber-Mojdehkar B. Carbamylated erythropoietin increases frataxin independent from the erythropoietin receptor. *Eur. J. Clin. Invest.* 2010 40, 561–565.

Suno M. and Nagaoka A. Inhibition of lipid peroxidation by a novel compound, idebenone (CV-2619). *Jpn. J. Pharmacol.* 1984 35, 196–200.

Tan G, Chen LS, Lonnerdal B, Gellera C, Taroni FA, Cortopassi GA. Frataxin expression rescues mitochondrial dysfunctions in FRDA cells. *Hum Mol Genet.* 2001. 10:2099–2107

Tarng D.C, Huang T.P, Wei Y.H, Liu T.Y, Chen H.W, Wen Chen T, Yang WC. 8-hydroxy-2'-deoxyguanosine of leukocyte DNA as a marker of oxidative stress in chronic hemodialysis patients. *Am J Kidney Dis.* 2000 Nov;36(5):934-44.

Tarpey M.M, Wink D.A, Grisham M.B. Methods for detection of reactive metabolites of oxygen and nitrogen: in vitro and in vivo considerations. *Am J Physiol Regul Integr Comp Physiol.* 2004; 286:R431-44.

Theriault A., Chao J.T, Gapor A. Tocotrienol is the most effective vitamin E for reducing endothelial expression of adhesion molecules and adhesion to monocytes. *Atherosclerosis* 2002;160:21–30.

Tomassini B., Arcuri G., Fortuni S., Sandi C., Ezzatizadeh V., Casali, C. Condò, I. Malisan, F. Al-Mahdaw, S., Pook, M., Testi R. Interferon gamma upregulates frataxin and corrects the functional deficits in a Friedreich ataxia model. *Hum Mol Genet.* 2012; 21(13):2855-61.

Uchida K. 4-Hydroxy-2-nonenal: a product and mediator of oxidative stress. *Prog Lipid Res* 2003; 42:318-43

Valko M., Rhodes CJ., Moncol J., Izakovic M., Mazur M. (2006). Free radicals, metals and antioxidants in oxidative stress-induced cancer. *Chemico-Biological Interactions*;160:1–40.

Vazzola V., Losa A., Soave C., Murgia I. Knockout of frataxin gene causes embryo lethality in *Arabidopsis*. *FEBS Lett.*2007 581: 667-672.

Vlassara H, Bucala R, Striker L. Pathogenic effects of advanced glycosylation: biochemical, biologic, and clinical implications for diabetes and aging. *Lab Invest.* 1994; 70:138-51.

Vankan P., Prevalence gradients of Friedreich's Ataxia and R1b haplotype in Europe co-localize, suggesting a common Palaeolithic origin in the Franco-Cantabrian ice age refuge. *Journal of Neurochemistry.* 2013.126 (11-20).

Viviani Anselmi C., Ferreri C., Novelli V., et al. Fatty acid percentage in erythrocyte membranes of atrial flutter/fibrillation patients and controls. *J. Interv. Card. Electrophysiol.* 2010; 27:95-9.

Voisine C., Schilke B., Ohlson M., Beinert H., Marszalek J., and Craig E.A. Role of the mitochondrial Hsp70s, Ssc1 and Ssq1, in the maturation of Yfh1. *Mol Cell Biol.*2000. 20: 3677-3684, 2000.

Waldvogel D., van Gelderen P., Hallett M. Increased iron in the dentate nucleus of patients with Friedreich's ataxia. *Ann Neurol* 1999;46(1):123–125

Wall R., Ross R.P, Fitzgerald G.F, et al. Fatty acids from fish: the anti-inflammatory potential of long-chain omega-3 fatty acids. *Nutr Rev* 2010; 268:280-9.

Weidemann F., Stork.S., Liu D., Hu K. Herrmann, S., Ertl G., and Niemann M. Cardiomyopathy of Friedreich Ataxia. *Journal of Neurochemistry.* 2013, 126 (88-93).

Wilks A., Ortiz de Montellano P.R. Intramolecular translocation of the protein radical formed in the reaction of recombinant sperm whale myoglobin with H₂O₂. *J Biol Chem.* 1992; 267:8827-33.

Wilson R. Iron dysregulation in Friedreich ataxia. *Semin Pediatr Neurol* 2006;13(3):166–175.

Xia H., Cao Y, Dai X., Marelia Z., Zhou D., Mo R., Al-Mahdawi S., Leimkuhler S., Rouault T.A., Li K. “Novel frataxin isoforms may contribute to the pathological mechanism of friedreich ataxia,” *PLoS ONE.* 2012, vol. 7, no. 10.

Yang H., Magilnick N., Lee C., Kalmaz D., Ou X., et al. Nrf1 and Nrf2 regulate rat glutamate-cysteine ligase catalytic subunit transcription indirectly via NF-kappaB and AP-1. *Mol Cell Biol* 2005. 25: 5933–46.

Zambonin L., Ferreri C., Cabrini L., et al. Occurrence of trans fatty acids in rats fed a trans-free diet: a free radical-mediated formation? *Free Rad Biol Med* 2006; 40:549-56.

Zhu H., Itoh K., Yamamoto M., Zweier J.L, Li Y. Role of Nrf2 signaling in regulation of antioxidants and phase 2 enzymes in cardiac fibroblasts: protection against reactive oxygen and nitrogen species-induced cell injury. *FEBS Lett.* 2005 579: 3029–36.